

FEASIBILITY STUDY OF USING LEAKY COAXIAL CABLE (LCX)
FOR RURAL COMMUNICATIONS

DSS Contract Serial No. OSU76-00154

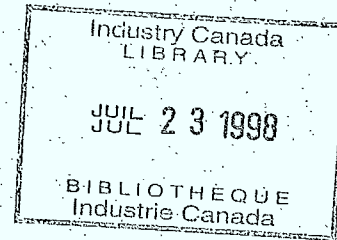
FINAL REPORT

September 1977

Submitted by: Professor Michael Hamid

Department of Electrical Engineering
University of Manitoba
Winnipeg, Manitoba
R3T 3C4

QUEEN
P
92 92
.C2
H34
1977



FEASIBILITY STUDY OF USING LEAKY COAXIAL CABLE (LCX)
FOR RURAL COMMUNICATIONS

DSS Contract Serial No. OSU76-00154

FINAL REPORT

September 1977

Submitted by: Professor Michael Hamid

Department of Electrical Engineering
University of Manitoba
Winnipeg, Manitoba
R3T 3C4



FEASIBILITY STUDY OF USING LEAKY COAXIAL CABLE (LCX)
FOR RURAL COMMUNICATIONS

DSS Contract Serial No. OSU76-00154

FINAL REPORT

September 1977

Research Personnel: Dr. M. Hamid, Professor
Dr. T.C.K. Rao, Research Associate
Dr. M.F. Iskander, Research Associate
Mr. D.A. Copeland, Technician
Mr. A. Ittipiboon, Graduate Student
Mr. C.S. Kim, Graduate Student

DOC Scientific Authority: Dr. George D. Cormack

Department of Communications
Journal Tower North
300 Slater Street
Ottawa, Ontario
K1A 0C8

P
92
C2
H34

TABLE OF CONTENTS

	Page
ACKNOWLEDGEMENTS	i
LIST OF TABLES	ii
LIST OF FIGURES	iv
LIST OF PRINCIPAL SYMBOLS AND ABBREVIATIONS	vi
RESEARCH OBJECTIVES	viii
CHAPTER 1 INTRODUCTION	1
1.1 Common Types of Leaky Transmission Lines	2
1.2 Frequency Considerations	4
1.3 References	7
CHAPTER 2 STUDIES ON COMMERCIAL LCX CABLES	
2.1 Introduction	12
2.2 Basic Parameters of LCX Cables	13
2.2.1 Transmission Loss	14
2.2.2 Coupling Loss	14
2.2.3 Group Delay	15
2.2.4 Return Loss vs Frequency	15
2.2.5 Two-Way Coupling	16
2.2.6 Radiation Pattern and Gain	16
2.3 Measurement Methods	17
2.3.1 Measurement of Transmission Loss	18
2.3.2 Measurement of Group Delay	30
2.3.3 VSWR Measurement	36
2.3.4 Coupling Loss Measurements	36
2.4 Coupling Loss Measurements at 150 KHZ-10 MHZ	38
2.5 Coupling Loss Measurements at 100 KHZ	43
2.6 Time Domain Reflectometer Technique	45
2.7 References	48
CHAPTER 3 THE MODIFIED GOUBAU LINE	
3.1 Introduction	49
3.2 Theoretical Model	50
3.3 Operating Physical Mechanism	52
3.4 Line Excitation	53
3.5 Operating Frequency Bandwidth	54

	Page
3.6 Transverse Field Decay	55
3.7 Leaky MGL	55
3.8 Experimental Line	57
3.9 Experimental Results	62
3.10 Discussion	80
3.11 References	82
 CHAPTER 4 LEAKY COIL-COUPLED COAXIAL SYSTEM (LCCX)	
4.1 Introduction	84
4.2 Theory	87
4.2.1 Characteristic Impedance of a Coaxial Line	87
4.2.2 Magnetic Field Inside a Coaxial Line	87
4.2.3 Coupling by a Rectangular Loop	90
4.2.4 Radiation by a Short Wire	91
4.2.5 Radiation Pattern of a Short Loop Antenna	93
4.3 Experimental Investigations	96
4.3.1 Experimental Line	96
4.3.2 Indoor Experiments	97
Experiment No. 1	99
" No. 2	99
" No. 3	99
" No. 4	99
" No. 5	99
4.3.3 Outdoor Experiments	104
4.4 Discussion	104
4.5 References	112
 CHAPTER 5 GENERAL DISCUSSION	113
 CHAPTER 6 GENERAL CONCLUSIONS AND RECOMMENDATIONS	124

ACKNOWLEDGEMENTS

The valuable assistance of A. Symmons, T.J. White and K. Podaima of the Electrical Engineering Department, University of Manitoba, towards the technical aspects of this study is acknowledged. The administrative assistance of Professor R.E. Chant and Miss Janet Gourlay of the Office of Industrial Research, University of Manitoba, as well as Judith Moroz Bade of the Electrical Engineering Department, University of Manitoba, is also gratefully acknowledged. Thanks are also due to Hitachi Cable, Ltd. and the Andrew Antenna Company for providing test cable samples, the Manitoba Telephone System for lending the Time Domain Reflectometer equipment and the Department of Communications, Winnipeg, for lending the Spectrum Analyzer and Field Strength measuring equipment. Thanks are also due to Dr. A. Watanabe of the Canadian Embassy, Tokyo, Japan, for arranging cable samples from Sumitomo Electric Industries, Ltd. and Fujikura Cable Works, Ltd., Japan, and to Dr. L. Shafai of the University of Manitoba for proofreading the manuscript.

Finally, the contribution of Dr. G.D. Cormack of the Department of Communications, Ottawa, through many profitable discussions throughout this project is also gratefully acknowledged.

LIST OF TABLES

TABLE		Page
2.1	Attenuation Constant vs Frequency in dB/20 ft	21
2.2	Transmission Loss and Phase Angle of Hitachi HW-46 LCX	32
2.3	Phase Angle Measurement	34
2.4	Measurement of Coupling Loss of RX4-3A Radiax Cable	39
2.5	Measurement of Coupling Loss of HW-46 LCX	40
2.6	Measurement of Field Intensity (at 20 ft) vs Frequency	41
2.7	Measurement of Field Intensity (at 20 ft) vs Frequency	41
2.8	Variation of Electric Field Intensity with Distance	42
2.9	Measurement of Coupling Loss at 100 KHZ	44
3.1	Comparison Between the Calculated and Measured Values of λ_g (Dipole Probe)	63
3.2	Measured Values of the Guide Wavelength (cm) - Monopole Probe	63
3.3	Measured Values of the Decay Coefficient for the MGL	67
3.4	Variation of VSWR with Disc Position	75
3.5	Measurement of Radial Power Decay at 150 MHZ	76
3.6	Measurement of Field Intensity at 150 KHZ (Vertical Polarization)	77
3.7	Measurement of Field Intensity at 150 KHZ (Horizontal Polarization)	78
3.8	Variation of Field Intensity with Frequency at 20 ft	79
4.1	Voltage Induced by a Single Turn Loop Using an RMS Voltmeter (Experiment No. 2)	100
4.2	Voltage Induced by a Single Turn Loop Using HP Spectrum Analyzer (Experiment No. 2)	101
4.3	Measured Field Strength at 20 ft vs Frequency (Experiment No. 4)	102
4.4	Measurement of Voltage Induced with a 4-turn Coil Inside the the Coaxial Line	103
4.5	Variation of Field Intensity ($\mu\text{V}/\text{m}$) with Frequency (Single Turn)	105
4.6	Variation of Field Intensity ($\mu\text{V}/\text{m}$) with Distance (Single Turn)	106
4.7	Variation of Field Intensity ($\mu\text{V}/\text{m}$) with Frequency (4-turn Coil)	107

		Page
4.8	Variation of Field Intensity ($\mu\text{V}/\text{m}$) with Distance (4-turn Coil)	108
4.9	Variation of Electric Field Intensity with Frequency (4-turn Coil)	109
4.10	Variation of Electric Field Intensity with Distance (4-turn Coil)	110
Summary 1	Electric Field Strength at 20 ft (in $\mu\text{V}/\text{m}$) vs Frequency (in MHz)	118
Summary 2	Attenuation Loss in dB/20 ft	119
Summary 3	Coupling Loss in dB (at 20 ft)	120

LIST OF FIGURES

FIGURE		Page
1.1	Types of 'Leaky Cables'	3
2.1	Block Diagram Used for the Measurement of Attenuation	19
2.2	Variation of Attenuation vs Frequency (10-100 MHz)	22
2.3	" (100-450 MHz)	23
2.4	" RX4-3A, RX5-1 (100-550 MHz)	24
2.5	" RX4-3A, RX5-1 (450-900 MHz)	25
2.6	" RX4-1 (450-900 MHz)	26
2.7	" RX5, RX4-3A (800-1250 MHz)	27
2.8	" RX4-1 (800-2150 MHz)	28
2.9	" RX4-1 (1200-1650 MHz)	29
2.10	Experimental Set-up Used for Measuring Transmission Loss	31
2.11	Transmission Loss of HW-46 LCX vs Frequency	33
2.12	Group Delay vs Frequency	35
2.13	Variation of VSWR with Frequency	37
3.1	Junction Between the Modified Goubau Line and the Coaxial Waveguide	51
3.2	Details of the MGL, Launchers and Spacers	58
3.3	Details of Launchers	59
3.4	Experimental Set-up Used for Near-Field Measurements	60
3.5	Radial Power Decay	65
3.6	Standing Wave Pattern Along the Structure	66
3.7	Normalized Power vs Radial Distance (in cm) for Loaded and Unloaded Cases	68
3.8	Comparison of Normalized Power vs Radial Distance (in cm) on Either Side of Discontinuity	69
3.9	Normalized Power on Load Side vs Radial Distance (in cm) for Brass Disc Loaded MGL for Different Frequencies	70
4.1	Schematic Diagram of the Proposed System (LCCX)	86
4.2	Schematic Diagram of Coaxial Cable Cross-Section	88
4.3	Coordinates and Radiation Pattern of a Short Wire Antenna	92
4.4	Coordinate System Used for Determining the Radiation from a Loop Antenna	94

FIGURE

Page

4.5 Radiation Pattern of a Loop Antenna

95

4.6 Geometry of the Experimental Line

98

LIST OF PRINCIPAL SYMBOLS AND ABBREVIATIONS

- ϵ_r - Relative dielectric constant of the dielectric medium
 $\tan\delta$ - Loss tangent of the dielectric material
 LCX - Leaky Coaxial Cable
 GL - Goubau Line
 MGL - Modified Goubau Line
 ω - Angular frequency in radians
 γ - Axial propagation constant in cm^{-1}
 α - Attenuation constant (real part of γ)
 β - Phase constant (imaginary part of γ)
 λ_g - Guide wavelength
 ϵ_d - Decay coefficient
 Radiax - Type name of Andrew Antenna Company LCX
 N - Number of turns of coil
 A - Area of the coil
 R_1 - Radius of inner conductor of a coaxial cable
 R_2 - Inner radius of outer conductor of coaxial cable
 R_3 - Outer radius of outer conductor of coaxial cable
 \vec{J}_1, \vec{J}_2 - Current densities in the inner and outer conductors
 μ - Permeability of the medium
 L_1, L_2, L_3 - Self inductances in the three regions of a coaxial cable
 L - Total self inductance of a coaxial cable
 l_1, l_2, l_3, l_4 - Lengths of arms 1, 2, 3, and 4 of coil
 d_2 - Distance between arm 2 and inner conductor
 d_4 - Inside distance between arm 4 and outer conductor
 d'_4 - Outside distance between arm 4 and outer conductor

- (R, θ , z) - Cylindrical coordinate system
- V - Voltage induced in a coil
- ϕ - Magnetic flux linkage
- I - Current flowing in the coaxial line
- \vec{B} - Magnetic Induction
- λ - Wavelength

RESEARCH OBJECTIVES *

- (a) Review of existing literature on *leaky cable* communication systems presently used in tunnels, mines, highways, railways, buildings and rural areas with low density populations.
- (b) Identification and evaluation of the basic parameters of a leaky coaxial cable so that the radiation and transmission characteristics would be optimized for design purposes for both the broad band and narrow band applications. *The frequency range of interest is 10 KHz to 500 MHz and low loss is an obvious requirement in rural communications.*
- (c) Experimental verification of basic properties of a *conventional* leaky coaxial cable and a *proposed novel cable*, including methods for two-way signal coupling, transmission loss, coupling loss, *differential phase*, VSWR vs frequency, measurement of field components, radiation pattern and gain for experimental models. The investigation will also include plans for a physical layout of an LCX cable in rural Manitoba and optimization of its path for maximum continuous access. *Desirable attributes of the cables and detrimental features (crosstalk, interference, line loss etc.) will be discussed in the final report in the context of rural communications.*
- (d) Formulation of recommendations for future research on selected topics in the same general area.

*As reproduced from original contract proposal.

INTRODUCTION

For many years the need for a reliable communication system within and around special environments like mines, tunnels, subways, etc. has been recognized, particularly for such reasons as safety, more efficient production and maintenance as well as convenience of personnel. A similar need has also been recognized for communications in special environments above ground such as buildings, railways, highways, etc. In all these applications the design of a continuous access communication system is unconventional and complex due to the problems associated with radio wave propagation within each environment or with the outside. Similar problems also arise in the case of rural communications, particularly in large countries like Canada where small communities are often far removed from large cities and hence deprived of modern communication facilities.

Attempts were therefore initiated to solve the communication problem in general using a driven loop and an earth or metallic return [1.1]. In 1956 Monk and Winbigler used an open pair transmission line laid in a rail tunnel and driven from a VHF transmitter and achieved two-way communication over a distance of 1Km [1.2]. Based on the pioneering work of Monk and Winbigler, Martin [1.3-1.6] carried out experimental investigations which led to the conclusion that the loosely braided coaxial cable, or "leaky feeder" as it is now called, was the

best choice for the transmission line. Liegeois and Leclercq in Belgium developed non-driven twin feeders to improve the coupling between mobile stations in the mine galleries. Consequently, the concept of a leaky transmission line received more attention and subsequent development led to different systems for different applications.

1.1. Common Types of Leaky Transmission Lines:

The six most common types of leaky coaxial cables (LCX) which emerged in recent years are shown schematically in Fig. 1.1. The Loose-braid system was developed by Martin for mine communications [1.1]. The Radiax type consists of periodically-spaced slots in the outer conductor of a coaxial cable and is manufactured in North America by Andrew Corporation [1.7-1.8]. The continuous longitudinal slot in the outer conductor design was developed by Siemens [1.9] and Kabelmetal Cables [1.10] in West Germany. Inix-Delogne system was developed in Belgium and consists of a pair of radiating devices connected at approximate intervals along a normal coaxial cable [1.11-1.15]. The zig-zag slot design on the outer conductor was suggested by the Japanese National Railways for radio communication with trains, and is designed as a radiating-receiving structure [1.16-1.20]. The CERT system consists of a continuous slot in the outer conductor with a helically wound continuous radiating element surrounding the inner dielectric of the cable [1.21].

Theoretical analysis and experimental implementation of some of these cable systems have been presented by Wait *et al*

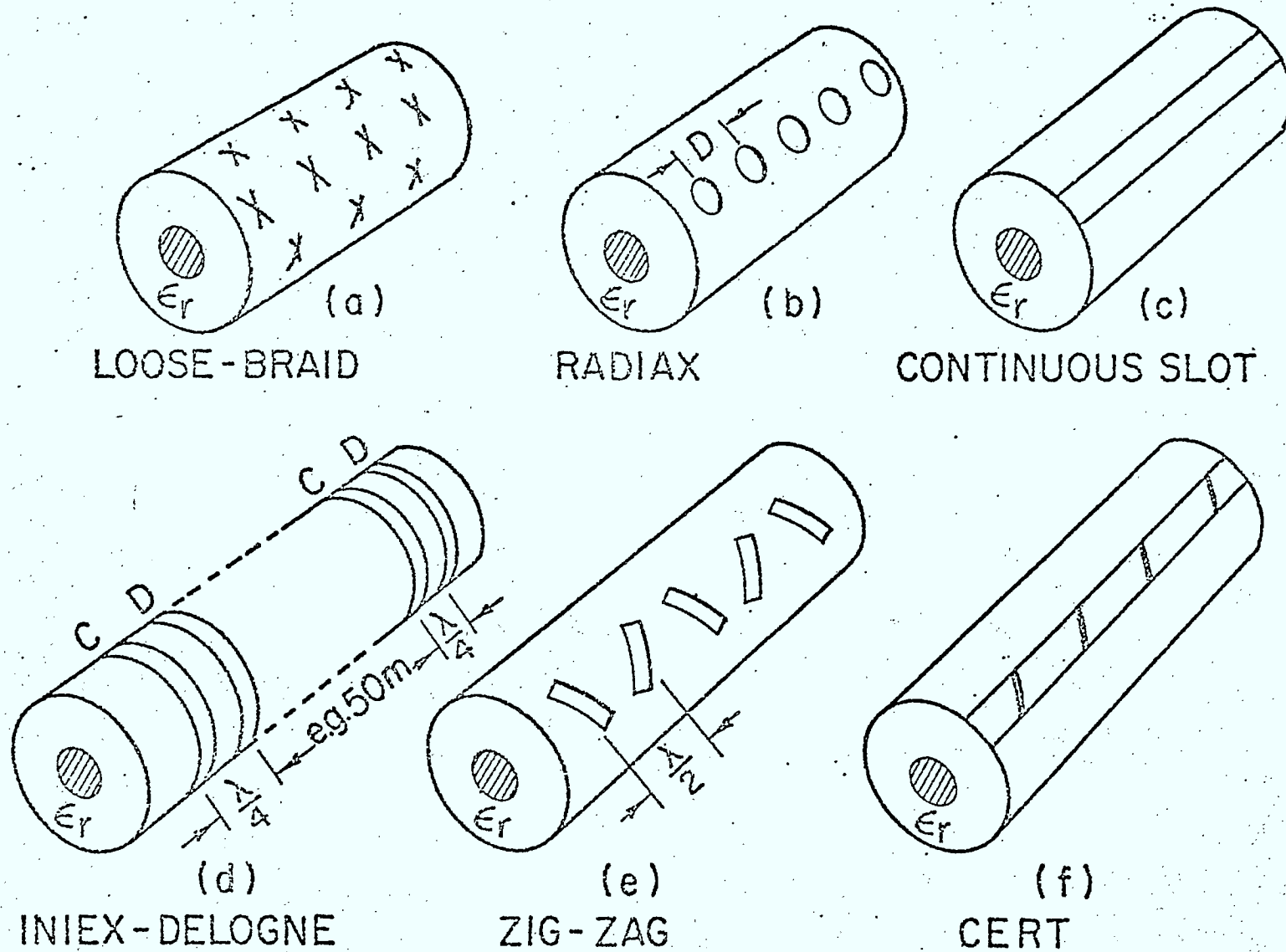


Fig. 1.1 Types of "Leaky Cables"

[1.22-1.39] and Brennan [1.40]. In particular, a common two-way communication system for tunnels includes a transmitter/receiver connected to a duplexer which is in turn connected to a splitter in series with the leaky cable [1.41].

1.2. Frequency Considerations:

For any given frequency, a leaky coaxial cable has transmission loss, coupling loss (to a halfwave dipole at 20 ft distance away from cable), return loss, power handling capacity, radiation pattern depending on its geometrical and electrical parameters, and the details of its construction. As the frequency increases, it is expected that the transmission loss will increase, while the coupling loss may or may not increase. This is because the mechanism of radiation in a leaky coaxial cable is based on the radiation by an array of slots where any individual slot is not excited by a voltage source as a resonant antenna. The radiation mechanism by a slot, well below half wave resonance, is similar to that of an aperture whose edges represent charge singularities due to interruption of current in the outer conductor. It is well known that a charge accumulation at a conducting edge radiates an electric field oriented parallel to the edge, and in a plane perpendicular to the edge. However, the mechanism of interaction between parallel edges of a slot is the same as in the case of a resonant slot. Also, the mechanism of interaction between adjacent slots on the curved outer conductor of a leaky coaxial cable is similar to that of resonant slots on a conducting plane. Therefore, until the

analytical studies are completed for the leaky feeder structures, there is no basis for optimal design or selection of one type over the other except on the basis of experience and experimentation. For instance, the salient features of the zig-zag design are to control the radiation angle, to suppress space harmonic waves and to cancel over one period the longitudinal component of the electric field, while maintaining the same orientation of the circumferential component. However, knowledge of the interaction between edges of the same slot and adjacent slots could possibly lead to a better design in the future. Until the formidable mathematical problems are solved, there is no hope of an analytical procedure to determine the optimum frequency for leaky coaxial lines. This opinion is also shared by Chick [1.1].

For the specific application to rural communications it would be most advantageous to operate at very low frequencies where the transmission losses are the lowest, thus permitting long lengths of coaxial cable at practically no loss. In addition, such very low frequencies would, in principle, help to achieve larger coupling distances which is of particular interest to sparsely populated remote areas of Canada. However, it must be borne in mind that the usual disadvantages at the lower frequencies like extraneous interferences from the surroundings, larger skin depth, etc., would impose severe restrictions on the cable size and operating frequency. Such difficulties are not easy to overcome with any of the six existing types of LCX cables. For this reason a novel technique, in which magnetic, rather than electric, coupling techniques are employed, is

proposed later, and may be more suitable for overcoming these problems once fully understood and developed. Details of this magnetic coupling and the preliminary measurements carried out on an experimental line constructed for this purpose are described in Chapter 4.

Since the problems regarding the operating frequency and optimum cable size are not completely resolved, it would be too early to consider applications involving wide or narrow bandwidths or the optimum choice of modulation. However, it may be mentioned that in general for narrow-band applications, the usual modulation is either of the amplitude or angle type.

Chapter 2 deals with the commercial leaky coaxial cables and their basic parameters like transmission and coupling loss. Chapter 3 deals with *the proposed novel cable*, called the modified Goubau line, and the measurements carried out on the line. Chapter 4 deals with an alternative and new technique called the Leaky coil coupled coaxial (LCCX) system which seems to have advantages at low frequencies. Chapter 5 presents a brief general discussion, while Chapter 6 deals with the important qualitative conclusions and suggestions for further work.

1.3 References:

- [1.1] Proceedings of the colloquium on Leaky Feeder Radio Communication Systems, University of Surrey, Electronic and Electrical Engineering Department, 8-10 April, 1974.
- [1.2] N. Monk and H. S. Winbigler, "Communication with Moving Trains in Tunnels", IRE Trans. on Vehicular Communications, PGVC-7, pp. 21-28, Dec. 1956.
- [1.3] D. J. R. Martin, "Radiocommunication in Mines and Tunnels", Electronics Letters, Vol. 6, No. 18, 3 Sept., 1970.
- [1.4] D. J. R. Martin, "Transferred Surface currents in Braided Coaxial Cables", Electronics Letters, Vol. 8, No. 18, 7 Sept., 1972.
- [1.5] D. J. R. Martin, "A General Study of the Leaky-Feeder Principle", The Radio and Electronic Engineer, Vol. 45, No. 5, pp. 205-214, May, 1975.
- [1.6] D. J. R. Martin, "The Bicoaxial Leaky Line and its Applications to Underground Radio Communication", Radio Science, Vol. 11, No. 10, pp. 779-785, October, 1976.
- [1.7] E. H. Johnson, "Foam Heliac - A New Foam Coaxial Cable", IRE Transactions on Vehicular Communications, Vol. VC-11, No. 1, August, 1962.
- [1.8] Andrew Antenna Corporation, "A Slotted Cable for Short Range Communications", Telecommunications Vol. 7, No. 10, pp. 44-45, 1972.
- [1.9] M. Hahns and H. Haselhorst, "Radiating RF cables for underground Transport Radio Communication Systems", Siemens Review, Vol. 9, pp. 345-347, 1969.

- [1.10] Kabelmetal Report entitled, "Radio Frequency Line for Remote Control Systems", Kabelmetal, 8500 Nurnberg 2, West Germany.
- [1.11] P. Delogne and R. Liegeois, "Radio Transmission Systems Recommended by Iniex", proceedings of International Electrical, Electronics conference and Exposition, Sept. 29--Oct. 1, 1975, Toronto, Canada.
- [1.12] P. Delogne and R. Liegeois, "Le Rayonnement D'une Interruption Du Conducteur Exterieur D'une Cable Coaxial", Annales Des Telecommunications, Vol. 26, No. 3-4, pp. 85-100, March-April, 1971.
- [1.13] P. Delogne, "Basic Mechanisms of Tunnel Propagation", Radio Science, Vol. 11, No. 4, pp 295-303, April, 1976.
- [1.14] P. Delogne, "Les Liaisons Radio-Electriques Par Cable Coaxial Dans La Mine", Extrait Des Annales Des Mines De Belgique, pp. 967-975, 1970.
- [1.15] P. Delogne, "Les Systemes INIEX de Communication Par Radio" Extrait Des Annales Des Mines De Belgique, pp. 951-962, 1974.
- [1.16] Sumitomo Electric Industries, Ltd., "Zig-zag Slot Leaky Coaxial Cable for Vehicular Communication System" Industrial Report, Tokyo, 1971.
- [1.17] T. Yoshiyasu *et al*, "Leaky Coaxial Cable for Train Communication", Hitachi Review, Vol. 20, No. 5, pp. 204-211, (undated).
- [1.18] T. Kishimoto *et al*, "Wide Band Leaky Coaxial Cable for a 800 MHz Band", 8 pages, Private Communication.
- [1.19] T. Sako *et al*, "Large size Coaxial Cable for 400 and 800 MHz Frequency Band", (undated private communication).
- [1.20] K. Mikoshiba and Y. Nurita, "Guided Radiation by Coaxial Cable for Train Wireless Systems in Tunnels", IEEE Trans. on Vehicular Technology, Vol. VT-18; pp. 66-69, Aug. 1969.

- [1.21] Antenna Transmission Line, Technical Memo No. 49, Times Wire and Cable Company, 358 Hall Avenue, Wallingford, Connecticut 06492, U.S.A., 1973.
- [1.22] D. A. Hill and J. R. Wait, "Analysis of Electromagnetic Scattering from Wire-Mesh Structures", Electronics Letters, Vol. 12, No. 17, p. 427, 19 August, 1976.
- [1.23] J. R. Wait and D. A. Hill, "Low Frequency Radio Transmission in a Circular Tunnel Containing a Wire Conductor Near the Wall", Electronics Letters, 1 June, 1976.
- [1.24] J. R. Wait, "On the Impedance of Long Wire Suspended over the Ground", Proc. IRE, Vol. 49, No. 10, Oct., 1961.
- [1.25] J. R. Wait, "Effective Impedance of a Wire Grid Parallel to the Earth's Surface", IRE Trans on Antennas and Propagation, Vol. AP-10, No. 5, pp. 538-542, Sept., 1962.
- [1.26] J. R. Wait, "Note on the Theory of Transmission of Electromagnetic Waves in a Coal Seam", Radio Science, Vol. 11, No. 4, pp. 263-265, April, 1976.
- [1.27] D. A. Hill and J. R. Wait, "Gap Excitation of an Axial Conductor in a circular Tunnel", Journal of Applied Physics, Vol. 45, No. 11, pp. 4774-4777, Nov., 1974.
- [1.28] J. R. Wait and D. A. Hill, "On the Electromagnetic Field of a Dielectric Coated Coaxial Cable with an Interrupted Shield", IEEE Trans. on Antennas and Propagation, Vol. AP-23, No. 4, pp. 470-479, July, 1975.
- [1.29] J. R. Wait, "Comments on the Horizontal Wire Antenna over a Conducting or Dielectric Half Space: Current and Admittance", Radio Science, Vol 9, No. 12, p. 1165, Dec., 1974.

- [1.30] J. R. Wait and D. A. Hill, "Theory of the Transmission of Electromagnetic Waves Down a Mine Hoist", Radio Science, Vol. 10, No. 6, pp. 625-632, June, 1975.
- [1.31] C. H. Stoyer and J. R. Wait, "Analysis of Source Location Errors for a Magnetic Dipole Buried in a Laterally Inhomogeneous Conducting Earth", Pure and Applied Geophysics, Vol. 114, 1976.
- [1.32] J. A. Fuller and J. R. Wait, "A Pulsed Dipole in the Earth", Topics in Applied Physics, Springer-Verlag, Vol. 10, Chapter 5 (L.B. Felsen Editor), pp. 237-269, 1976.
- [1.33] J. R. Wait and D. A. Hill, "Propagation Along a Braided Coaxial Cable in circular Tunnel", IEEE Trans. on Microwave Theory and Techniques, Vol. MTT-23, No. 5, pp. 401-405, May, 1975.
- [1.34] J. R. Wait, "Theory of Wave Propagation Along a Thin Wire Parallel to an Interface", Radio Science, Vol. 7, No. 6, pp. 675-679, June, 1972.
- [1.35] D. A. Hill and J. R. Wait, "Scattering from a Break in the Shield of a Braided Coaxial Cable-Numerical Results", AEU, Vol 30, pp. 117-121, 1976.
- [1.36] J.R. Wait, L. Thrane and R. J. King, "The Transient Electric Field Response of an Array of Parallel Wires on the Earth's Surface", IEEE Trans. on Antennas and Propagation, Vol. AP-23, No. 2, pp. 261-264, March, 1975.
- [1.37] J. R. Wait and D. C. Chang, "Theory of Electromagnetic Scattering from a Layered Medium with a Laterally Varying Substrate", Radio Science, Vol 11, No. 3, pp. 221-229, March, 1976.

- [1.38] J. R. Wait, "Some Basic Electromagnetic Aspects of ULF Field Variations in the Atmosphere", Pure and Applied Geophysics, Vol. 114, pp. 15-28, 1976.
- [1.39] D. A. Hill and J. R. Wait, "Propagation Along a Braided Coaxial Cable Located Close to a Tunnel Wall", IEEE Trans. on Microwave Theory and Techniques, pp. 476-480, July, 1976.
- [1.40] G. R. Brennan, "Slotted Coax Solves Tunnel Radio Problem," Communications News, June, 1975.
- [1.41] Cablewave Systems, Inc., "Tenna/Flex Radiating Transmission Line", Technical Bulletin No. 26, August, 1975.

STUDIES ON COMMERCIAL LCX CABLES

2.1. Introduction:

Having reviewed the existing literature, and surveyed the basic features, applications, methods of coupling, etc., of leaky coaxial cables in general, one must recognize at the same time that no single LCX cable has been designed to suit all desirable applications in the field of communications. Different manufacturers have, as a result, undertaken the task of constructing LCX cables for specific applications, using their own modified designs. These designs include the continuous slot design, zig-zag slot design, loose braided coax and Radiax cables. In particular, the authors of papers presented at the 1976 International IEEE/AP-S and USNC/URSI meeting, University of Massachusetts, Amherest, October 11-15, 1976, session on "Telecommunications via Leaky Cables" were contacted. As a result, useful literature was received on the current state of the art.

Various attempts were subsequently initiated to acquire samples of commercially available leaky coaxial cables for the experimental program. Thus, three sets of Radiax cables (RX4-1, RX4-3A and RX5-1) from Andrew Antenna Company, Whitby, Ontario, were procured, along with the necessary accessories (connectors types 44AN, 44AW, 45AN and 45AW and 50 ohm terminations type 32299-5). Contacts were also made with

Hitachi Cable Company (New York), Sumitomo Electrical Industries (Japan), Fujikura Cables (Japan), Cablewave Systems (U.S.) and Belden Corp. (U.S.). Although every manufacturer contacted supplied literature and technical data sheets, some could not supply short cable samples, or were out of stock. Hitachi Cable Company offered free of charge 165 ft. of their LCX cable type HW-46 and a purchase order was subsequently placed to pay for transportation and one 50 ohm termination and two N-connectors (type N-J-42) to be installed in their factory in Japan at each end of the cable prior to shipping. Sumitomo supplied through the Canadian Embassy in Tokyo three (3) meters of their LCX cable type 72D, but could not supply the necessary connectors. Fujikura also supplied a 6 inch sample of their LCX cable type 43D, which was obviously for display and not testing. Hence our experimental program was restricted to the Radiax design of Andrew and the zig-zag slot design of Hitachi.

2.2. Basic Parameters of LCX Cable:

LCX cables are usually designed to function as continuous antennas as well as transmission lines. The slots in the outer conductor allow a certain portion of the transmitted RF power to be radiated along the entire length of the cable. The losses in such a system are grouped under two categories, *namely* the transmission loss (cable attenuation) and coupling loss (associated with the radiation aspect). In addition, there may be signal distortion due to group delay or differential phase, which depends on the operating frequency and bandwidth. As an

example, in a typical mobile LCX communication system inside a coal mine the sum of the two loss components equals 134 dB which corresponds to a transmitted power of 0.5 watts and a receiver sensitivity of $1\mu\text{V}$ into 50Ω for a usable received signal.

2.2.1. Transmission Loss:

The basic factors which influence the transmission loss are the intrinsic parameters of the line and the carrier frequency. The loss is independent of orientation, position and environmental conditions. For conventional transmission lines this loss is predictable from well known expressions. It is obvious that one can modify the incremental equivalent circuit for a conventional transmission line to include an element which accounts for the radiation. Such an element is by definition proportional to the radiation resistance of an equivalent single slot provided that the equivalent circuit is for an incremental length which includes one slot only, and that all the slots are identical in every respect.

2.2.2. Coupling Loss:

The coupling loss is a property of the transmission line as well as its environment [2.1]. It is usually defined as the average difference between signal level in the cable and the signal received by a 0 dB gain antenna (i.e. equivalent isotropic radiator). The usual convention is to use a $\lambda/2$ dipole at a distance of 20 ft from the test cable. The data

usually supplied by manufacturers gives a tolerance of $\pm 10\text{dB}$.

The above definition of the coupling loss becomes somewhat unrealistic in low frequency applications. This is due to the difficulties encountered in making half wavelength resonant dipoles at such low frequencies. Also the rigidity of the 20 ft physical separation distance and the $\lambda/2$ dipole receiver are unrealistic, and have little significance at low frequencies, particularly in connection with rural communications. A more realistic definition would probably be over a fixed distance to wavelength ratio, i.e. fixed electrical distance.

2.2.3. Group Delay:

An important characteristic of any transmission device is the ability to transmit a signal over a wide frequency band with minimum distortion. Distortion results when the phase shift through the device is a nonlinear function of frequency. A convenient indication of nonlinear phase shift is the group delay which is defined as:

$$t_D = \frac{d\phi}{d\omega} \text{ seconds}$$

and is proportional to the slope of the phase vs frequency characteristic.

2.2.4 Return Loss vs Frequency:

As the operating frequency is varied, the input reflection coefficient changes and a convenient measure of this change is the return loss or alternatively the VSWR. It is to be expected that the VSWR will be minimum near the design resonant frequency and increases on either side.

2.2.5 Two-way Signal Coupling:

For communication applications (either stationary or mobile) it is necessary to be able to transmit a signal from the cable to a receiving antenna and *vice versa* with high fidelity. In some applications (e.g. railway communications) the receiving antenna is a short section of LCX cable identical to the main line and mounted on either the top or the sides. In other applications (e.g. mines) inductive loop coupling to the transmitter and receiver is preferable, particularly at HF frequencies.

2.2.6 Radiation Pattern and Gain:

The radiation from leaky coaxial cables can be viewed as a linear slot array with tapered illumination in both the amplitude and phase at each slot. Since each slot cuts the wall current flowing in the outer conductor, the orientation and size of each slot and the separation between adjacent slots determine the radiation intensity, radiation angle and field components. In the case of zig-zag slots the period is approximately one wavelength at the transmission frequency and the axial field components (E_z) of two adjacent slots cancel, while the circumferential components (E_θ) are in the same direction. In other words, the longitudinal E_z components are suppressed, while the perpendicular E_θ components contribute to the radiated field. The resulting radiation pattern and gain for the zig-zag slot design have been reported by Sako et al [2.2] on the basis of theory and experiment.

2.3 Measurement Methods:

The purpose of measuring the preceding parameters for the experimental LCX cables is two-fold. First, to verify the data supplied by the manufacturer which, if successful, could give confidence if the same measurement method is used outside the design frequency band specified by the manufacturer. Second, to evaluate these parameters in the frequency range specified in the contract proposal (10 KHz to 500 MHz). As a result, different measurement methods and equipment were used in different frequency ranges. It is well known that no single measurement method is applicable for the entire frequency range of interest. For instance, microwave laboratory type of equipment was used to test over microwave frequencies while mobile field intensity measuring equipment was employed in the 150 KHz to 3 MHz range. At still lower frequencies above 10 KHz Spectrum Analyzer equipment was employed. The Field Intensity meter was borrowed from the Dept. of Communications in Winnipeg and consisted of a Singer R.I.F.I. (Radio Interference Field Intensity) Meter model NM-25T, along with a loop probe (15.5" diameter and antenna factors submitted separately) and a Radio Frequency Interference calculator, Stoddart part no. 21518. The Spectrum Analyzer was also borrowed from the Dept. of Communications in Winnipeg, and consisted of an HP 8553 B Spectrum Analyzer RF section (0-11, 0-110 MHz), HP 8552 B Spectrum Analyzer IF section, HP 8443 A tracking generator and counter, and an HP 141 T Display section.

2.3.1. Measurement of Transmission Loss:

The experimental set up used is shown schematically in Fig. 2.1. It consists of a sweep oscillator (HP 8690 A) connected to a directional coupler (Narda 3001-20) and an oscilloscope (HP 180 T) and swept amplitude analyzer (HP 8755). The output from the oscilloscope is fed to an X-Y recorder (HP 7035 A).

Two experimental methods, which should yield equivalent results, were employed. In the first method, which is a reflection type measurement, the coupled arm of the directional coupler is fed to the test cable, which is terminated by a short circuit. As a result of the reflection from the load end, a standing wave is set up along the cable. The reflection coefficient is thus measured and this, in turn, is related to the attenuation constant. However, when the experiment is performed indoors, this method may give rise to some errors if there are reflections from the surrounding objects.

Alternatively, the signal is picked up from the load end by connecting a detector in place of the short circuit. In this method, which is referred to as the substitution method, the output of the directional coupler is first directly connected to the oscilloscope and later connected through the test cable. The difference between the two readings obtained is the attenuation for the actual length of the test cable (20 ft for each of the Radiax cables and 165 ft for the Hitachi cable). Care is taken to see that there are no excessive interconnections

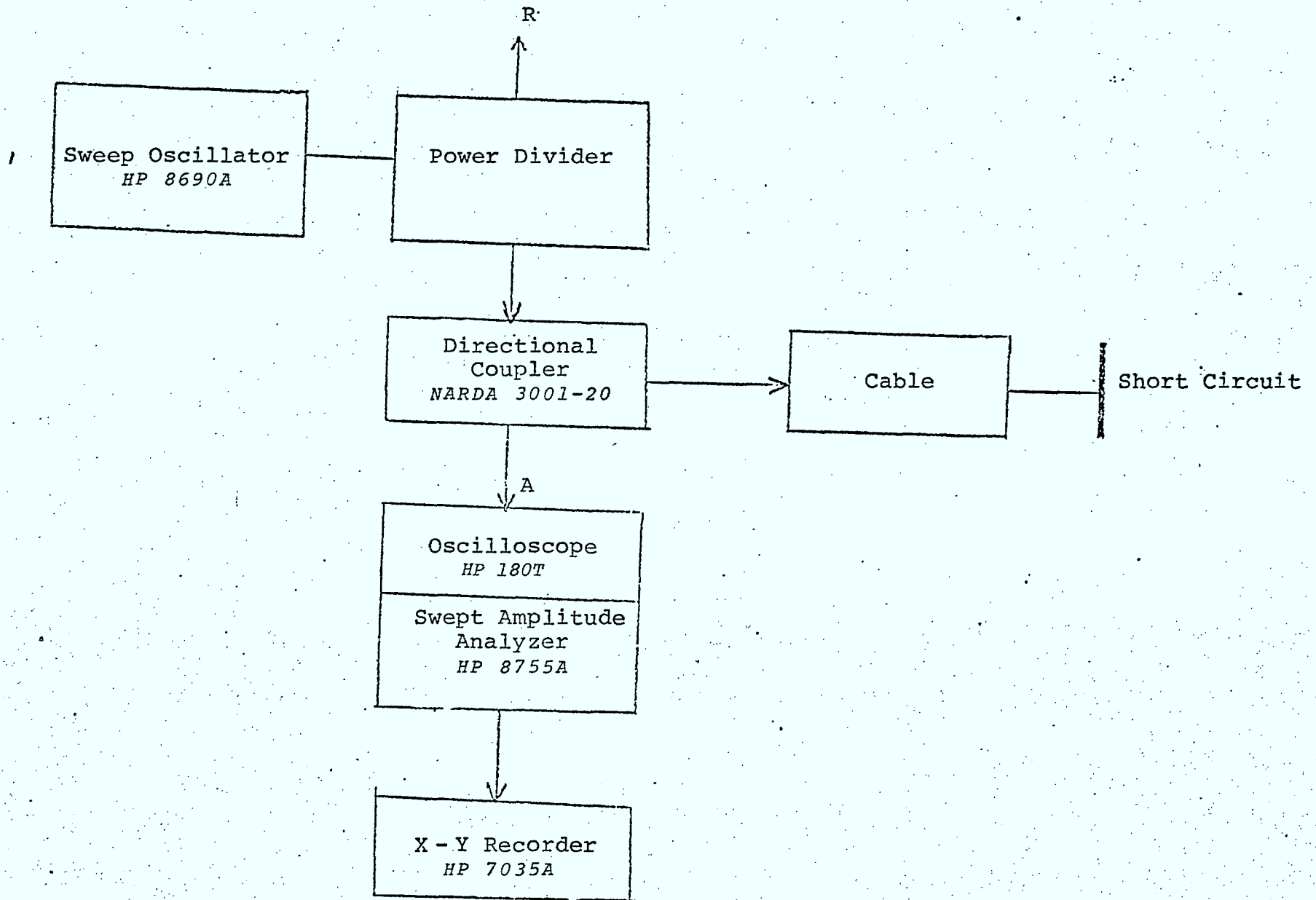


Fig. 2.1 Block Diagram Used for the Measurement of Attenuation

and transitions as they are likely to affect the measured values. The measurements were repeated on all the three sets of Radiax cable samples by the substitution method, and some typical results are presented in Figures 2.2 to 2.9 for different frequency ranges. In all the graphs the frequency is along the abscissa, and the upper curve is for the case when the cable is not included in the circuit, while the lower curve is when the cable is included. The value of attenuation at any given frequency is the difference between the two curves in dB. Examination of the curves shows that the variation of the attenuation with frequency is reasonably smooth in the 100 to 550 MHz range, but is not so smooth in the 450 to 900 MHz range. This is especially true for the RX4-3A cable which has a higher attenuation constant according to the Andrew catalogue [2.1]. For still higher frequency bands, the fluctuations are much more predominant, the reason being the deteriorating performance of the directional coupler. In the 10 to 100 MHz band the attenuation constant of all Radiax cables tested is negligible, and it is, in fact, difficult to distinguish between them. For the still lower bands of 1 to 10 MHz and 400 KHz to 1 MHz spot frequency attenuation measurements were carried out and are shown in Table 2.1.

With respect to the Hitachi HW-46 LCX, the transmission loss is measured using a vector voltmeter (HP type 8405 A). The experimental arrangement is shown schematically in Fig.2.10. Table 2.2 shows the comparison between this cable and ordinary

Table 2.1: Attenuation Constant vs Frequency
in dB/20 ft.

Reference: 0 dB (without Radiax cable)

Frequency (MHZ)	RADIAX TYPE	
	RX4-3A	RX5-1
0.4	0.01	0
0.5	0.01	0
0.6	0.02	0.01
0.7	0.02	0.01
0.8	0.02	0.01
0.9	0.04	0.02
1.0	0.05	0.02
2.0	0.09	0.04
3.0	0.11	0.06
4.0	0.12	0.06
5.0	0.13	0.08
6.0	0.17	0.10
7.0	0.12	0.10
8.0	0.28	0.20
9.0	0.28	0.18
10.0	0.38	0.25

VERTICAL SCALE 0.5 dB/div

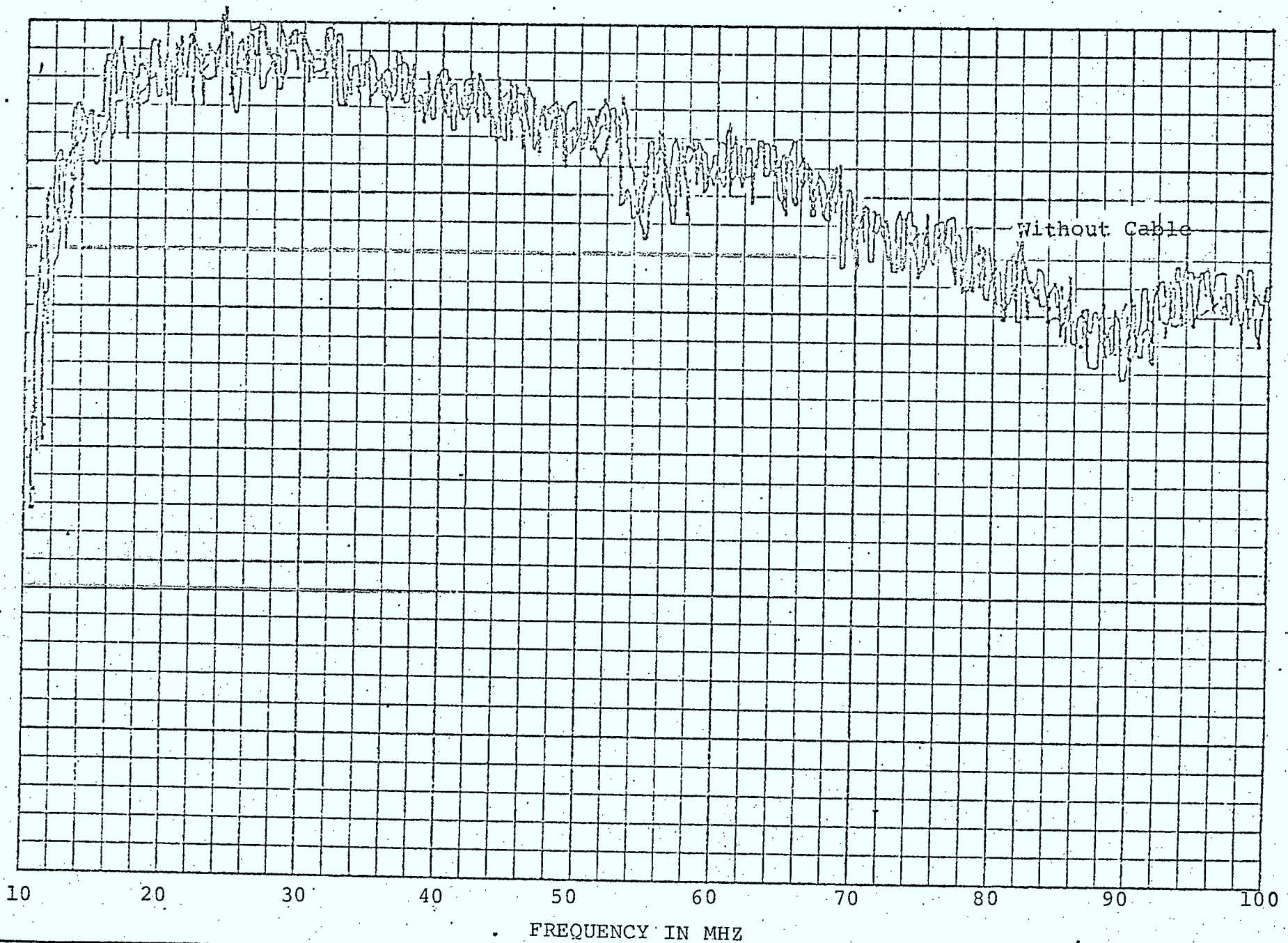


Fig. 2.2 Variation of Attenuation vs Frequency (10-100 MHz)

VERTICAL SCALE 0.5 dB/div.

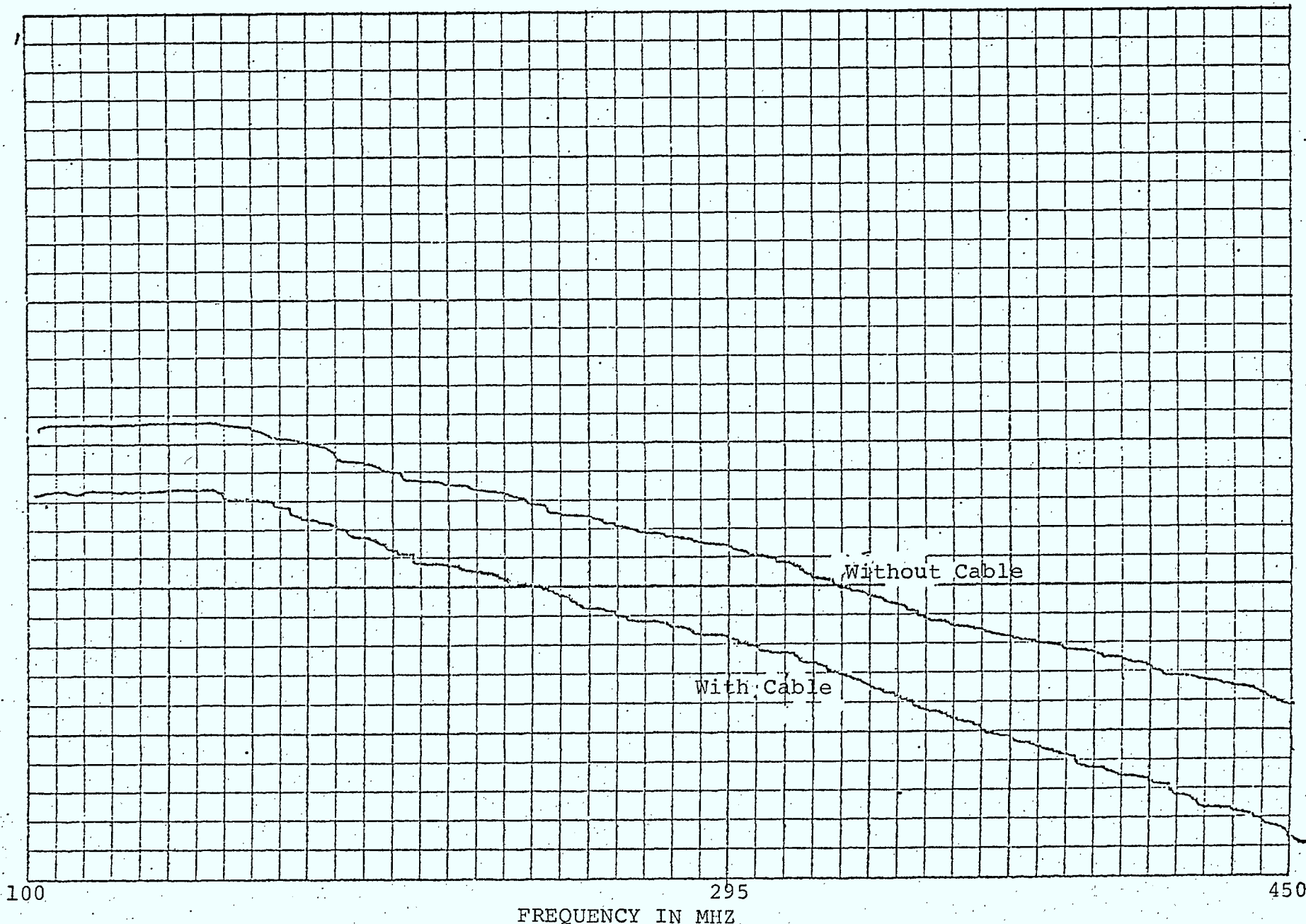


Fig. 2.3 Variation of Attenuation vs Frequency (100-450 MHz)

VERTICAL SCALE 0.5 dB/div

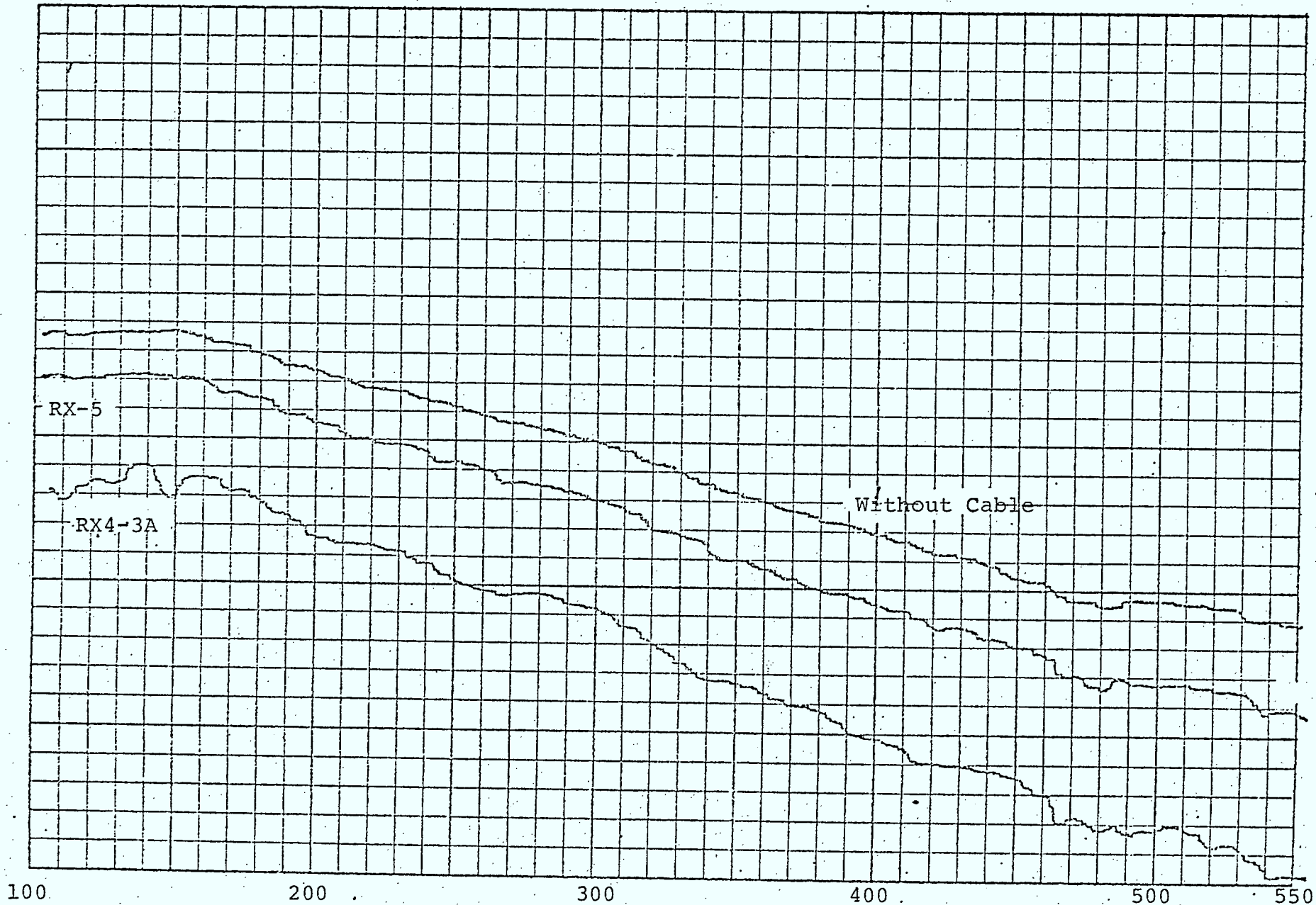
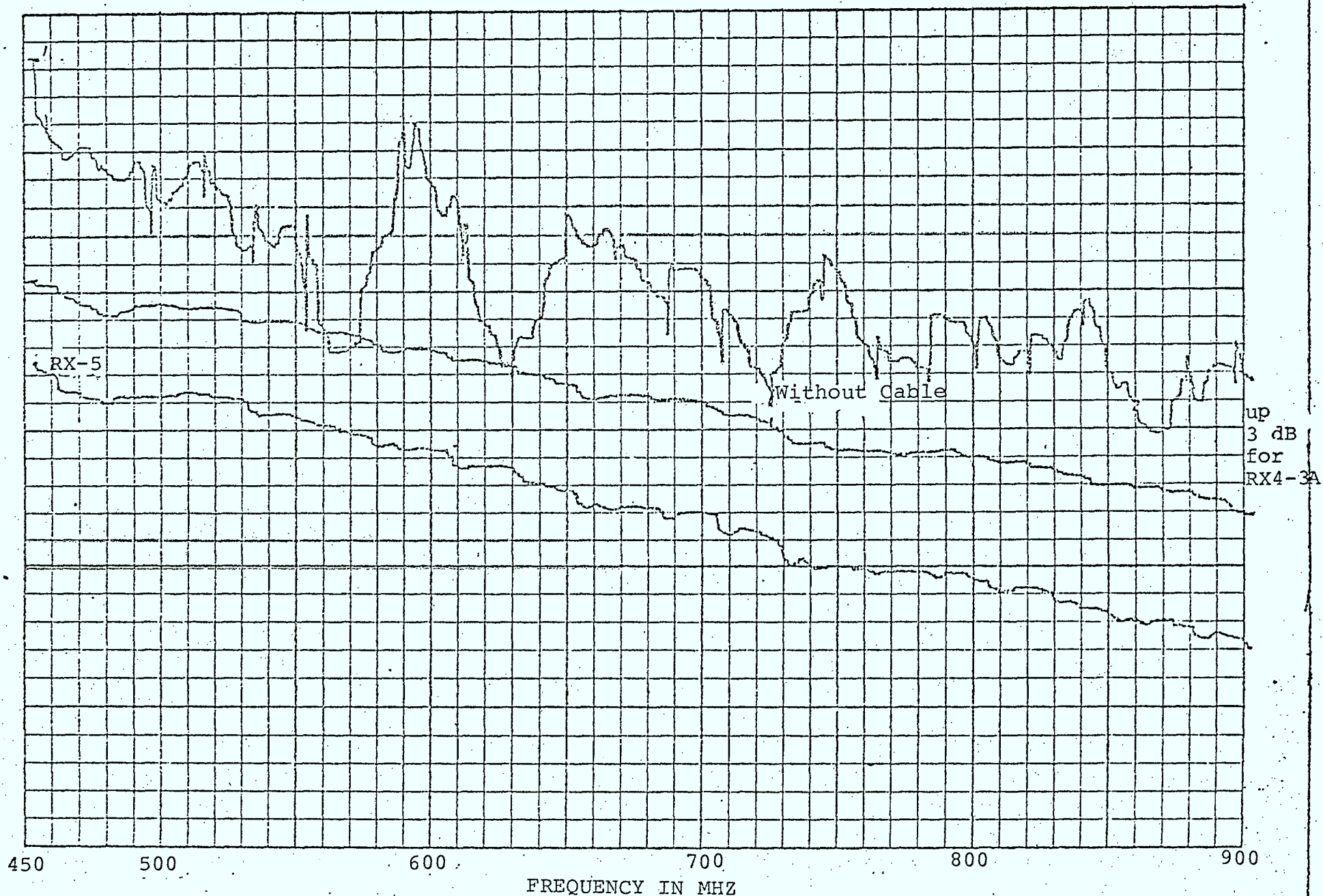


Fig. 2.4 FREQUENCY IN MHZ

Fig. 2.4 Variation of Attenuation vs Frequency RX4-3A, RX5-1 (100-500 MHZ)

VERTICAL SCALE 0.5 dB/div



25

Fig. 2.5 Variation of Attenuation vs Frequency RX-3A, RX5-1 (450-900 MHz)

VERTICAL SCALE 1 dB/div

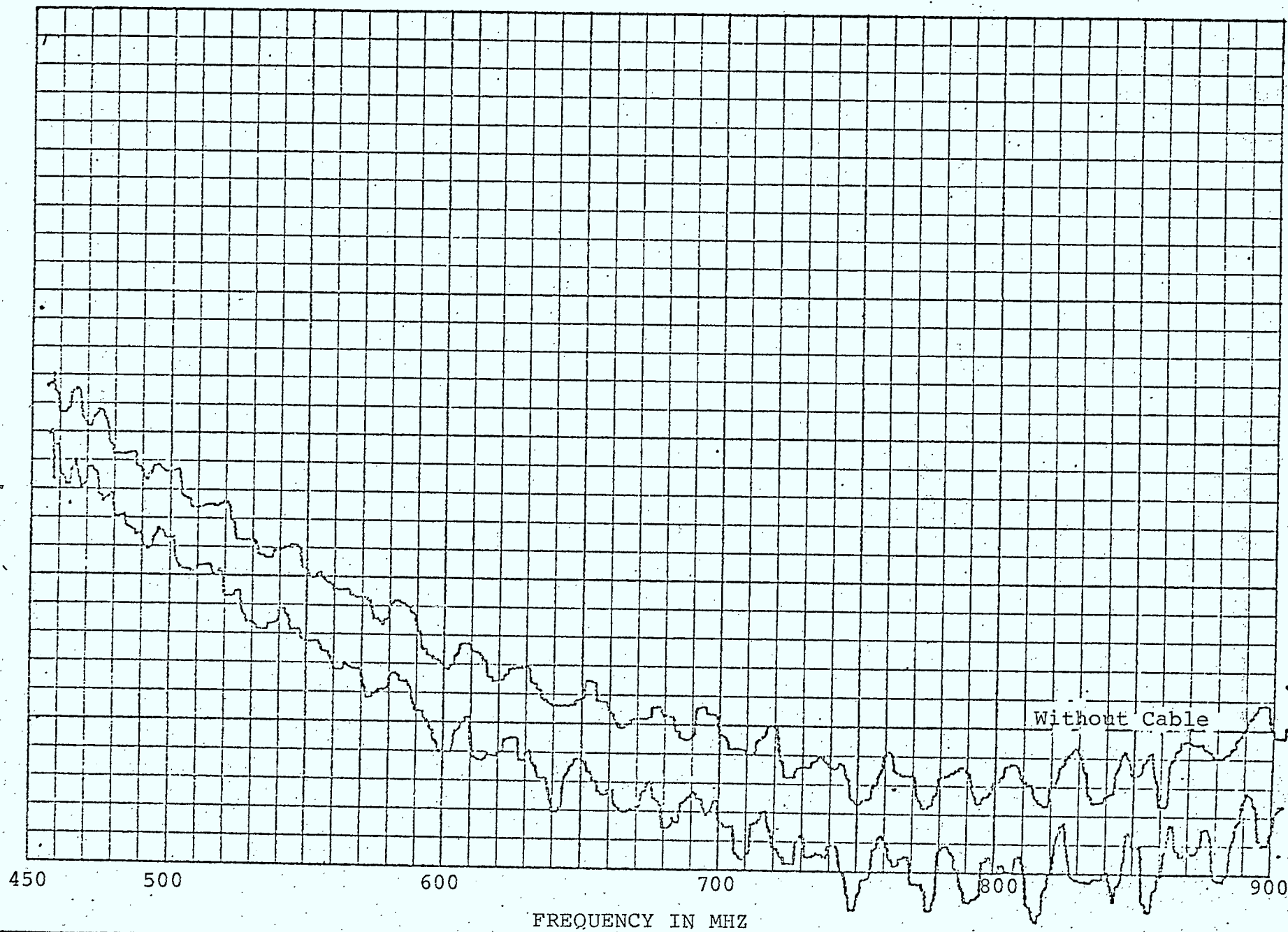


Fig. 2.6 Variation of Attenuation vs Frequency RX4-1 (450-900 MHz)

VERTICAL SCALE 0.5 dB/div

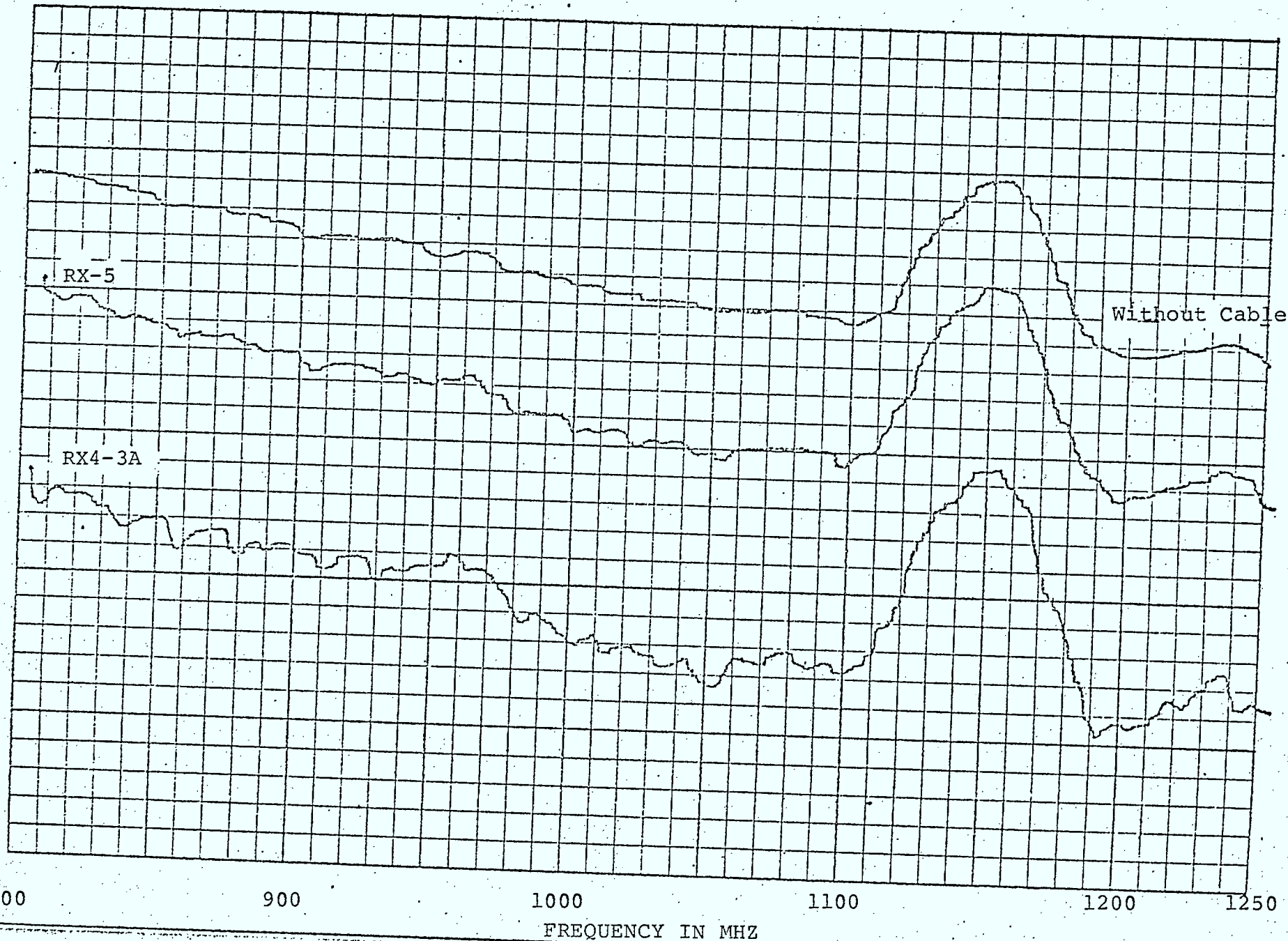


Fig. 2.7 Variation of Attenuation vs Frequency RX5, RX4-3A (800-1250-MHZ)

VERTICAL SCALE 1 dB/div

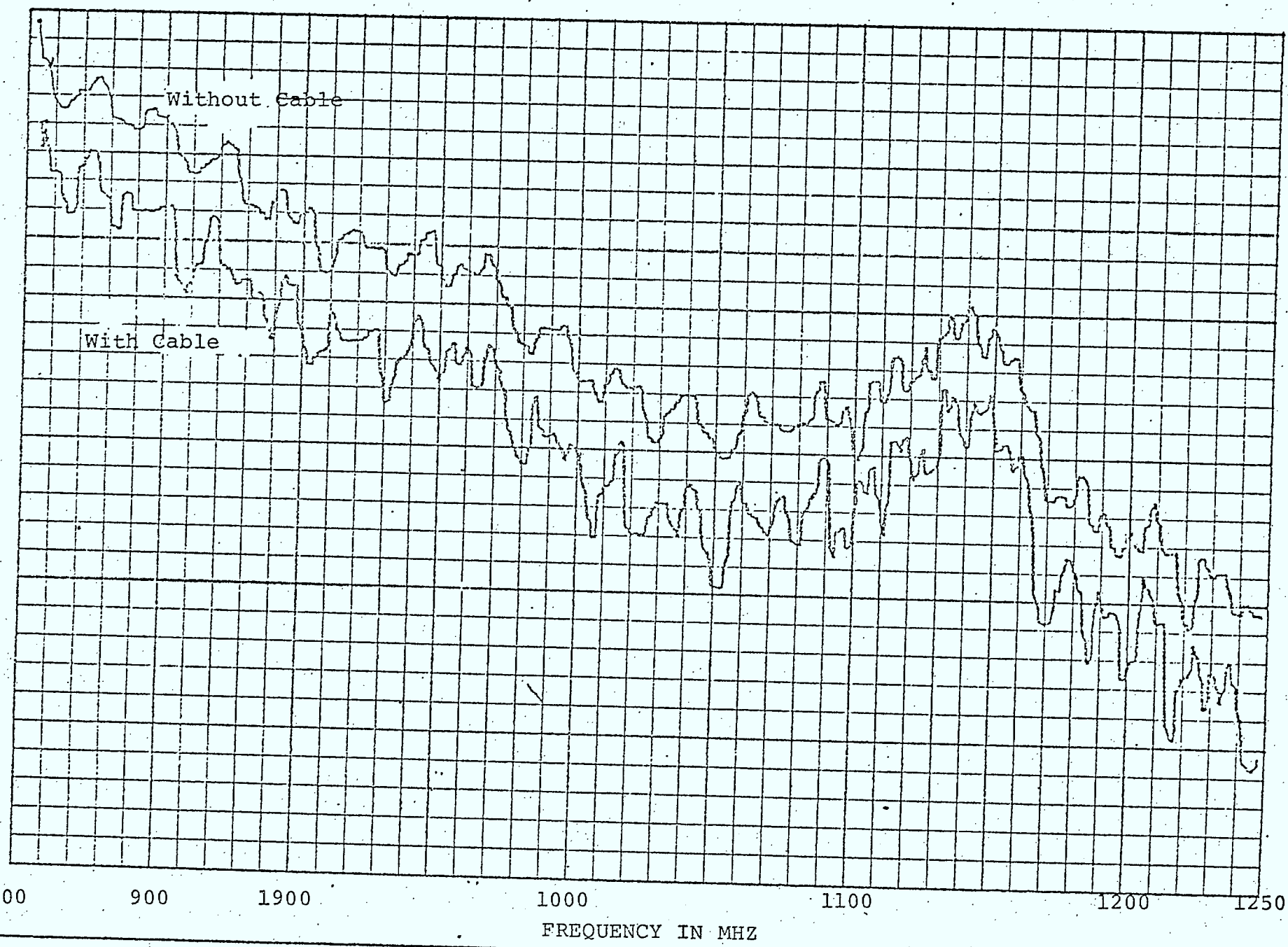


Fig. 2.8 Variation of Attenuation vs Frequency RX4-1 (800-1250 MHz)

VERTICAL SCALE 1 dB/div

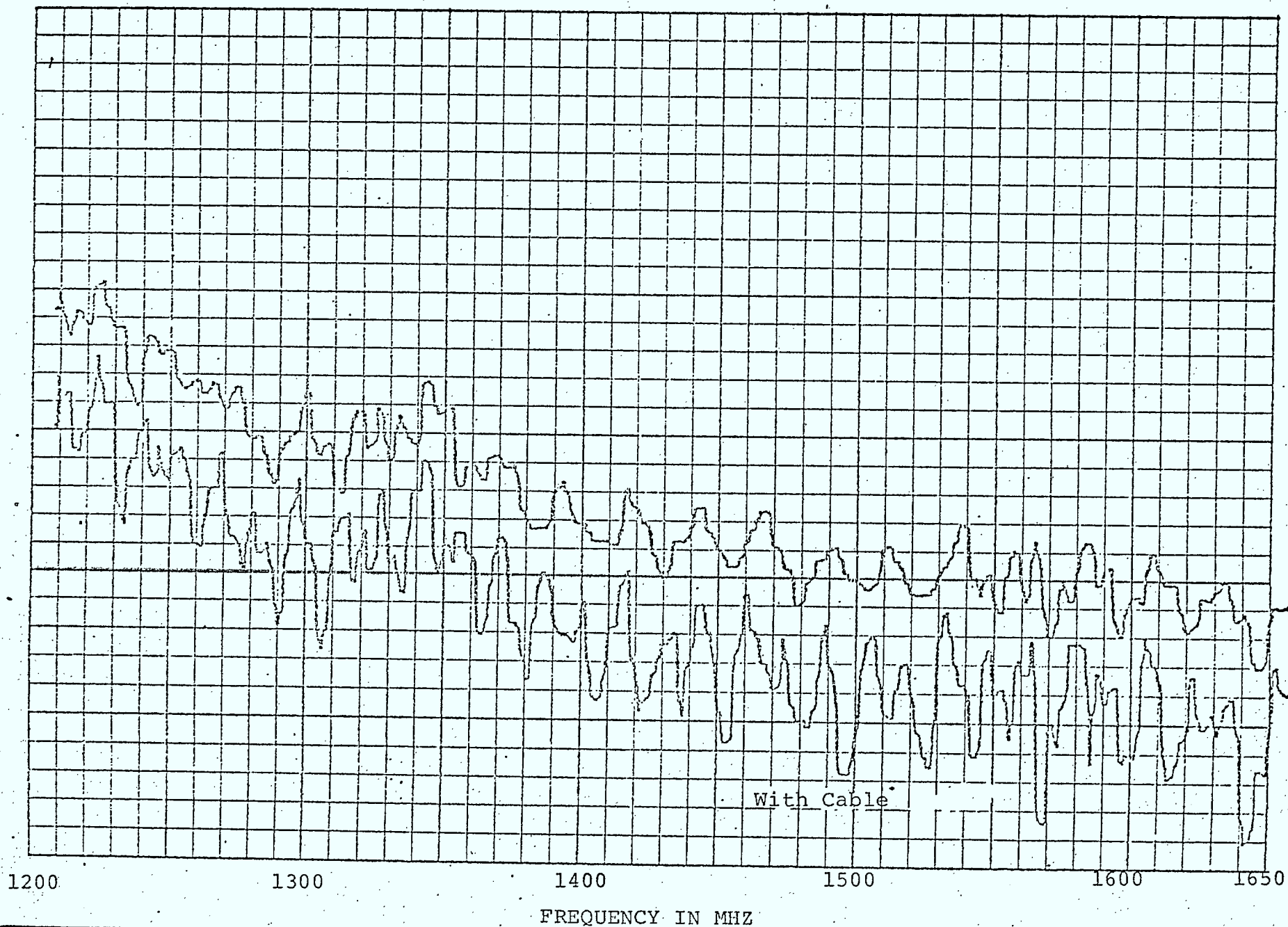


Fig. 2.9 Variation of Attenuation vs Frequency RX4-1 (1200-1650 MHz)

RG 212/U coaxial cable insofar as the transmission loss and phase shift are concerned. In the 10 to 100 MHz frequency range the transmission loss is shown graphically in Fig. 2.11. It is to be noted that the loss in this cable (165 ft long) is only 0.5 dB higher than a coaxial line of 20 ft length. It is, therefore, encouraging to see that the Hitachi cable is better suited for long distance communications than any of the three Radiax cables.

2.3.2 Measurement of Group Delay:

The experimental setup used to measure the group delay is the same as shown in Fig. 2.10. Each time the frequency setting is varied, the phase shift through the test cable is noted from the vector voltmeter. Some of the results for the Radiax cables are shown in Table 2.3. When the phase angles at two frequencies, which are reasonably close to one another, are known, the group delay can be calculated using the simple relation

$$t_D = \frac{d\phi}{d\omega} = \frac{\Delta\phi(\text{degrees})}{360 \Delta f(\text{HZ})} \quad \text{seconds}$$

Figure 2.12 shows graphically the variation of the group delay (in nanoseconds) with frequency (in MHz) in the 1 to 500 MHz range. The test cables include two of the 20 ft long Radiax cable samples and the 165 ft long Hitachi cable. Also shown for comparison is the group delay of a standard coaxial cable RG 212/U of 20 ft length. The results for the Hitachi cable were normalized to 20 ft length for comparison purposes, while the results for the Radiax RX4-3A are not shown since they appear to be unreliable. It is to be observed that the group delay with frequency for the Hitachi cable is smaller and less oscillatory in the 1 - 10 MHz range than the

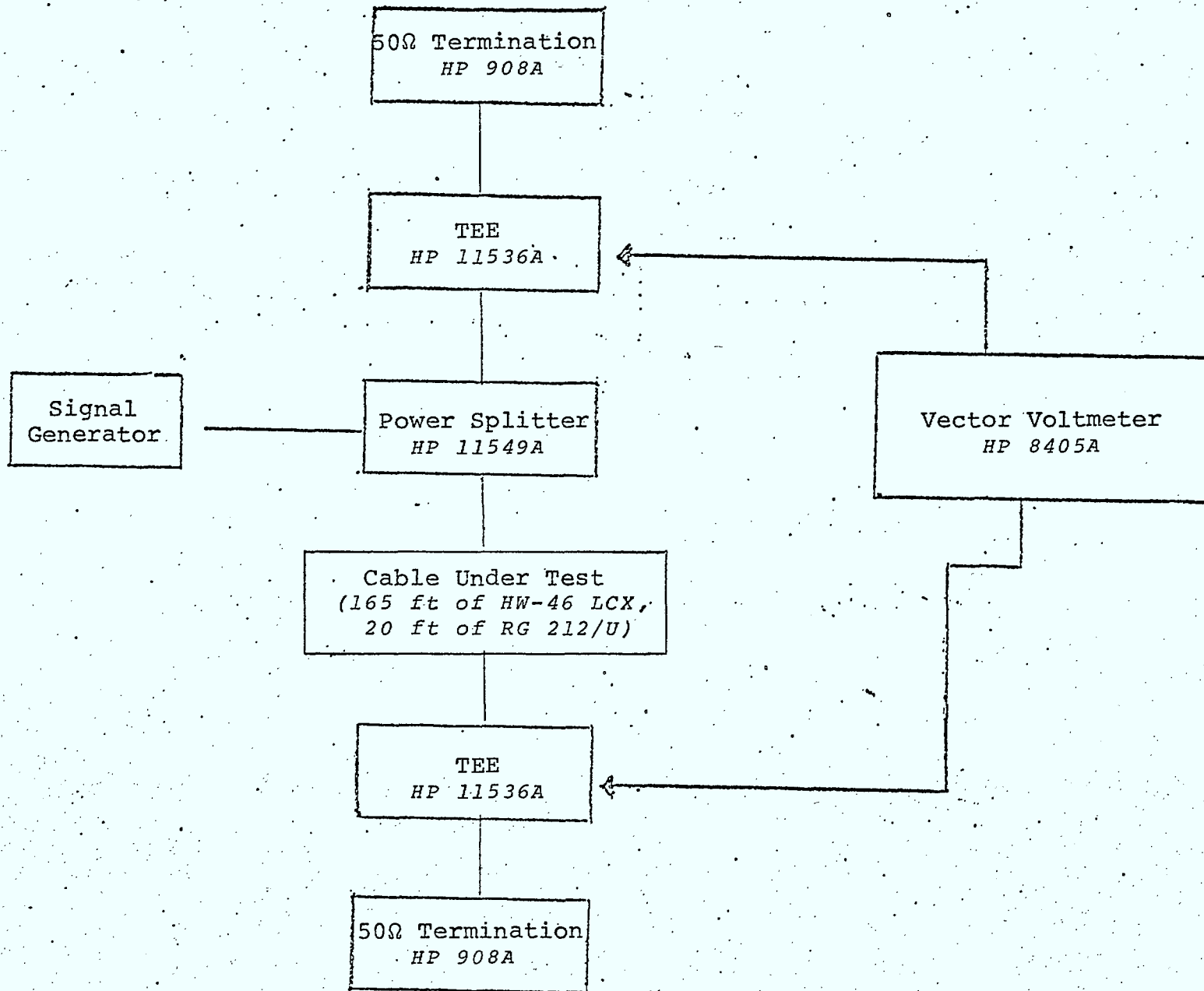


Fig. 2.10 Experimental Set-Up Used for Measuring Transmission Loss

Table 2.2 TRANSMISSION LOSS AND PHASE ANGLE OF HITACHI HW-46 LCX

Frequency (MHz)	Coaxial Cable		HW-46 LCX	
	Transmission loss (dB)	Phaseangle (degrees)	Transmission loss (dB)	Phaseangle (degrees)
1	} < 0.05	32	} < 0.1	- 94
2		43		-181
3		56		+101
4		88		+ 24
5		80		- 55
6		89		-126
7	0.05	101	0.1	+149
8	0.05	113	0.2	+ 72
9	0.1	125	0.18	- 2
10	0.1	137	0.2	- 73
150	0.6	+ 77	1.5	+106
200	0.7	-123	1.4	- 82
250	0.8	+ 48	1.8	+172
300	0.9	-150	1.8	+ 40
350	0.9	- 8	2.1	- 60
400	1.2	+120	2.4	+ 90
450	1.0	- 75	2.4	- 98
500	1.1	100	2.6	+139

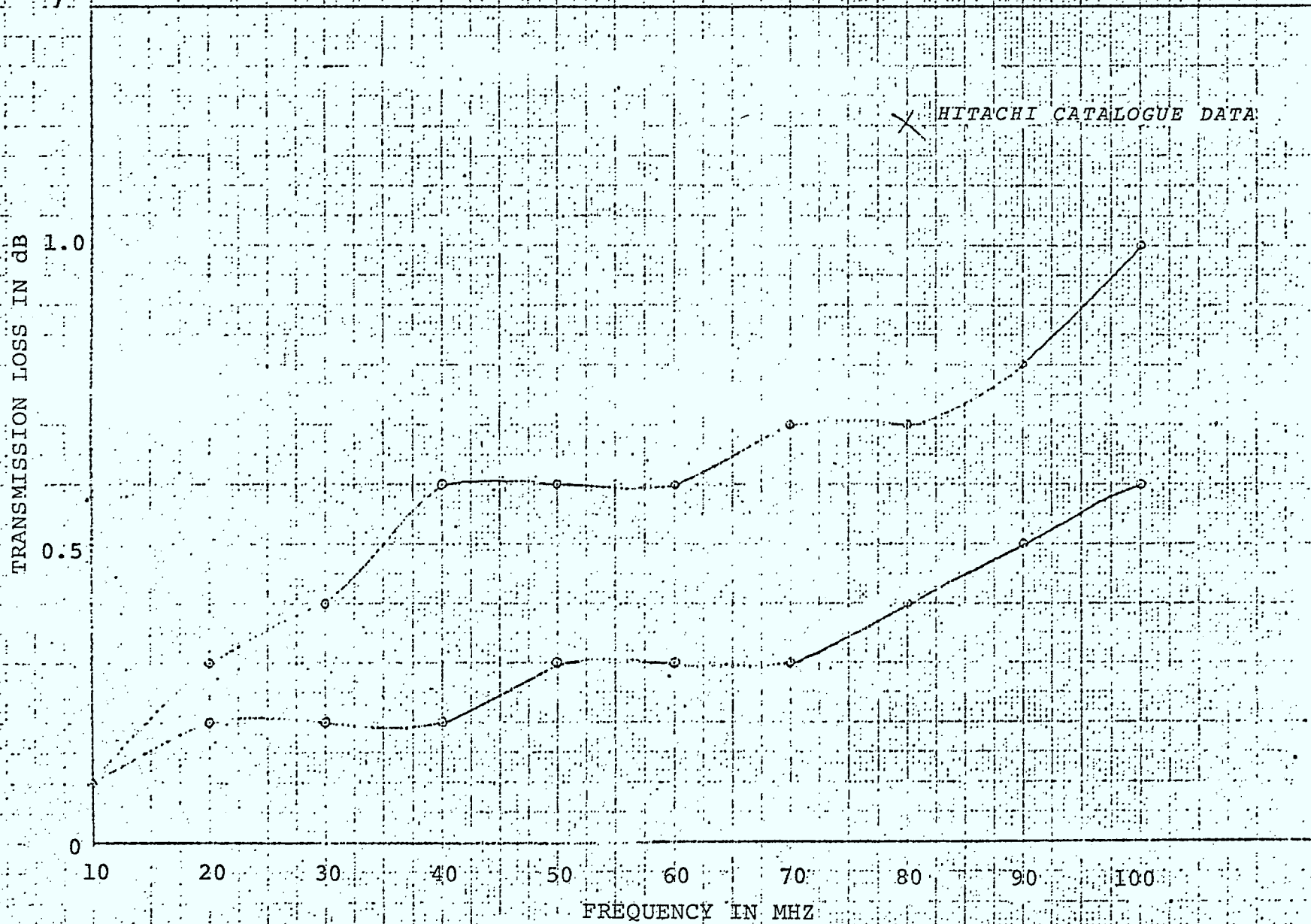


Fig. 2.11 Transmission Loss of HW-46 LCX vs Frequency

Table 2.3: PHASE ANGLE MEASUREMENT

All Phase Angles are in Degrees

Frequency (MHZ)	Radiax Cable Type		
	Rx4-3A	Rx5-1	Rx4-1A
	(Degrees)		
3	+ 12	27	40
4	- 36	38	51
5	- 39	41	61
6	- 44	53	68
7	- 46	66	78
8	- 60	75	89
9	+ 60	88	100
10	+ 18	72	98
150	- 74	+115	- 1
200	+134	- 67	-133
250	+ 56	-113	+174
300	-124	+126	+ 34
350	+ 81	112	- 76
400	- 99	-121	+136
450	+150	+168	+ 36
500	+ 55	+ 71	- 60

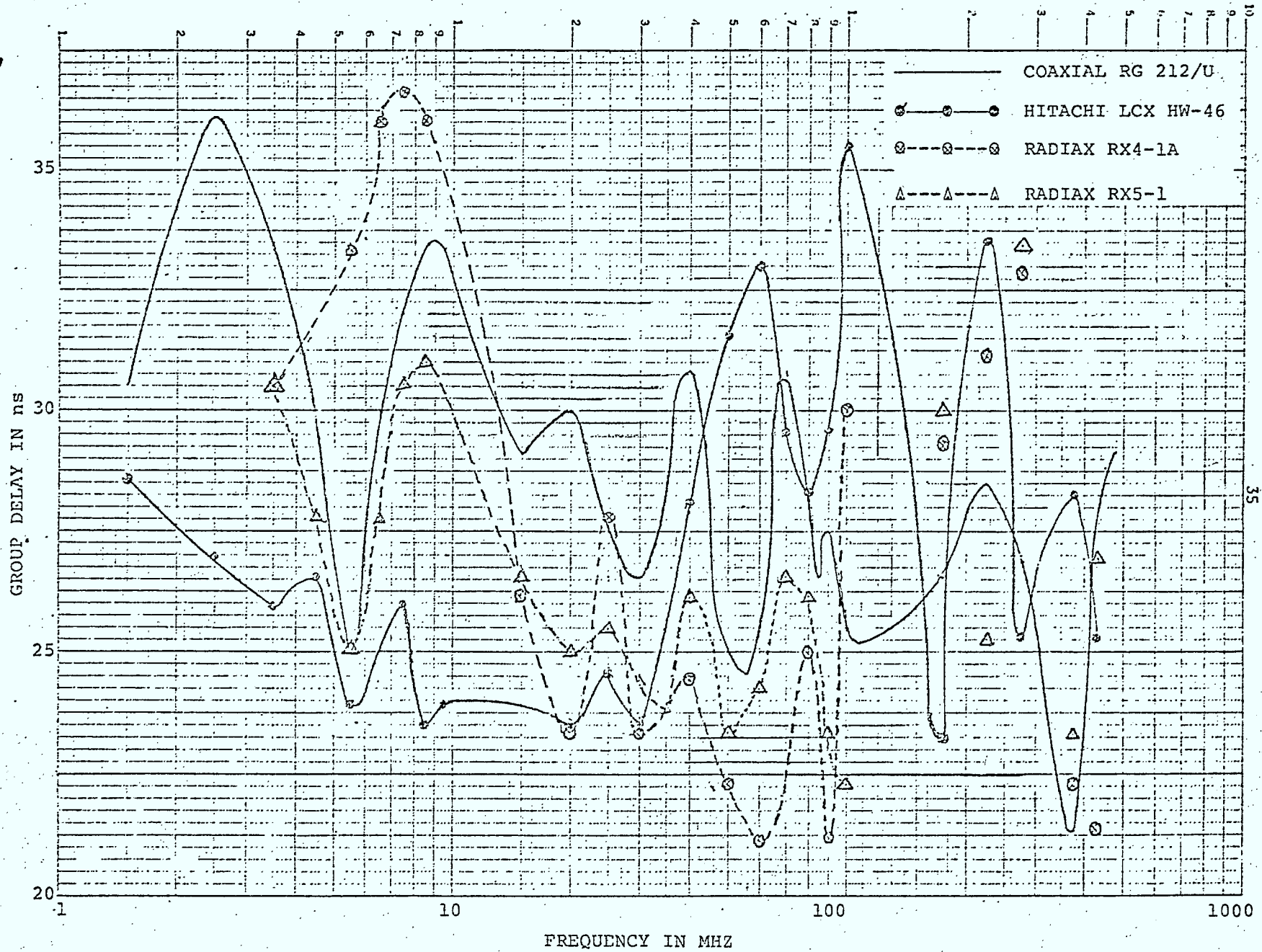


Fig. 2.12 Group Delay vs Frequency

remaining cables, which include the RG 212/U coaxial line. However, in the 10 - 100 MHz range, the Radiax cables appear to perform better insofar as the group delay is concerned.

2.3.3. VSWR Measurement:

The VSWR of the three 20 ft long Radiax cables was measured using conventional slotted line techniques. In the 100 to 500 MHz frequency range the variation of VSWR is shown for the Radiax samples RX4-3A and RX4-1 in Fig. 2.13. For lower frequencies and for the third Radiax sample type RX5-1 the conventional slotted line technique of measuring VSWR did not give consistent results. This is to be expected, since the slotted line is not sufficiently long to accommodate a maximum and a minimum. Moreover, at lower frequencies the test cables are so short electrically and correspond to a fraction of the wavelength and the return loss measurement by microwave techniques therefore has no significance. Alternative techniques must be employed at such frequencies for which no equipment is available at present.

The VSWR for the Hitachi cable was measured within the band specified by the manufacturer and was found in agreement with the published value [2.3].

2.3.4 Coupling Loss Measurements:

Early attempts to measure the coupling loss using a standard dipole receiving antenna fixed at a radial distance of 20 ft did not yield consistent results. The measurements were performed in a microwave anechoic chamber where multiple reflections from surrounding metallic objects gave rise to fluctuations, particularly below 300 MHz.

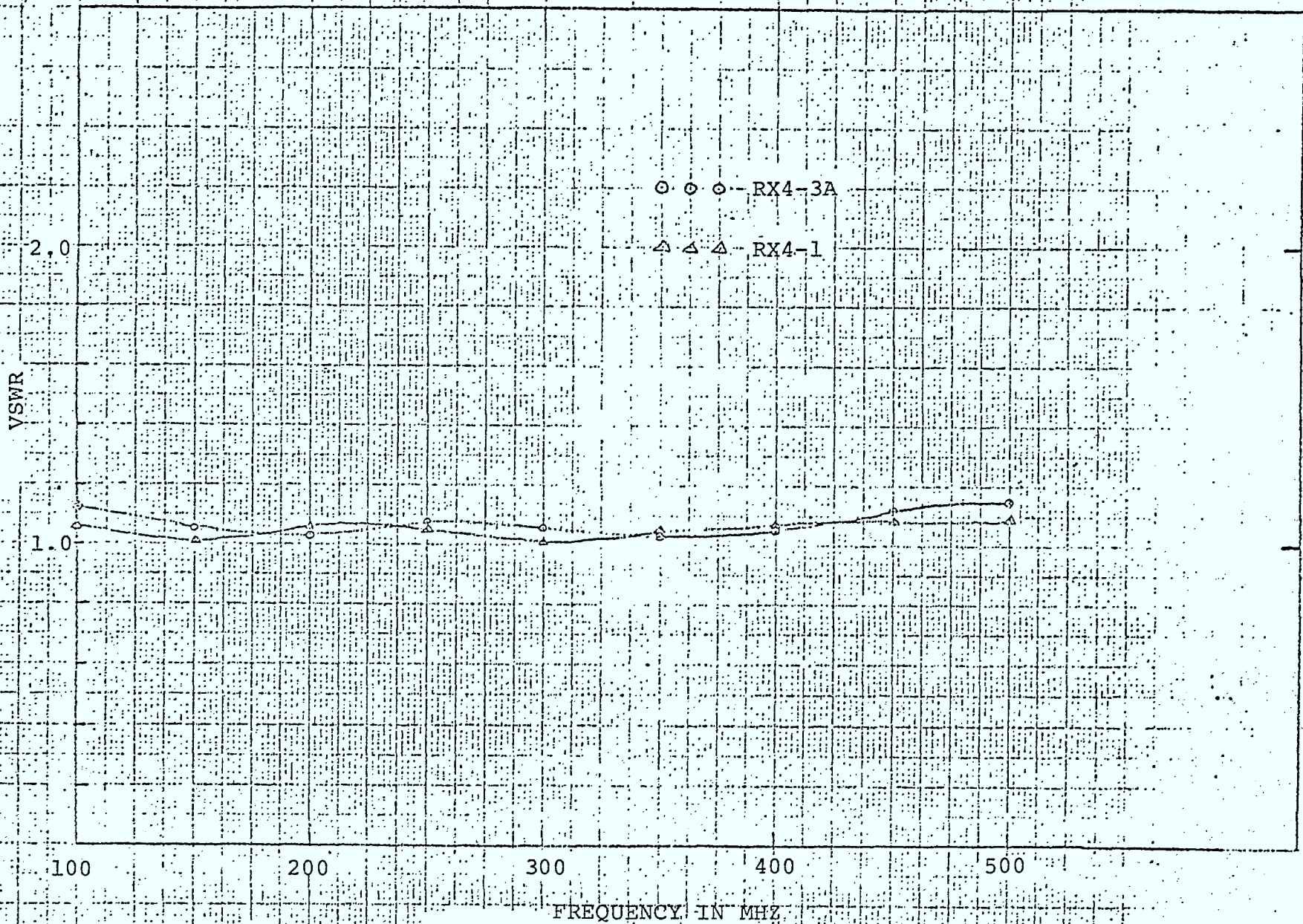


Fig. 2.13 Variation of VSWR with Frequency

To overcome these difficulties, the outdoor antenna lab was employed at the end of the winter season. The lab consists primarily of two 30 ft high steel towers over a ground plane, one fixed and the other movable on rail tracks and driven by a motor up to a maximum separation of approximately 70 ft. The cable (Radiax RX4-3A and Hitachi HW-46) is mounted vertically along the fixed tower and facing a receiving antenna located on a positioner on top of the movable tower.[†] Both horizontal and vertical polarizations were tested at three frequencies, *namely* 250, 300 and 350 MHz. The results are given in Tables 2.4 and 2.5 for distances ranging from 2.5 to 27.5 ft. No tests were made over the other two Radiax cables since they are similar to the Radiax cable tested.

2.4 Electric Field Intensity Measurements at 150 KHz to 10 MHz:

The electric field from the Hitachi HW-46 LCX and Radiax RX4-3A were also measured in the outdoor antenna laboratory over the 150 KHz to 10 MHz range, using the NM-25 T R:I.F.I. meter mentioned earlier. This meter operates over several bands ranging from 150 KHz to 32 MHz and the 150 KHz to 10 MHz range was selected for measurements. The results are given for horizontal and vertical polarizations in Tables 2.6 - 2.8.

[†] The receiving antenna or probe is adjusted for both the vertical and horizontal polarization by simple rotation. Its height above the ground plane is also adjustable with the aid of the positioner, but it was almost constantly maintained at 20 ft above the ground plane and aiming approximately at the center of the test cable. In the case of the Hitachi cable only 30 ft were used in the measurement with the remaining 135 ft coiled and covered with aluminum foil to prevent it from radiating towards the probe.

Table 2.4: Measurement of Coupling Loss of RX4-3A Radiax Cable

Zero distance is the minimum distance between
the cable and dipole (29")

Coupling Loss (dB)

<u>Distance (feet)</u>	<u>f = 250 MHz</u>		<u>f = 300 MHz</u>		<u>f = 350 MHz</u>	
	<u>Horizontal</u>	<u>Vertical</u>	<u>Horizontal</u>	<u>Vertical</u>	<u>Horizontal</u>	<u>Vertical</u>
0	66	63	67	68	70	69
1	71	67	63	72	70	70
2	71	68	63	68.5	77	65
3	70	69	63	71.0	67	65
4	69	68	63	70.5	66	66
5	68	69	65	73	65	69
6	68	68	66	72.5	64	70
7	70	69	66	73.5	67	73
8	71	71	69	74.5	72	81
9	74	72	70	77	78	80
10	79	75	73	75	81	90
11	81	77	73	76	75	90
12	78	78	72	76.5	75	86
13	79	80	75	78.5	74	85
14	77	77	71	78	80	90
15	79	77	69	75.5	79	84
16	79	79	68	76.5	78	81
17	79	78	68	75.5	78	80
18	79	79	68	75	76	78
19	81	81	68	74	76	78
20	78	92	68	74	76	80
21	77.5	86	70	77	77	79
22	77	82	73	78.5	77	80
23	72	79	75	78.5	81	81
24	75	76	79	79	84	80
25	75	76	82	79.5	76	78

Table 2.5: Measurement of Coupling Loss of HW-46 LCXCoupling Loss (dB)

Distance (feet)	f = 250 MHz		f = 300 MHz		f = 350 MHz	
	Horizontal Polarization	Vertical Polarization	Horizontal Polarization	Vertical Polarization	Horizontal Polarization	Vertical Polarization
2	47	54	54	45	54	68
3	58	57	53	60	66	63
4	60	70	55	58	58	61
5	66	70	51	50	76	64
6	70	67	48	54	68	72
7	61	63	57	58	58	63
8	58	63	50	58	57	60
9	62	63	55	60	62	60
10	64	64	49	52	74	60
11	65	62	49	55	78	66
12	64	64	60	57	65	64
13	61	65	51	59	62	61
14	57	65	49	58	62	62
15	57	69	60	62	65	75
16	65	74	58	50	61	60
17	65	64	50	58	63	59
18	67	62	52	56	64	62
19	60	63	64	60	60	73
20	64	71	57	57	58	63
21	70	71	60	50	70	64
22	70	71	59	50	62	70

Table 2.6: Measurement of Field Intensity (at 20 ft) vs Frequency
RX4-3A Radiax Cable (Horizontal Polarization)

Frequency (MHZ)	Electric Field Intensity ($\mu\text{V/m}$)
0.15	6.2
0.20	8.0
0.25	11.4
0.30	12.0
0.60	36.0
0.75	
1.00	
2.00	45.0
3.00	62.0
4.00	80.0
5.00	
6.00	160.0
7.00	
8.00	225.0
9.00	400.0
10.00	800.0

Table 2.7: Measurement of Field Intensity (at 20 ft) vs Frequency
Hitachi HW-46 LCX

Frequency (MHZ)	Electric Field Intensity ($\mu\text{V/m}$)	
	Horizontal Pol.	Vertical Pol.
0.150	7.0	3.0
0.600	12.5	4.5
1.500	70.0	28.0
3.000	220.0	--

Table 2.8: Variation of Electric Field Intensity with DistanceHitachi HW-46 LCXFrequency = 150 KHz

<u>Distance</u> <u>(feet)</u>	<u>Electric Field Intensity</u> <u>(μV/m)</u>	
	<u>Horizontal Pol.</u>	<u>Vertical Pol.</u>
3	250	62
4	180	56
5	125	40
6	90	32
7	70	22
8	56	17.5
9	50	14.0
10	40	11.0
11	32	9.0
12	26	7.0
13	20	6.3
14	17	5.0
15	16	4.5
16	14	3.5
17	12.5	3.5
18	11.0	2.8
19	10.0	2.5
20	9.0	2.8

2.5 Coupling Loss Measurements at 100 KHz:

The coupling loss of the Hitachi test cable was measured outdoors with the cable vertically mounted along the fixed tower and facing the probe. The receiving antenna was the Singer loop already mentioned, which was mounted on the movable tower so as to measure the coupling loss at 100 KHz as a function of distance. Using the HP spectrum analyzer the results for horizontal and vertical polarizations are shown in Table 2.9. It must be pointed out that the signal was too small and was rather difficult to record beyond a distance of 6 ft. Since the cable was designed to be operated in a much higher frequency band, the slots are not expected to radiate with any significant field strength at 100 KHz or at lower frequencies.

Table 2.9: Measurement of Coupling Loss at 100 KHz
Hitachi HW - 46 LCX

<u>Distance</u> <u>(feet)</u>	<u>Horizontal</u> <u>Polarization</u>	<u>Vertical</u> <u>Polarization</u>
2	-106	- 96
3	*-110	-102
4	<-110	-106
5	<-110	<-110
6	<-110	<-110

All measurements in dBm and with test cable terminated in 50 Ω
0 dBm = Generator output (10v peak to peak)

2.6. Time Domain Reflectometer Technique:

As mentioned previously, the performance of leaky coaxial cables is basically determined by the coupling loss measured between the radiating cable and a fixed antenna, the attenuation per unit length and the optimum operating frequency. In addition, the sensitivity of the performance of the cable to mounting problems is of practical importance.

Apart from the frequency domain measurements already reported, it is desirable to employ a complementary method, such as the time domain technique, in order to describe the cable performance over a wide frequency band using a single measurement for each quantity of interest. Hence the behaviour of the line beyond its operating band, and in particular below its empirical optimum frequency, can be studied. Additional advantages of time domain techniques are to reduce errors due to mismatch of the measurement system components and to separate (in time) the so called "end effects" from the overall characteristics of the line. This separation can also facilitate an isolated study of the periodic effects due to mode convergence at the beginning and end of the line.

The proposed technique is described in a separate article [2.4] and briefly employs equations derived from a signal flow graph procedure where the leaky cable is represented as a three-port network with two ports representing the end port of the cable and the third port representing the leakage. Thus, cable mounting effects such as reflections from the surroundings etc.,

are described by means of the third port. Only segments of the transient response to an impulse waveform need be sampled so that the scattering parameters describing the performance of the cable can be obtained.

In order to test the feasibility of the method, comparative measurements were made on the Radiax and MGL[†] cable samples. The time domain reflectometer was an HP-1415A TDR system where the transmitted pulse was generated from a 150 ps step using a 25 Ω short circuited stub as a pulse forming network. Also, a 28 ps HP 184A TDR system with accessories (1815B sampler, 1817A sampling head, 1106B tunnel diode and 1104A trigger countdown) borrowed from the Manitoba Telephone System was used for a short period. The appropriate segments from the analog signals were sampled and stored in a buffer of PDP-11/40 computer system, while their Fourier transforms were calculated using the FFT subroutine in the same computer.

The technique was attempted only on an exploratory basis, with the hope that further and more elaborate measurements could be carried out when the TDR equipment could be procured for a reasonable period of time. Preliminary measurements indicate the Radiax Cable samples are very close to 50 ohm lines, while the MGL test line has a characteristic impedance of approximately 300 ohms. The effect of bending the Radiax Cables was noticed, while the effects of connectors and transitions were also observed. It is unfortunate that the waveforms and other TDR measurement records could not be reported here, since the measurements were only exploratory and done during the very brief period in which

[†] This cable is described in Chapter 3.

the TDR equipment was borrowed. Since time domain measurements were not part of this contract, it is hoped that detailed measurements could be carried out at a later date in a future contract.

2.7. References:

- [2.1] Radiax Slotted Coaxial Cable System Design Consideration Andrew Bulletin 1058B, Andrew Antenna Company Ltd.
- [2.2] Sako, T. et al: 'Large Size Leaky Coaxial Cable for 400 and 800 MHz Frequency Band', The Fujikura Cable Works Ltd., Tokyo.
- [2.3] Hitachi Leaky Coaxial Cable, Hitachi Cable Ltd., CAT No. EF-701.
- [2.4] Iskander, M.F. and Hamid, M. A. K.: 'A Time-Domain Technique for Characterizing Leaky Coaxial Cables', 1977 IEEE/MTT-S International Microwave Symposium, San Diego, California, June 1977.

THE MODIFIED GOUBAU LINE

3.1. Introduction:

Ever since the pioneering theoretical and experimental work of Goubau [3.1. 3.2] on surface wave transmission lines, a considerable number of investigations has been carried out on different types of surface wave lines and other related topics [3.3 - 3.5]. All such lines have one common characteristic, in that they are open lines, i.e. part of the electromagnetic energy travels in the air surrounding an unshielded guiding structure. The importance of such a study of these 'open waveguides' arises because the attenuation factors of the propagating electromagnetic wave are considerably lower than in 'closed waveguides'. This is especially true when the surface wave structure is excited in its lowest order mode.

One of the most recent members of this family of lines is the modified Goubau line (MGL) where a suitably designed airgap is introduced between the conductor and the dielectric layer of a conventional Goubau line (GL). This line, while fully retaining the merits of the GL, appears to have, at least in theory, a lower attenuation constant [3.6]. It was also noted that, as the airgap size increased, the calculated attenuation constant

decreased in a monotonic fashion. The line also shows considerable promise to have a wider bandwidth as compared with the GL of identical outer diameters of the conductor and the dielectric layer and propagating the same mode [3.7].

In the following sections the theoretical model will be presented first in order to explain the mechanism responsible for the basic advantages over the conventional Goubau line. This will be followed by sections dealing with the design of surface wave launchers, radiation and matching elements, as well as the details of an experimental line constructed for laboratory testing where return loss and near-field measurements are presented.

3.2. Theoretical Model:

The geometry of the MGL is shown in Fig. 4.1, along with the basic electrical parameters of the three media. The wave is assumed to be propagating in the positive z direction, and the field components are assumed to vary as $\exp[-\gamma z]$ where $\gamma = \alpha + j\beta$. A time variation of $\exp[j\omega t]$ is assumed.

For the symmetric TM_0 mode propagating on the structure, the three non-vanishing components are E_z , E_ρ and H_ϕ , and they are independent of ϕ . The wave equation is solved in the three media as shown elsewhere [3.6], and the expressions for the field components can be written down. Imposing the boundary

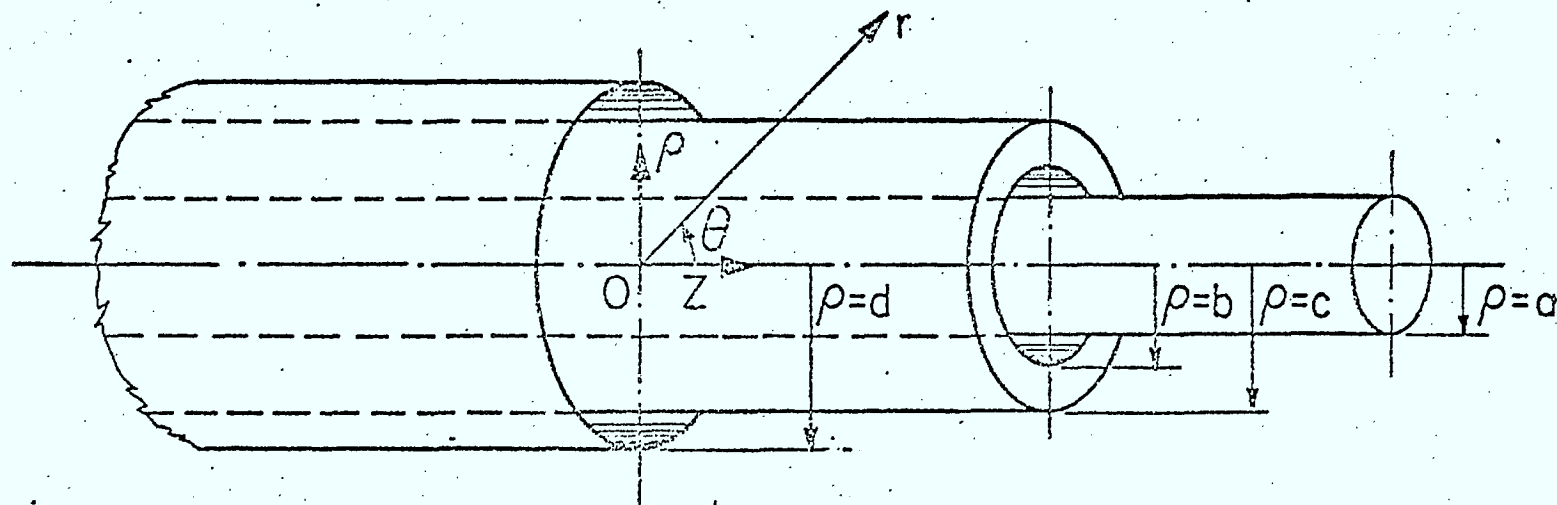


Fig. 3.1 Junction Between the Modified Goubau Line and the Coaxial Waveguide.

conditions for the general case of a lossy conductor and lossy dielectric layer, the characteristic equation is derived and is solved for various combinations of parameters. In particular, the low frequency approximation is studied as a separate case [3.6].

The unique solution of the characteristic equation determines such propagation characteristics as the phase and attenuation constants, guide wavelength and phase velocity, decay coefficient, surface resistance, and reactance and characteristic impedance. The power launched onto the MGL travels entirely in the z direction, which is the direction of propagation, and is obtained by integrating the Poynting vector over the transverse cross-section over the three media.

Some representative numerical results are given elsewhere [3.6] in the form of tables and graphs.

3.3. Operating Physical Mechanism:

All the computations performed up to the present time indicate clearly that the MGL has a lower attenuation constant, and a wider bandwidth as compared to the GL.

The reasons presently attributed to these observations are that part of the wave is made to travel in a relatively loss free airgap medium, instead of the dielectric layer. In other words, the field is pulled away from the conductor surface, where the losses are usually high, and there is a redistribution of the transverse power profile which increases the field concentration in the dielectric layer. Similar observations were also made

earlier at the University of Manitoba in the case of antennas [3.8] and conventional metallic waveguides [3.9]. For narrow airgap sizes, the possibility of existence of a backward wave is suspected. On the other hand, the size of the airgap may not be so critical for the MGL as it is in the case of center-fed dielectric dipole antennas. The so called quarter wave effect (3.8) may not be noticeable in the case of open surface wave lines like the MGL.

3.4. Line Excitation:

The field configuration of the dominant mode of the MGL is similar to the TEM coaxial line mode in the transverse plane. It is therefore quite logical to use the open end of a coaxial line as the feed point for launching a surface wave on the MGL, provided that the two lines share the same inner conductor, as shown in Fig. 3.1. The mathematical model for this type of excitation has been recently derived, and the resulting problem of scattering at the abrupt junction has been formulated and solved by the Wiener-Hopf method [3.10]. This analysis led to expressions and representative numerical results for the reflection and transmission coefficients and launching efficiency.

However, in practice the outer conductor of the coaxial line is flared in the form of a conical launcher over a few wavelengths in order to create a smooth variation of transverse impedance. The flared section is normally referred to as a horn surface wave launcher. The design procedure to determine

the flare angle, electrical length and impedance is given elsewhere [3.1] and is employed in the design of the experimental line discussed later.

As the operating frequency is decreased, the electrical length of the horn launcher decreases unless the physical length is increased. This could become a serious disadvantage since the length may become too prohibitive for practical systems. An alternative procedure has to be, therefore, investigated for the lower frequencies. The most promising approach at present is to use shaped dielectric inserts inside the launcher as already reported from the University of Manitoba in the case of circular and rectangular waveguides [3.11 and 3.12].

3.5. Operating Frequency Bandwidth:

The presence of a narrow airgap in the MGL leads to a wider operating frequency bandwidth than the GL for the same mode [3.7]. In this case the definition of the operating frequency bandwidth is based on Semenov's criterion of limits, set on the transverse propagation constant in the surrounding medium [3.13]. These limits amount to attenuation limits where the MGL losses are lower than a coaxial line of comparable dimensions and composition. In addition it must be noted that the guide wavelength for surface wave lines lies between the free space wavelength and the wavelength in the dielectric.

The wider bandwidth of the MGL in conjunction with the lower attenuation constant suggests numerous practical applications such as in point to point line communications.

3.6. Transverse Field Decay:

The transverse field distribution of any surface wave line is an important characteristic since it is indicative of the effectiveness of the structure as a waveguide. For this reason, the decay coefficient is normally used to give an idea of the radial field decay in the transverse direction. This coefficient is given elsewhere [3.6] and is a function of the operating frequency and physical dimensions as expected. The higher the frequency for any given line, the higher is the decay coefficient, and tighter the coupling of the surface wave to the line, and *vice versa*.

In case of the MGL the decay coefficient is smaller than that of a GL of unmodified dimensions which implies that the surface wave is more loosely bound to the outer surface. With a shorter section of a similar line and as the receiving antenna, possible applications could be found in continuous access guided communication (CAGC) on ground transportation systems such as railways, highways, and monorails [3.14]. Gallawa et al [3.15] have reported an extensive investigation of the GL for two-way continuous communications and, especially for such applications, the reduced attenuation and larger field spread of the MGL are obviously of advantage.

3.7. Leaky MGL:

So far the MGL has been presented as a surface wave transmission line, where part of the energy travels in the dielectric layer and the rest in the airgap and the surrounding air medium.

In other words, the surface wave is still a guided wave and the wave impedance has a unique and calculable value for any cross section along the length of the line. However, when the MGL is loaded at some position, the wave impedance changes and this is associated with a radiated wave originating from the load discontinuity. At the same time, we expect that scattered waves and higher order modes are excited particularly in the immediate vicinity of the discontinuity. This loading, therefore, converts the MGL to a leaky surface wave line with similar characteristics to the LCX with analogous engineering design procedures and associated problems.

There are many possible methods of achieving an impedance discontinuity in an MGL on a continuous or discrete basis. The corresponding radiation patterns could be directive or omnidirectional (i.e. independent of the azimuthal angle). Examples of continuous discontinuities are longitudinal, straight or helical slots or metallic tapes. Examples of discrete discontinuities are circular metallic or dielectric discs or conducting strips. Some results dealing with conducting and dielectric discs and conducting strips are reported elsewhere [3.16].

Because an abrupt discontinuity is likely to create additional mismatch on the line, it would be ideal if the discontinuity can be a sliding type, in order to obtain radiation and higher power transfer from the generator to the line. This is the particular advantage of a sliding disc type discontinuity, which is somewhat analogous to the case of

conventional tuners where power transfer from the generator to the load is controllable. Because of its simplicity and convenience, this type of discontinuity has been investigated experimentally in some detail, and results are presented in the following sections for the return loss or VSWR.

3.8. Experimental Line:

An experimental MGL line was constructed from a 6 ft long copper tube of 0.5" outside diameter and an acrylic tube ($\epsilon_r = 2.6$, $\tan \delta = 0.0057$) of 0.75" inside diameter and 0.875" outside diameter. The inner conductor is supported by three 0.25" wide acrylic spacers, as shown in Fig. 3.2. Two of these three spacers are at the opposing ends of the line and the third is approximately at the middle of the line. The copper tube is closed at the ends by means of a pin-plug arrangement, where the centrally located pin ensures a good electrical contact and D.C. continuity with a coaxial N-type connector. The line is excited from a coaxial line and the outer conductor is flared in the form of a conical horn launcher. The launchers are designed and constructed by known techniques [3.1] and the details of the geometry are given in Fig. 3.3.

The experimental set-up used is shown schematically in Fig. 3.4. The method of measurement is based on a technique originally proposed by Barlow and Karbowskiak [3.3], and is fairly well known and established. Thus, the output of the sweep oscillator is fed through a frequency meter to a 1KHz

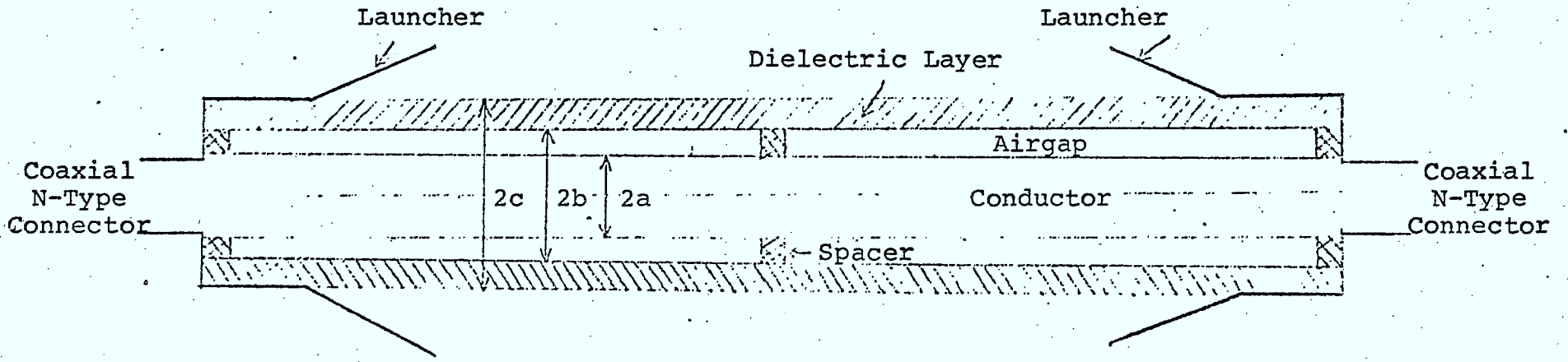
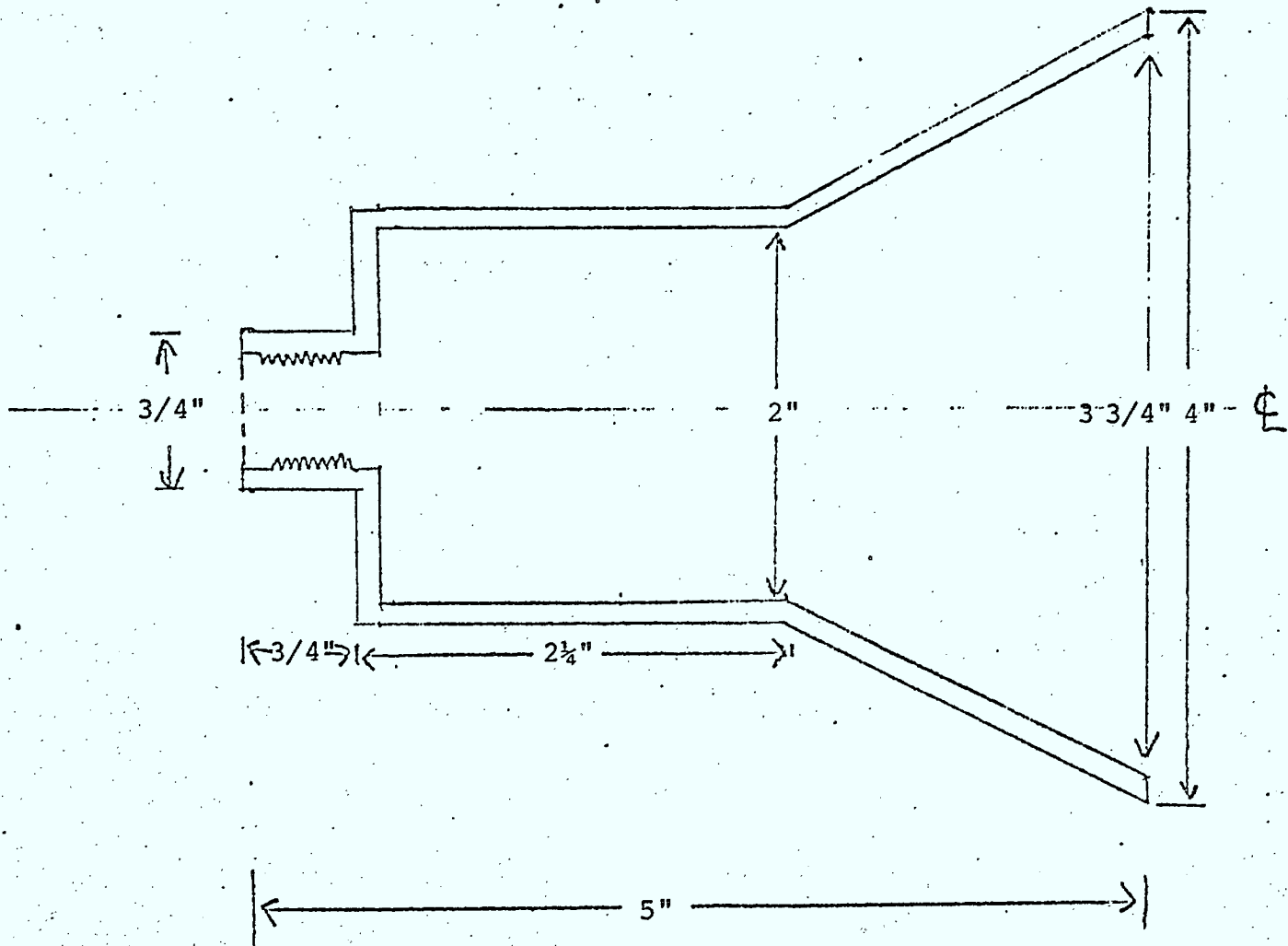


Fig. 3.2 Details of the MGL, Launchers and Spacers



*all sides 1/8" thick
 **threads are for N-type connector

Fig. 3.3 Sketch of Launcher

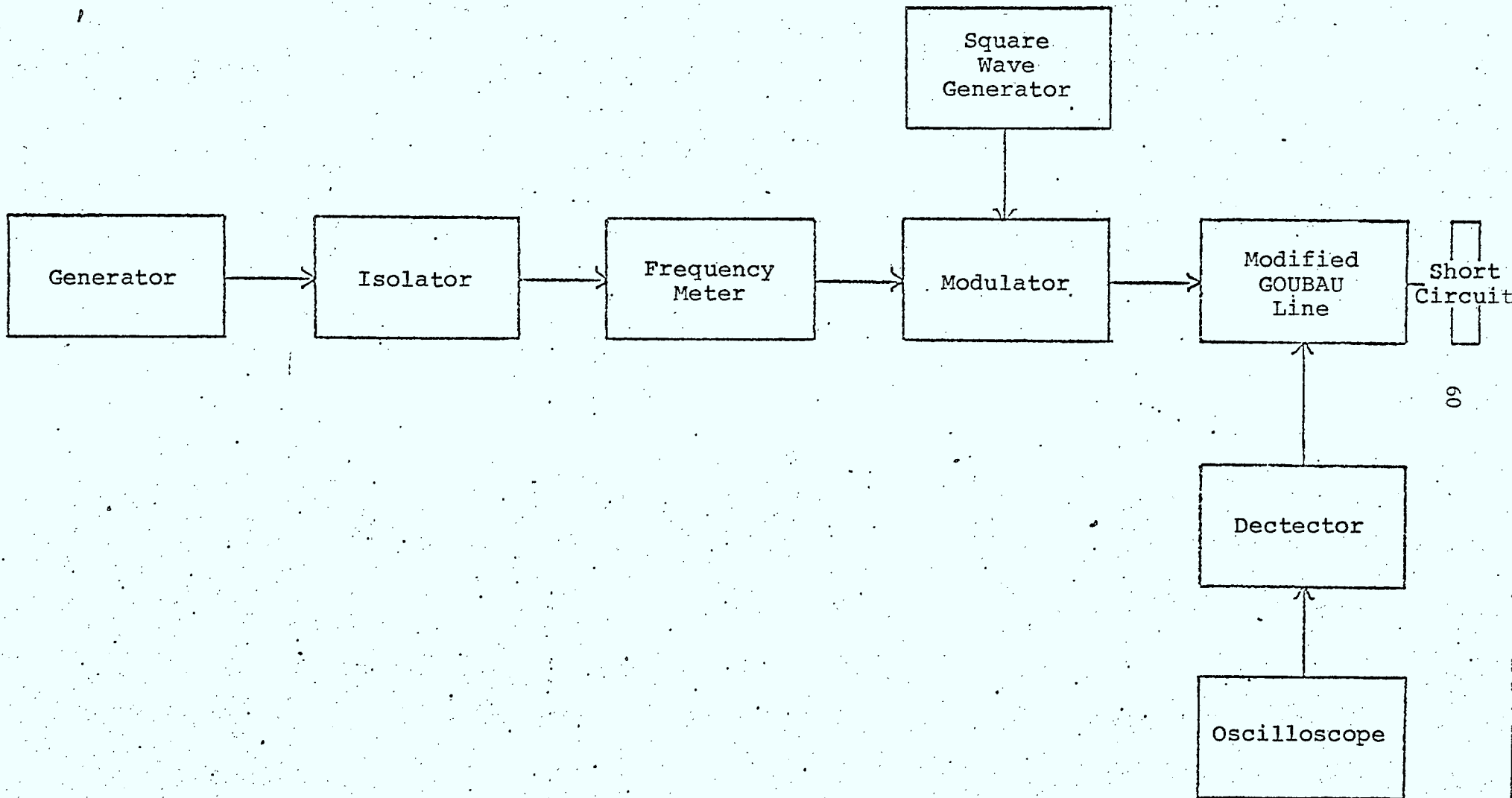


Fig. 3.4 Experimental Set-up Used for the Near-Field Measurement

square wave modulator. The output of the modulator is in turn fed to the line which is short circuited at the far end, and hence standing waves are set up on the line. The axial electric field component is detected with the aid of the dipole probe and detector. The radial component is detected by using a monopole probe constructed for this purpose, in which the inner conductor protrudes over and above the outer conductor by approximately 5 to 6 mm. The probe is mounted on the probe carriage of an optical bench covered with absorbing pads (to minimize reflections) and oriented parallel to the line so that the appropriate electric field component is detected inside a microwave anechoic chamber suitable above 300 MHz. In the case of the monopole probe, the probe position is adjusted to a height so that the tip is approximately 1.5 cm from the outer surface of the line. A similar procedure is adopted when the dipole probe is mounted so that the dipole arms are parallel to the axis of the line and separated from it by 1.5 cm. Since the dimensions of the probe are small, it may be assumed that the presence of the probe near the line does not significantly alter the surface wave distribution. The probe is moved along the bench parallel to the axis of the line in small steps of 5 mm, and each time the power detected is read from a calibrated oscilloscope display, which is connected to the probe through a detector. The standing wave pattern is measured near the launcher end, near the middle portion where the spacer is located, and near the short circuited end. No appreciable change in the value of the guide wavelength was observed, except for the difference that, in the middle portion

where the spacer was located, the minima were rather deep and more pronounced and the field more sensitive. The separation between either two successive minima or maxima gives half the guide wavelength. The agreement between calculated and measured values of the guide wavelength is better for the monopole than for the dipole measurements. This gave confidence in the validity of the experimental system, and the procedure was repeated with the aforementioned discontinuities.

The inner and outer diameters of the brass and acrylic rings are the same and equal 0.875" and 1.125", respectively, while their thickness is 0.125". The conducting tape is wrapped around the line and is 1 cm wide (with negligible thickness).

3.9 Experimental Results:

The experimental set-up already described in Fig. 3.4 was initially employed to measure the electric field components E_ρ and E_z . As mentioned earlier, these components are detected using the monopole and dipole probes, respectively.

Although the MGL can be used in principle in any frequency band, particularly when excited in the dominant E_0 mode, initial measurements were carried out in the 1.5 - 2.0 GHz range. This range was selected on the basis of the availability of dipole probes. The data was used to calculate the guide wavelength and decay coefficient as shown in Table 3.1. The measured values reported in this table are the result of averaging over total number of maxima and total number of minima in the standing wave pattern over the line [3.18].

Table 3.1: Comparison Between the Calculated and Measured Values of λ_g (Dipole Probe)

Frequency (MHz)	Wavelength λ_o (cm)	Guide Wavelength λ_g (cm)	
		Calculated	Measured
1500	20.00	19.7308	19.56
1600	18.75	18.4922	18.72
1666	18.00	17.7491	17.55
1800	16.66	16.4282	16.20
2000	15.00	14.774	14.36

Using the monopole probe it was possible to test the line in a different frequency band ranging from 1 to 4 GHz using different signal generators with manual adjustments. The results thus obtained are presented in Table 3.2, and show better agreement with theory than Table 3.1. The "left" and "right" positions indicated in Table 3.2 correspond to the generator and short-circuit sides of the discontinuity, respectively. The measured values reported in Tables 3.2 and 3.3 are the result of averaging over the total number of maxima and minima to the left and right sides of the discontinuity.

Table 3.2: Measured Values of the Guide Wavelength (cm) - Monopole Probe

λ_o	λ_g							
	MGL		Brass Ring		Acrylic Ring		Conducting Tape	
	Calculated	Measured	Left	Right	Left	Right	Left	Right
30	29.6429	29.50	29.50	29.40	28.50	29.33	29.00	28.80
20	19.7308	19.77	19.62	19.75	19.50	19.63	19.50	19.63
15	14.7774	14.82	14.40	14.75	14.50	14.57	14.81	14.71
10	9.8267	9.76	9.87	9.78	9.85	9.76	9.80	9.75
7.5	7.3528	7.34	7.33	7.31	7.36	7.38	7.35	7.62

The close agreement between the calculated [3.6] and measured values of the guide wavelength suggests that the surface wave is launched properly and is tightly bound to the outer surface. This gives some confidence that the system is feasible and, hence, the theoretical concept of the MGL is demonstrated experimentally.

The variation of power detected in the transverse plane was measured with the aid of an alternative experimental arrangement of the line and optical bench. The radial power variation thus measured was close to the expected values based on theoretical calculations [3.6] as shown in Figures 3.5 and 3.6. The deviation between the two can be attributed to the possibility of existence of a standing wave in the radial direction due to reflections from the probe and other surrounding metallic objects. However, no significant effects were observed due to movements of personnel in the vicinity of the probe. It may be noted here that the theory assumes a pure surface wave, while the experiment gives a slower rate of decay.

The experimental procedure for measuring the guide wavelength and power decay of the MGL was repeated in the presence of metallic and dielectric discontinuities and the results are presented in Tables 3.2 and 3.3.

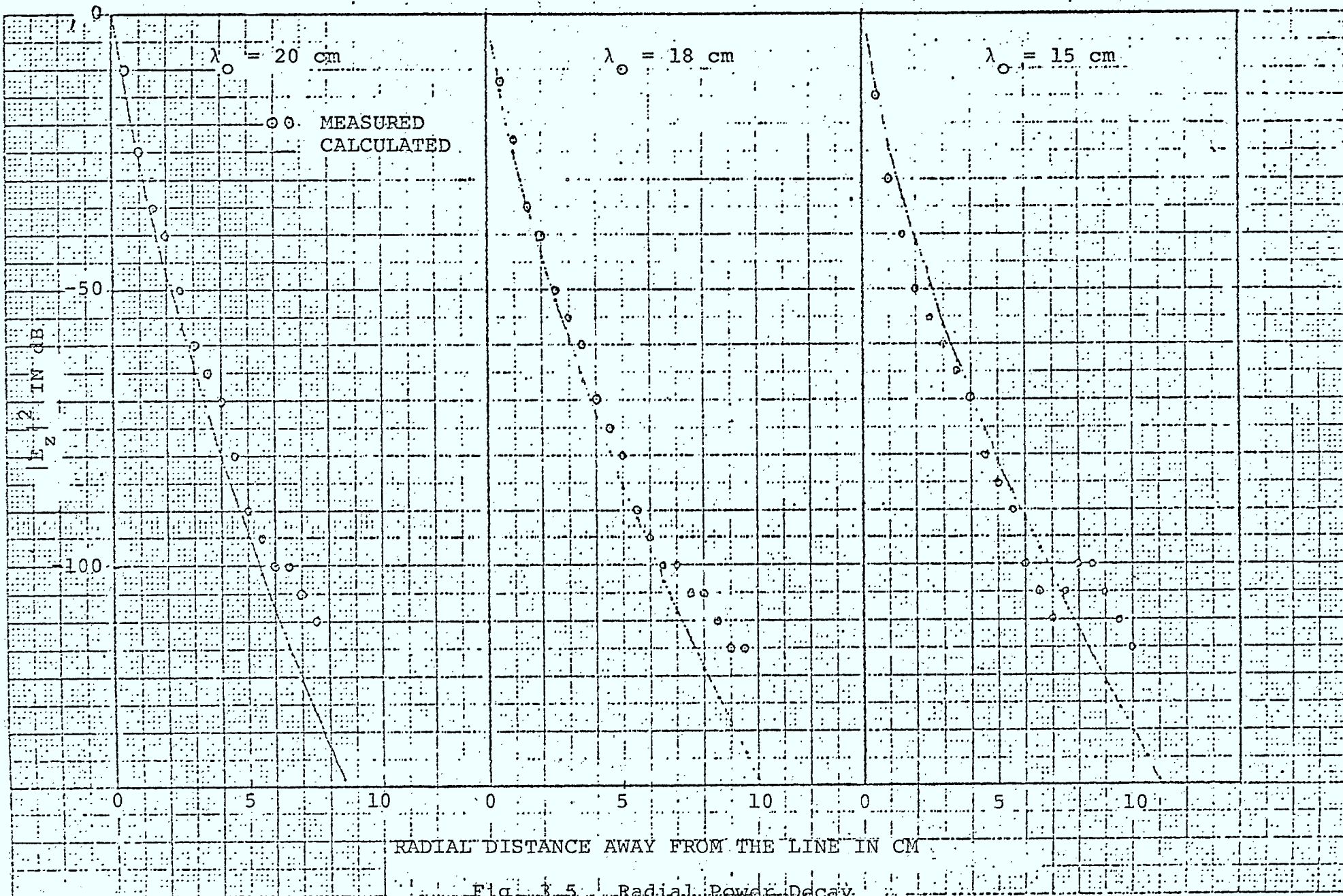


Fig. 3.5 Radial Power Decay

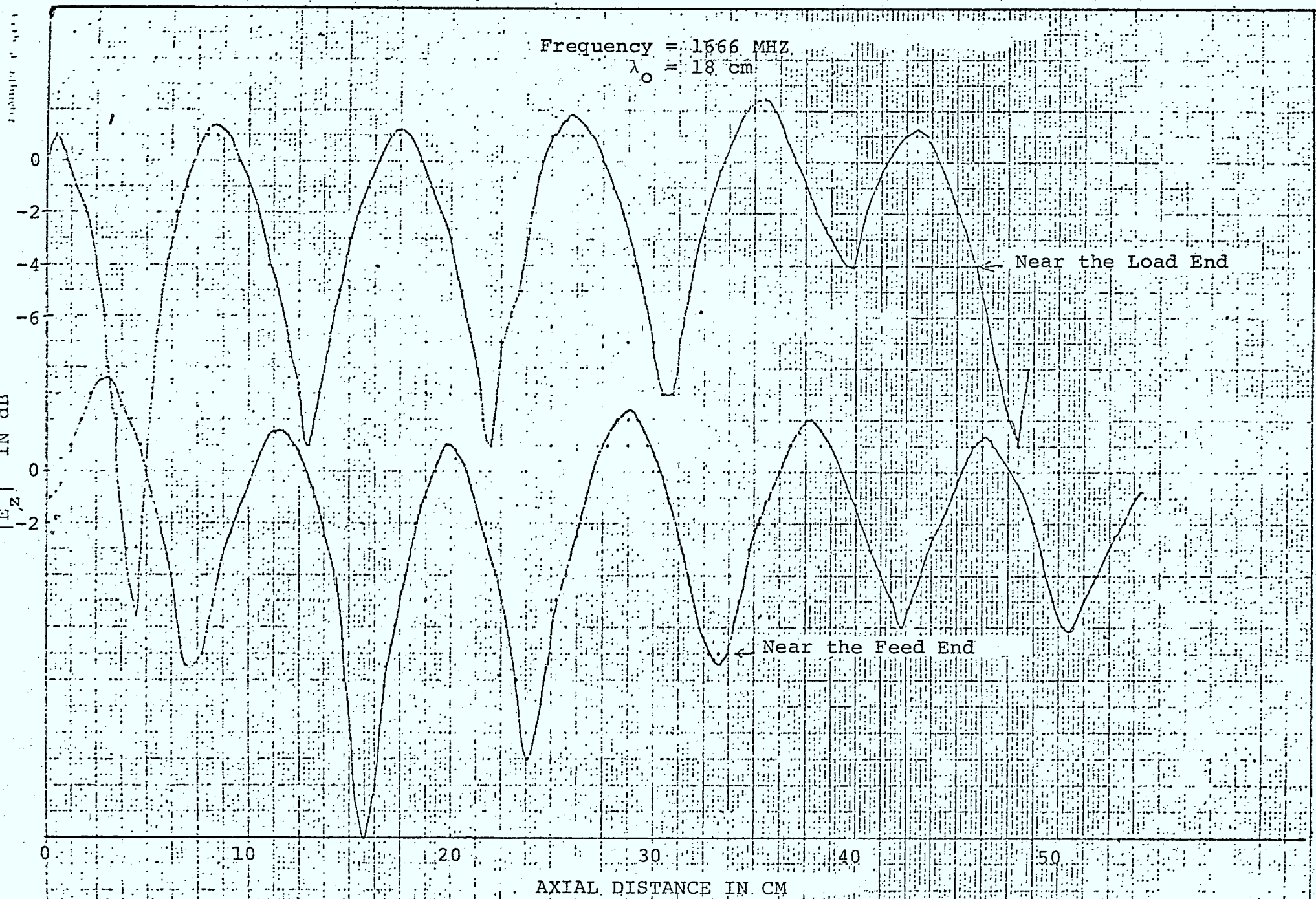


Fig. 3.6 Standing Wave Pattern Along the Structure

Table 3.3: Measured Values of the Decay Coefficient for the MGL

λ_0	Decay Coefficient (cm^{-1})							
	Unloaded		Brass Disc		Acrylic Ring		Conducting Tape	
	Calculated	Measured	Left	Right	Left	Right	Left	Right
30	0.0326	0.038	0.038	0.042	0.068	0.036	0.055	0.061
20	0.0521	0.047	0.061	0.050	0.071	0.060	0.071	0.060
15	0.0730	0.065	0.122	0.077	0.110	0.102	0.066	0.083
10	0.1185	0.139	0.100	0.133	0.110	0.139	0.125	0.143
7.5	0.1685	0.172	0.179	0.189	0.161	0.153	0.168	0.119

The "left" and "right" positions indicated in Table 3.3 correspond to the generator and short-circuit sides of the discontinuity, respectively. Figures 3.7 - 3.9 show the variation of the normalized power in the transverse plane with the radial distance away from the line.[†] Figure 3.7 shows a comparison between the unloaded MGL, brass disc-loaded MGL, and acrylic disc-loaded MGL at a fixed frequency of 1.5 GHz. Figure 3.8 shows the particular case of the brass disc-loaded MGL at a fixed frequency of 2.0 GHz where the variation is shown on either side as well as the center of the discontinuity. Figure 3.9 gives the radial decay to the right hand (or load end side) of the brass disc at various frequencies.

[†] It should be noted that this variation is independent of the axial position of the probe as also verified experimentally.

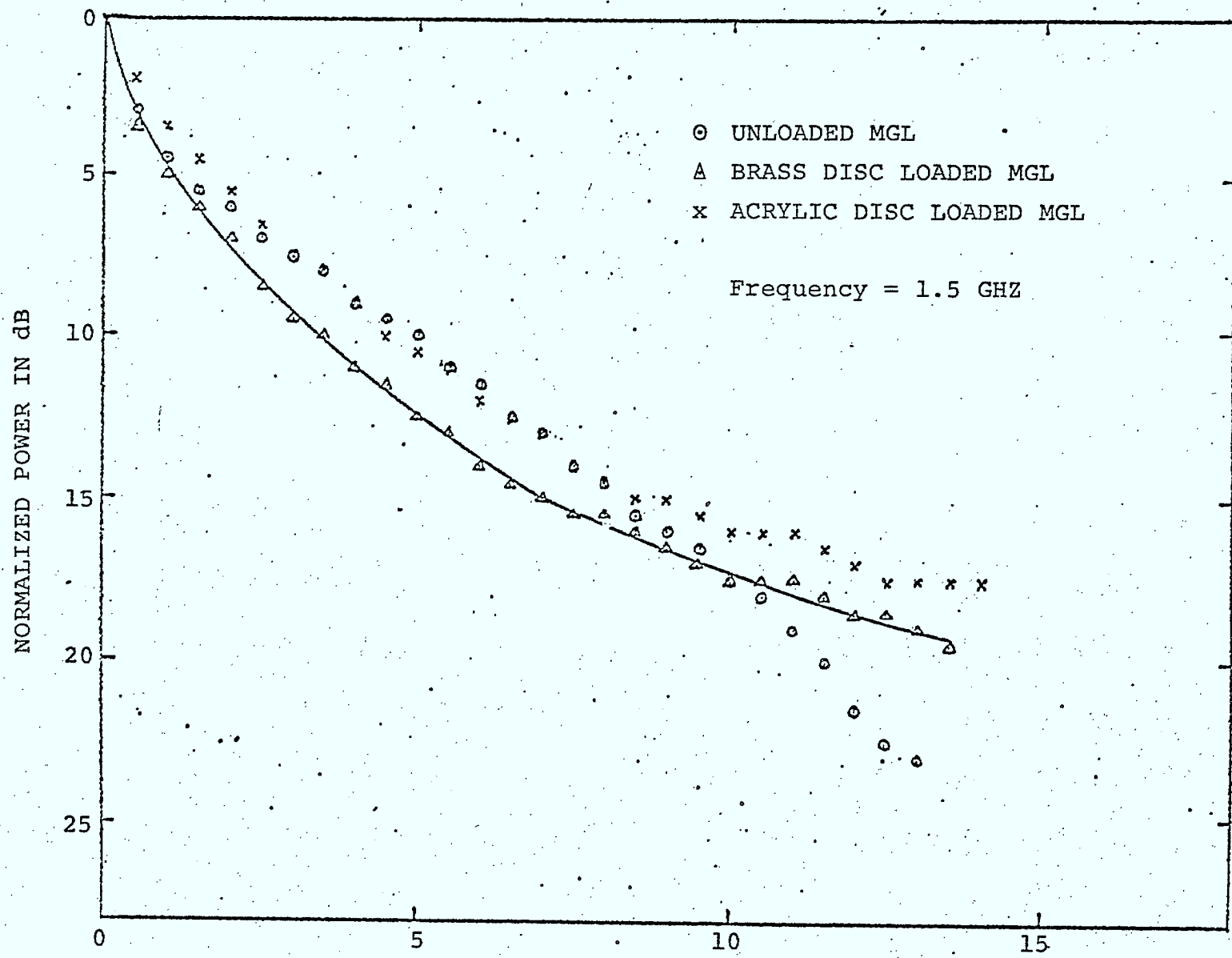


Fig. 3.7 Normalized Power vs Radial Distance (in cm) for Loaded and Unloaded Cases

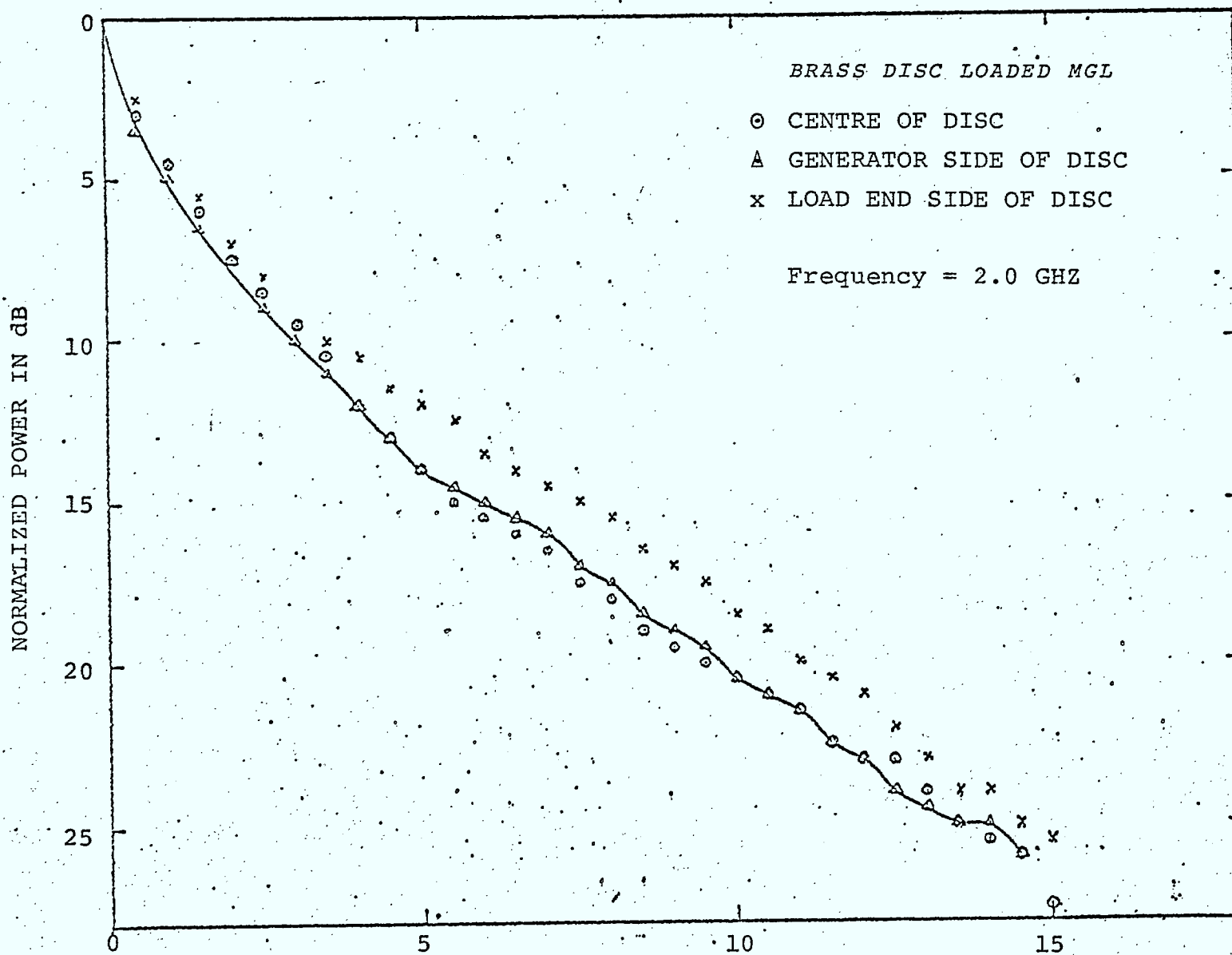


Fig. 3.8 Comparison of Normalized Power vs Radial Distance (in cm) on Either Side of Discontinuity

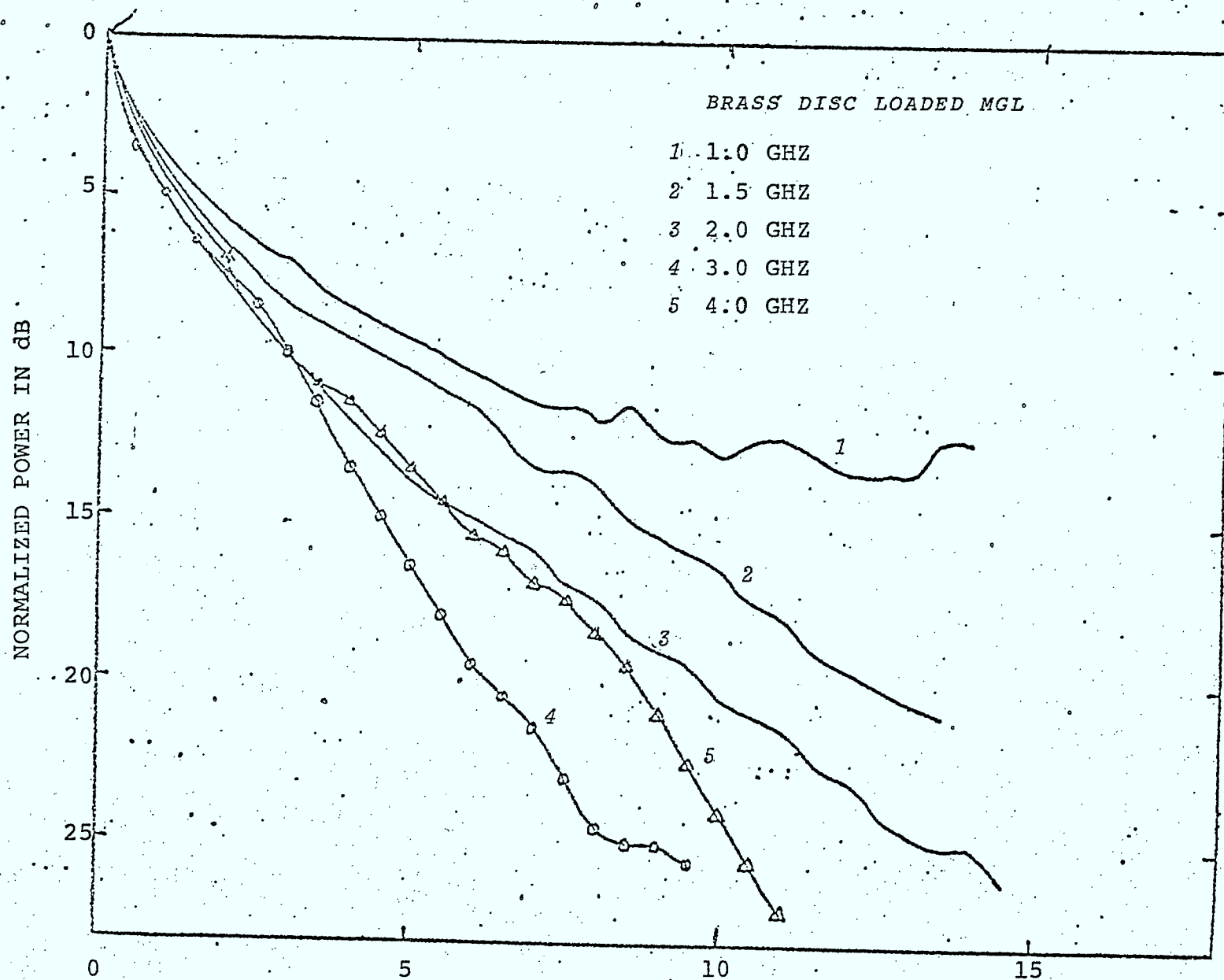


Fig. 3.9 Normalized Power on Load Side vs Radial Distance (in cm) for Brass Disc Loaded MGL for Different Frequencies

Since the interest in the MGL is based on its ability to propagate and radiate (with the aid of suitable discontinuities) e.m. energy, the question of characterizing the MGL as a leaky transmission line is of obvious interest. We note that little is reported in the literature on such engineering aspects as the equivalent circuit representation, frequency response and mechanism of radiation of surface wave transmission lines. In fact, the definition of a characteristic impedance for such lines does not exist and no procedure for its measurement is therefore available. Hence, for the experimental line of Fig. 3.2, we consider that the two launchers and end connectors are an integral part of the line. Also, we specifically adopt the concept of an equivalent characteristic impedance (Z_{oe}), equivalent propagation coefficient γ_e (or $\alpha_e + j\beta_e$). Obviously Z_{oe} is unknown and is needed to determine the optimum feed frequency for maximum transmitted and radiated power with minimum power reflected. The two methods described below were employed in our effort to characterize the line and both proved to be almost equally effective, although the second method proved to be more convenient and practical. It is unfortunate that a third method based on the TDR technique could not be employed, particularly to study the effects of connectors, launchers, bends, transitions, etc., due to the lack of equipment.

The first method is based on a two-port representation of the line with the radiation effect (when present) included in the attenuation constant α_e as a loss in the line. On this basis the input impedance Z_{in} for a line of length d

and terminated by a load impedance Z_R is given by

$$Z_{in} = Z_{oe} \frac{Z_R + Z_{oe} \tanh \gamma d}{Z_{oe} + Z_R \tanh \gamma d} \text{ ohms} \quad (3.1)$$

when such a line is fed from a 50 ohm line, the resulting reflection coefficient Γ in the feed line is

$$\Gamma = \frac{Z_{in} - 50}{Z_{in} + 50} \quad (3.2)$$

If Z_R is varied, with Γ being monitored at the same time, a point will be reached when $Z_R = Z_{oe}$ and the MGL becomes properly terminated with Z_{in} equal to Z_{oe} or Z_R . At that point the current value of Γ will be equal to the value calculated from (3.2). When this happens, the current value of Z_R equals Z_{oe} regardless of d and γ_e . Further measurements yield α_e and β_e as well as the frequency response of the line.

The second method is based on scattering matrix arguments for a three-port system consisting of the input, output and radiation ports. Here the value of S_{11} is monitored as a function of frequency for the line when the second port is open and short circuited. Since the line is bilateral, $S_{11} = S_{22}$ and $S_{12} = S_{21}$ and hence a maximum of S_{12} corresponds to a minimum in S_{11} . The frequency at which this is observed also corresponds to maximum power radiated by the line and received by a dipole probe located near the line (i.e. maximum S_{13}). The approximate value of this frequency for our experimental line was found to be 5 GHz corresponding to a minimum VSWR of 1.175 observed using a network analyzer.

The same procedure was adopted when the MGL was allowed to radiate in the presence of discontinuities. Since one of the discontinuities examined is of the disc type, the effect on the input VSWR of moving the disc relative to the mouth of the feed launcher was studied. Table 3.4 shows this variation and indicates the optimum disc position at a given frequency for minimum VSWR which was found experimentally to correspond to maximum radiated field, again using a dipole probe. In this sense the sliding disc does not only radiate, but is also analogous to a series transformer or sliding screw tuner on a conventional transmission line.

In order to study the coupling loss of the leaky MGL and compare the data with that of the Radiax and Hitachi LCX cables, measurements were performed at 150 MHz and 150 KHZ. The 150 MHz measurements allow direct comparison with the manufacturer's data on Radiax cables specifically. The results for the radial power decay with an acrylic disc loaded MGL are given in Table 3.5 and can be used to estimate the coupling loss as indicated in the table. The receiving antenna used was the monopole probe described earlier, which was moved away from the line in the transverse plane. The results indicate that even at a 20 ft distance away from the line (where the probe output may be used to estimate the coupling loss) the received power is only 22 dB below the reference value at the outer surface. Although the variation shown is oscillatory in nature, the received power is still significantly higher than with the Radiax cables. It is obvious that even better results could be obtained with a different size and composition of the disc, or with more discs, or both.

The 150 KHz data was obtained outdoors, using a function generator (Interstate Electronic Corporation type F36 AM/FM) with CW 10 volts peak to peak output across 50 ohms. The field strength was measured using a calibrated 150 KHz - 32MHz Singer Radio Interference Field Intensity Meter (R.I.F.I.) model no. NM-25T, in conjunction with a loop pickup antenna and Stoddart Calculator part no. 21518, all borrowed from Communications Canada, Winnipeg office. The results are given in Tables 3.6 and 3.7, which indicate that even at a distance of 42 ft the measured field strength is significant and shows little dependence on extraneous signals due to environmental interference.

Table 3.4: Variation of VSWR with Disc PositionCentre Frequency = 5000 MHz

<u>Distance from the mouth of launcher (cms)</u>	<u>VSWR</u>
1	1.288
2	1.230
3	1.202
4	1.210
5	1.175
6	1.260
7	1.380
8	1.350
9	1.380
10	1.380
11	1.380
12	1.350
	1.550

Table 3.5: Measurement of Radial Power Decay at 150 MHz

Distance (Inches)	Relative Power in dB
0.0	0.0
5.2	9.0
14.2	12.5
23.2	13.5
32.2	15.5
41.2	15.0
50.2	15.0
59.2	16.5
68.2	16.5
71.2	17.0
80.2	17.5
89.2	13.5
98.2	17.5
107.2	16.5
116.2	11.5
125.2	10.5
134.2	17.5
143.2	20.0
152.2	16.5
161.2	11.5
170.2	10.0
179.2	10.5
188.2	20.0
197.2	17.5
206.2	14.5
215.2	16.5
224.2	18.0
233.2	21.0
242.2*	22.0
251.2	22.0

*This number corresponds to approximately 20 ft separation distance and could be used to estimate the coupling loss using the relation:

$$\begin{aligned} \text{coupling loss} &= P_{\text{line}}/P_{20}^d \\ &= [P_{\text{line}}/P_0^m] [P_0^m/P_{20}^m] [P_{20}^m/P_{20}^d] \end{aligned}$$

where P_{line} is the total power flowing in the surface wave line, while P_0^m and P_{20}^m refer to the powers received by a monopole or half wave dipole (superscripted by m and d, respectively) at 0 or 20 ft separation distance. The first bracket can be estimated from the transverse power distribution in the structure, the second bracket is the quantity measured and shown in the table and the last bracket is well known. The resulting estimate for the coupling loss in the present case is 42 ± 10 dB, which is reasonably confirmed by comparing the outdoor field strength data (at different frequencies) for the LCCX and leaky MGL cables based on the same input power from the same generator.

Table 3.6: Measurement of Field Intensity at 150 KHz
(Vertical Polarization)

<u>Distance (in Feet)</u>	<u>Field Intensity ($\mu\text{V}/\text{m}$)</u>
2	4,250
3	2,850
4	2,000
5	1,500
6	1,070
7	680
8	570
9	400
10	320
11	270
12	180
13	145
14	115
15	80
16	68
17	58
18	58
19	30.6
20	28.0
21	24.0
22	20
23	18
24	16
25	13
26	12
27	11
28	10
29	9
30	8
31	7
32	7
33	7
34	6.8
35	8.8
36	6
37	6
38	5.2
39	5.6
40	6.0
41	5.6
42	5.2

Table 3.7: Measurement of Field Intensity at 150 KHz(Horizontal Pol.)

<u>Distance (in feet)</u>	<u>$\mu\text{V/m}$</u>
2	18,000
3	11,300
4	6,450
5	4,000
6	2,850
7	2,000
8	1,400
9	1,000
10	800
11	620
12	500
13	400
14	320
15	285
16	200
17	170
18	135
19	120
20	100
21	90
22	72

Table 3.8: Variation of Field Intensity with Frequency at 20 ft.

<u>Frequency</u> <u>(MHz)</u>	Field Intensity ($\mu\text{V/m}$)	
	<u>Loop in Vertical</u> <u>Plane</u>	<u>Loop in Horizontal</u> <u>Plane</u>
0.150	130	40
0.600	290	90
1.5	710	115
3.0	1150	900

3.10. Discussion:

From an examination of the near field measurements, we observe the experimental feasibility of the MGL and leaky MGL. As noted earlier, the surface wave properties are largely governed by the launcher design which is frequency sensitive. As a result, the experimental line constructed for testing purposes appears to be suited for frequencies above 100 MHz. This was necessary in order to use the microwave anechoic chamber during the winter months. As a consequence of testing at microwave frequencies the coupling distance was automatically restricted to a short range. All attempts to test the line indoors below 100 MHz gave rise to some experimental difficulties mainly due to launchers and multiple reflections from surrounding objects. This is the reason why outdoor measurements could not be carried out until the weather and climatic conditions permitted.

Examination of the radial power decay data at 150 MHz indicates that significant power can be picked up with a short monopole and a laboratory signal generator and the level received is higher than that of commercial LCX cables tested under identical conditions. Even more power could be picked up if the number, position, size and composition of the disc discontinuity were to be optimized. However, it should be recognized that in practical applications the disc type of discontinuity may not at all be ideal or preferable to shaped slots, grooves, tapes, etc. (e.g. rectangular, circumferential or helical slots).

With respect to the 150 KHz data, the measured field strength is significant for either polarization, and can be directly related to practical applications, particularly for rural communications. However, the mechanism of radiation may not be the same as in the case of higher operating frequencies. In other words, the experimental leaky MGL might not be acting as a surface wave line, but possibly as a conventional monopole antenna over a ground plane. In any case the concept of a leaky MGL appears to be quite promising and may be still adaptable to existing power line installations. Further work would, of course, be necessary to optimize methods of coupling, receiving antenna design and, above all, the frequency.

3.11. References:

- [3.1] Goubau, G: 'Surface Waves and their application to transmission lines', J. Appl. Phys., 1950, 21, pp. 1119-1128.
- [3.2] Goubau, G: 'Single-conductor surface-wave transmission lines', Proc. IRE, 1951, Vol. 39, pp. 619-624.
- [3.3] Barlow, H.M. and Karbowski, A.E.: 'An investigation of the characteristics of cylindrical surface waves', Proc. IEE, 1953, 100, Pt.III, pp. 321-328.
- [3.4] Barlow, H.M. and Brown, J.: 'Radio Surface Waves', (Oxford University Press, 1962).
- [3.5] Kiely, D.G.: 'Dielectric aerials', Methuen's Monographs on Physical Subjects (Methuen, 1953).
- [3.6] Rao, T.C.K. and Hamid, M.A.K.: 'Propagation characteristics of a dielectric-coated conducting surface-wave transmission line with an intervening airgap, Proc. IEEE, 1976, (10), pp. 973-980.
- [3.7] Rao, T.C.K. and Hamid, M.A.K.: 'Frequency bandwidth of the Modified Goubau Line', Proceedings IEE, in press, July 1977.
- [3.8] Towaij, S.J. and Hamid, M.A.K.: 'Radiation by a dielectric loaded cylindrical antenna with a wall airgap', Proc. IEE, 1972, 119, (1) pp. 48-54.
- [3.9] Mohnsen, A., Kashyap, S.C., Boerner, W.M., and Hamid, M.A.K. 'Field distribution in multi-layered dielectric-loaded rectangular waveguides', Proc. IEE, 1970, 117, pp. 709-712.
- [3.10] Rao, T.C.K. and Hamid, M.A.K.: 'On the excitation of surface waves over the Modified Goubau Line by a Coaxial Waveguide'. Paper presented at the URSI International Electromagnetic Symposium, June 20-24, 1977, Stanford University, Palo Alto.

- [3.11] Boulanger, R.J. and Hamid, M.A.K.: 'A new type of dielectric-loaded waveguide antenna', Microwave Journal, Vol.13, No.12, Dec. 70, pp. 67-68.
- [3.12] Towaij, S.J., Martens G. and Hamid, M.A.K.: 'A dielectric loaded circular waveguide antenna', IEEE Trans Ant and Propagation, Vol. AP-20, No.1, Jan. 1972, pp. 96-97.
- [3.13] Semenov, N.A.: 'Wavemodes in a surface waveline' Radio Engg. and Electron Phys., 1964, 1969, pp. 989-995.
- [3.14] Beal, J.C. et al: 'Continuous access guided communication (CAGC) for ground transporation systems', Proc. IEEE, 1973, 61 (5), pp. 562-568.
- [3.15] Gallawa et al: 'The surface wave transmission line and its use in communication with high-speed vehicles', IEEE Trans. Commun. Technol., COM-17, 1969, pp. 518-525.
- [3.16] Rao, T.C.K. and Hamid, M.A.K. 'Effects of disc and strip type discontinuities on the modified Goubau line', IEEE Trans. on Microwave Theory and Techniques, submitted for publication, May 1977.
- [3.17] Rao, T.C.K. and Hamid, M.A.K.: 'On the coaxial excitation of the modified Goubau line, Radio Science, submitted for publication, July 1977.
- [3.18] Rao, T.C.K. and Hamid, M.A.K.: 'Near-field measurements over an experimental modified Goubau line, Proceedings IEE, in press, July 1977.

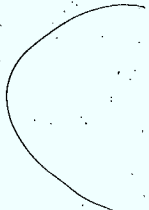
LEAKY COIL-COUPLED COAXIAL SYSTEM (LCCX)

4.1 Introduction:

As pointed out in Chapter 1 the existing leaky coaxial system designs are based on specific applications, none of which is suitable or economical at the lower frequencies where our real interest lies for rural communications. Thus, the six known commercial systems (Loose-braid, Radiax, Continuous Slot, Iniex-Delogne, Zig-zag and CERT) were not intended for low loss long distance rural communications as presently needed for sparsely populated areas of Canada. These systems involve somehow or another a disturbance of the wall current on the outer conductor resulting in radiation. The proposed system (LCCX) is based on the simple idea of duality, in the sense that the magnetic, rather than the electric, field is used for producing the radiated signal. It is anticipated that, once the proposed system is fully developed, it will retain the merits of the existing systems and will be applicable to new areas such as low frequency rural as well as urban communications.

Although the proposed system involves a coaxial line, it should be noted that adaptation to existing power lines may become feasible and economical, provided that the additional interference is resolved by proper design.

The proposed system is shown schematically in Fig. 4.1. It consists of an air-filled coaxial line, together with a rectangular four-arm coil where three of the arms (arms 1, 2 and 3) are inside the coaxial line while the fourth (arm 4) may be



inside or outside the line. Fig. 4.1 shows the latter case where arm 4 is outside the line and hence acts as the radiating element. If arm 4 is inside the line, it would be located close to the inner surface of the outer conductor, while arm 2 will be close to the inner conductor so that maximum flux linkage takes place while the induced voltage across the terminals will be used to feed an antenna, which could possibly be a loop (not shown). In either case, the dimensions of the coaxial line, the coupling coil (whether it is leaking through arm 4 or feeding a separate antenna), frequency, coil to coil separation along the coaxial line, determine the field strength at the observation point and are, therefore, subject to design optimization.

As is well known in electromagnetic theory, the flux linkage with a coil of fixed area A increases linearly with the number of turns N and the induced power increases by N^2 . A similar dependence is expected if the area rather than the number of turns is varied. The actual shape of the loop is immaterial provided that the field between the conductors is uniform, which is not the case in a coaxial line as will be shown later.

The basic theoretical concepts and relations underlying the proposed scheme are presented in the next section. It should be pointed out that although the system appears to be simple, there are, in fact, many unresolved questions which need further theoretical and experimental investigations.

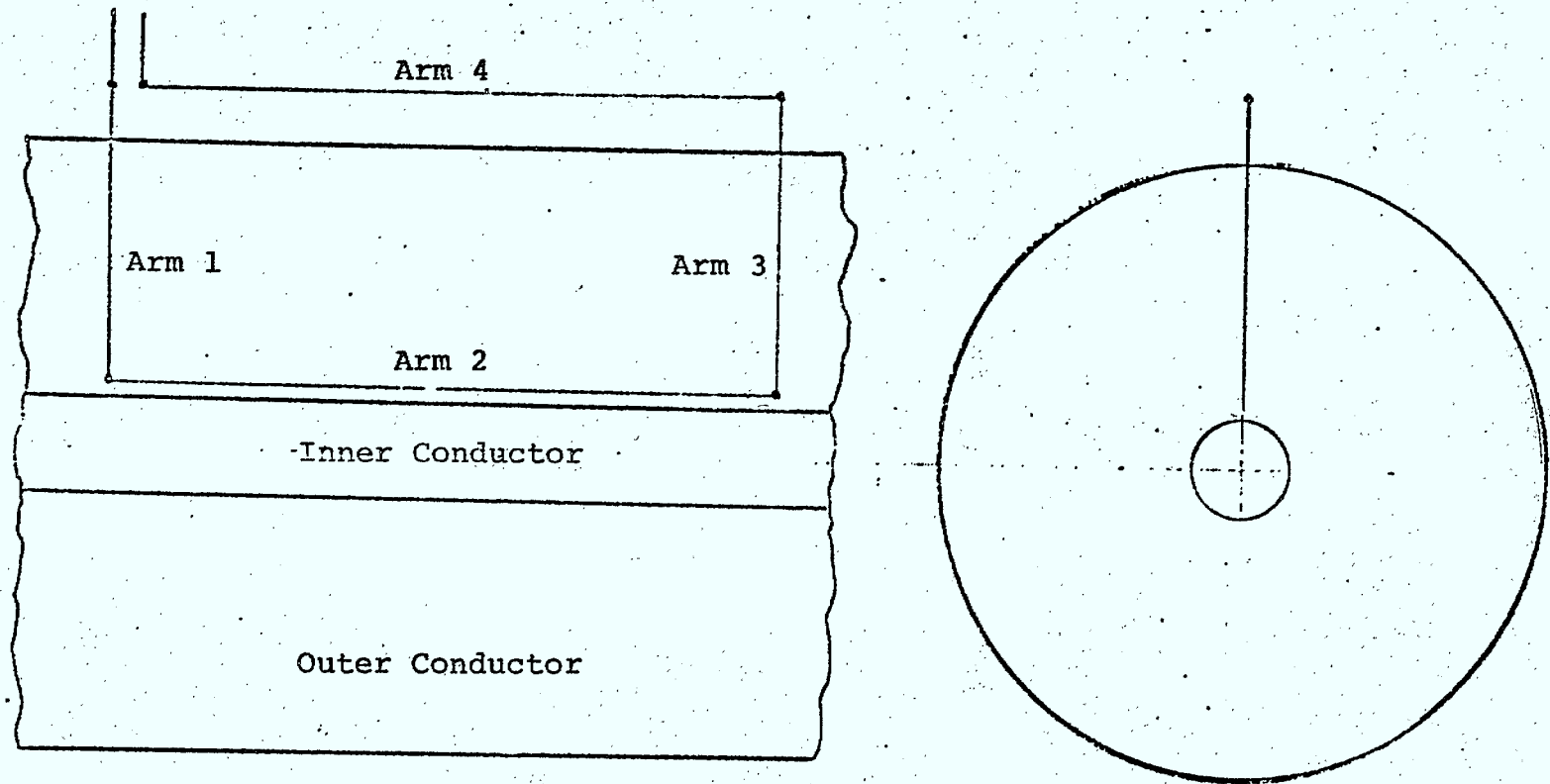


Fig. 4.1 Schematic Diagram of the Proposed System (LCCX)

4.2 Theory:

To understand the basic principles underlying the proposed system, it is necessary to review some of the theoretical concepts of a conventional coaxial line. This is done in the following sections.

4.2.1 Characteristic Impedance of a Coaxial Line:

The characteristic impedance of a coaxial line (see Fig. 4.2) of inner and outer radii equal to R_1 and R_2 , respectively, is given by [4.1]

$$\begin{aligned} Z_0 &= \frac{138}{\sqrt{\epsilon_r}} \log_{10} \frac{R_2}{R_1} \\ &= \frac{60}{\sqrt{\epsilon_r}} \log_e \frac{R_2}{R_1} \end{aligned}$$

where ϵ_r is the relative dielectric constant of the region between the conductors and equals unity in the case of an air region.

4.2.2 Magnetic Field Inside a Coaxial Line:

Figure 4.2 shows a coaxial cable cross-section where the radius of the inner conductor is denoted by R_1 and the radii of the inner and outer surfaces of the outer conductor are denoted by R_2 and R_3 , respectively. The current densities in the inner and outer conductors are denoted by \vec{J}_1 and \vec{J}_2 , respectively, and the permeability of the space in between is denoted by μ . If the central axis of the cable is along the z-axis and the frequency is low enough to ensure that the skin effect is negligible, then

$$\begin{aligned} \vec{J}_1 &= \frac{I}{\pi R_1^2} \hat{k}, & R < R_1 \\ \vec{J}_2 &= \frac{-I}{\pi(R_3^2 - R_2^2)} \hat{k}, & R_2 < R < R_3 \end{aligned}$$

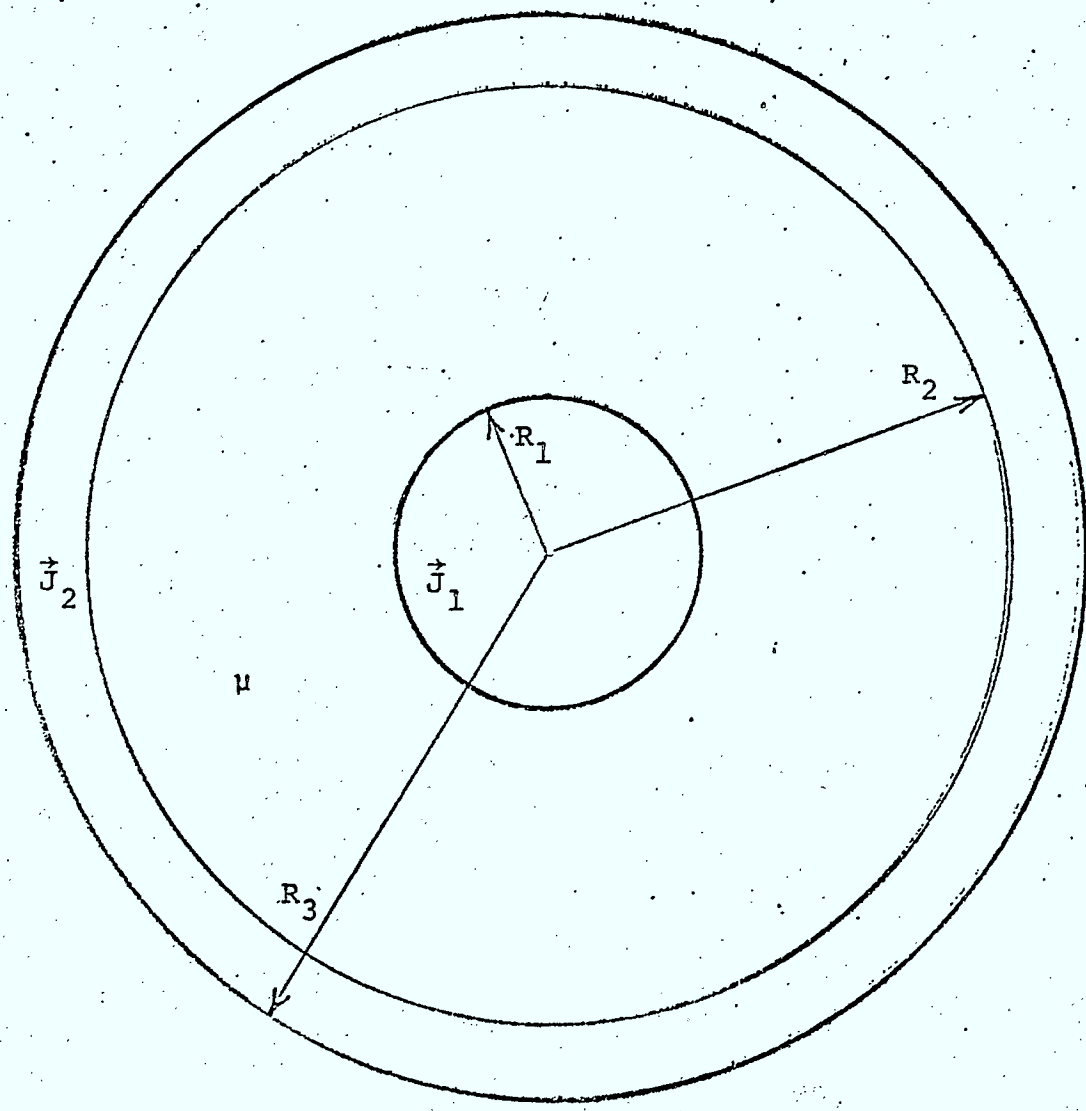


Fig. 4.2 Schematic Diagram of Coaxial Cable Cross-Section

where I is the total current in the line and \hat{k} is a unit vector along the z -axis. For $R < R_1$, Ampere's law gives

$$\oint_{C_1} \vec{H} \cdot d\vec{l} = \int_{S_1} \vec{J} \cdot \hat{n} \, dS$$

$$\int_0^{2\pi} H_\theta \hat{\theta} \cdot R d\theta \hat{\theta} = \int_0^R \int_0^{2\pi} \frac{I}{\pi R_1^2} \hat{k} \cdot \hat{k} \, R dR d\theta$$

which leads to the result

$$\vec{H} = \frac{I}{2\pi R_1^2} R \hat{\theta}, \quad 0 \leq R \leq R_1$$

where \hat{n} is a unit normal to a cylindrical surface of radius R while $\hat{\theta}$ is a unit vector in the polar direction or direction of the magnetic field H_θ . Similarly we can show that

$$\vec{H} = \frac{I}{2\pi R} \hat{\theta}, \quad R_1 \leq R \leq R_2$$

and

$$\vec{H} = \frac{I}{2\pi R} \left[\frac{R_3^2 - R^2}{R_3^2 - R_2^2} \right] \hat{\theta}, \quad R_2 \leq R \leq R_3$$

If the flux linkages in the inner conductor are denoted by λ_1 , then

$$\lambda_1 = \int_0^1 \int_0^{R_1} \frac{IR\mu}{2\pi R_1^2} \hat{\theta} \cdot \hat{\theta} \, dR \, dz \frac{\pi R^2}{\pi R_1^2} = \frac{\mu I}{8\pi}$$

hence

$$L_1 = \lambda_1 / I_1 = \mu / 8\pi \text{ henrys/meter}$$

similarly for region $R_1 < R < R_2$

$$L_2 = \frac{\mu}{2\pi} \ln \frac{R_2}{R_1}$$

while for the region $R_2 < R < R_3$

$$L_3 = \frac{\mu}{2\pi [R_3^2 - R_2^2]} \left[R_3^4 \ln \frac{R_3}{R_2} - \frac{R_3^2 (R_3^2 - R_2^2)}{R_2} - \frac{1}{4} (R_3^4 - R_2^4) \right] \text{ henrys/meter}$$

The total line self inductance is hence given by

$$L = L_1 + L_2 + L_3.$$

4.2.3 Coupling by a Rectangular Loop:

In order to predict the voltage induced by the loop, we designate the lengths of the four arms as l_1, l_2, l_3 and l_4 , respectively. Furthermore, we designate the distance between arm 2 and the inner conductor as d_2 , with the distance between arm 4 and the outer conductor as d_4 when arm 4 is inside the line and d_4' when it is outside. The radii of the inner and outer conductors are denoted by R_1 and R_2 , respectively.

Using the R, θ, z cylindrical coordinate system, we note that the voltage induced in the coil when arm 4 is inside the line is given by the time rate of change of the magnetic flux times the number of turns in the loop, i.e.

$$\begin{aligned} v &= -N \frac{d\phi}{dt} = j\omega N \int_S \vec{B} \cdot \hat{n} \, da, \quad (S = \text{loop area}) \\ &= -j\omega \mu N \int_S \frac{I}{2\pi R} \hat{\theta} \cdot \hat{\theta} \, dRdz \end{aligned}$$

$$\begin{aligned}
 &= \frac{-j\omega\mu N I \ell_2}{2\pi} \int_{d_2}^{R_2 - d_4} \frac{dR}{R} \\
 &= \frac{j\omega\mu N I \ell_2}{2\pi} \ln \frac{R_2 - d_4}{d_2}
 \end{aligned}$$

while in the case where arm 4 is outside the line, the induced voltage is given by

$$v = \frac{j\omega\mu N I \ell_2}{2\pi} \ln \frac{R_2}{d_2}$$

The above relations suggest that the induced voltage is linearly dependent on the radian frequency (ω), number of turns (N), permeability of the medium between the conductors (μ), driving current (I), length of the loop parallel to the inner conductor (ℓ_2) and nonlinearly on the separation distances between the loop and the conductors (d_2 and d_4). It should, however, be noted that the induced voltage is very sensitive to d_2 which suggests that v or v' can be adjusted in practice by varying d_2 possibly through a micrometer arrangement.

4.2.4 Radiation by a Short Wire:

Since arm 4 is the radiating element whose length L is short relative to the operating wavelength, it may be assumed that it is a short wire antenna or short dipole with uniform current distribution. If the peak current in the wire is denoted by I_0 , then the non-vanishing radiation field components are E_θ and H_ϕ which are given by [4.2]

$$E_\theta = \frac{j\omega I_0 L \sin\theta e^{j\omega(t - r/c)}}{4\pi\epsilon c^2 r}$$

$$H_\phi = E_\theta / 120\pi$$

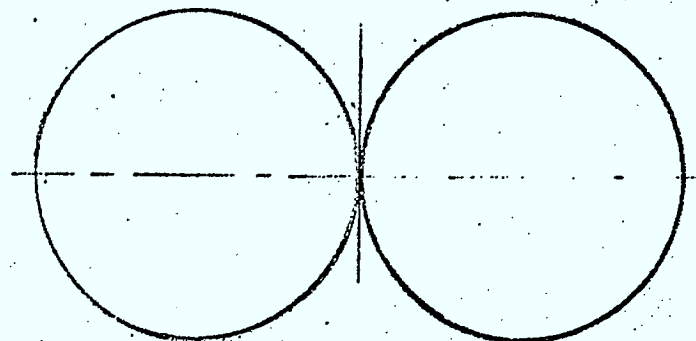
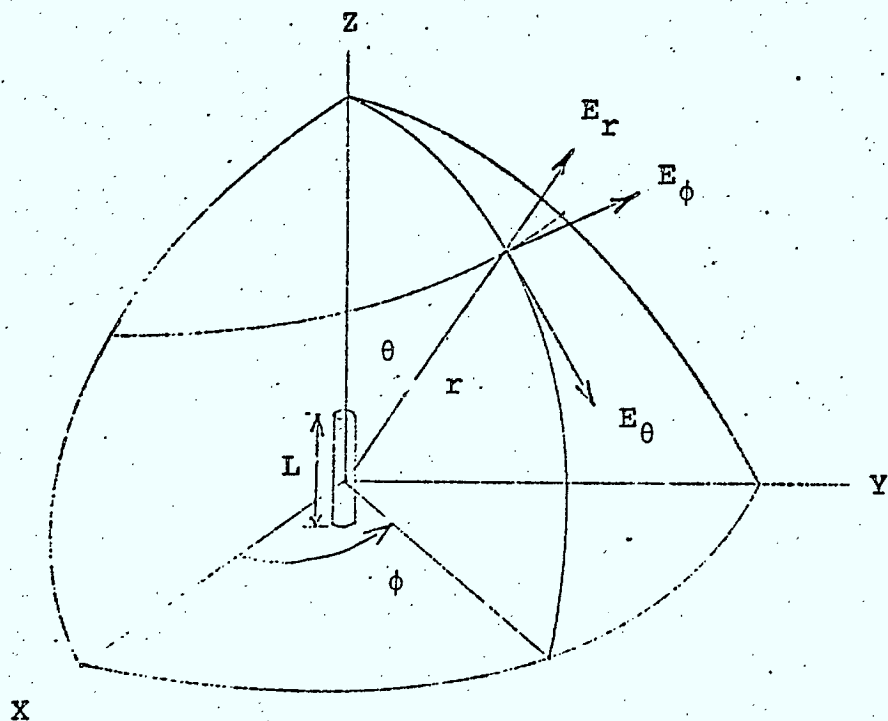


Fig. 4.3 Coordinates and Radiation Pattern of a Short Wire Antenna

where c is the velocity of light, ϵ is the permittivity of the medium and the coordinate system is as shown in Fig. 4.3. The resulting far electric field pattern is also shown in Fig. 4.3 and is in the form of a figure eight as is well known. However, it must be noted that the pattern will be modified by the presence of the cylinder forming the outer conductor of the line which is grounded.

4.2.5. Radiation Pattern of a Short Loop Antenna:

A short loop antenna may be circular or square in shape and is equivalent to a short magnetic dipole. The radiation pattern of a square or circular loop is the same and is given for the non-vanishing far field components by [4.2].

$$E_{\phi} \text{ (instantaneous)} = \frac{120\pi^2 [I] \sin\theta}{r} \frac{A}{\lambda^2}$$

where A is the area of the loop, $[I]$ is the retarded current, λ is the wavelength and r is the distance to the observation point (see Fig. 4.4). Alternatively $E_{\phi} \text{ (peak)} = \frac{120\pi^2 I_0 \sin\theta A}{r \lambda^2}$

where I_0 is the peak current in time in the loop and

$$[I] = I_0 e^{j\omega(t-r/c)}$$

and

$$H_{\theta} = E_{\phi} / 120\pi$$

Consequently, the field pattern in the plane of a circular loop with uniform current is a circle due to symmetry. In the elevation plane (i.e. off the polar axis) the power pattern is a figure eight as shown in Fig. 4.5. It should be noted that the approximation of a circular loop by a square loop is only good up to loop diameters equal to $\lambda/10$.

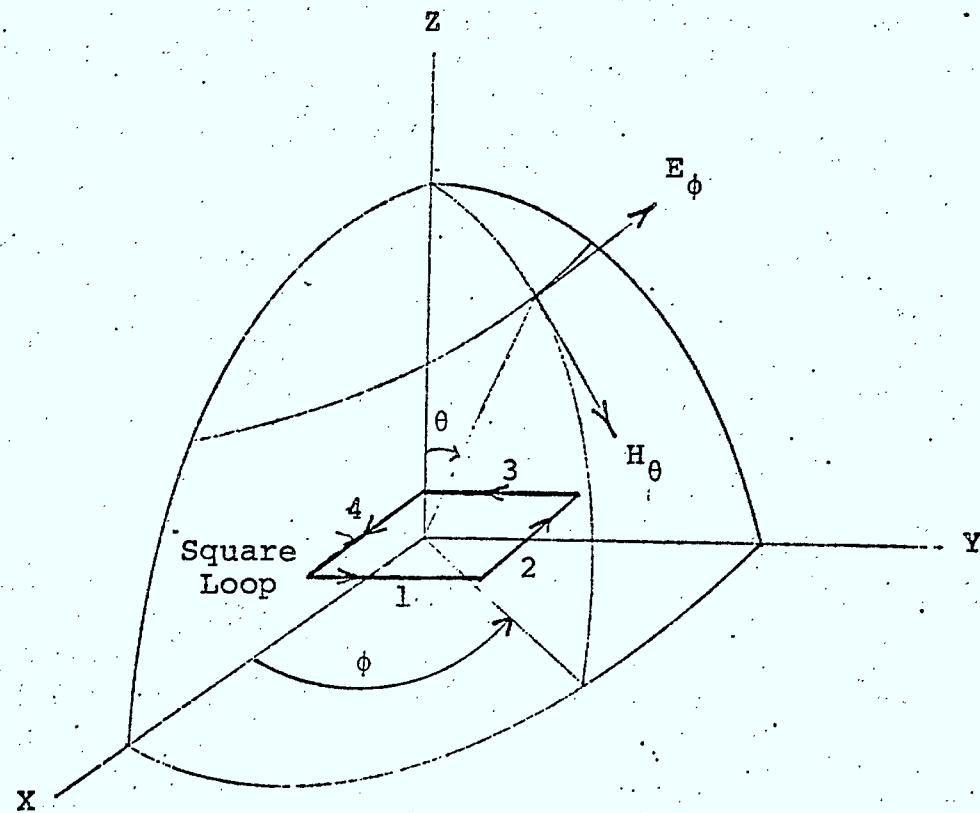


Fig. 4.4 Coordinate System Used for Determining Radiation from a Loop Antenna

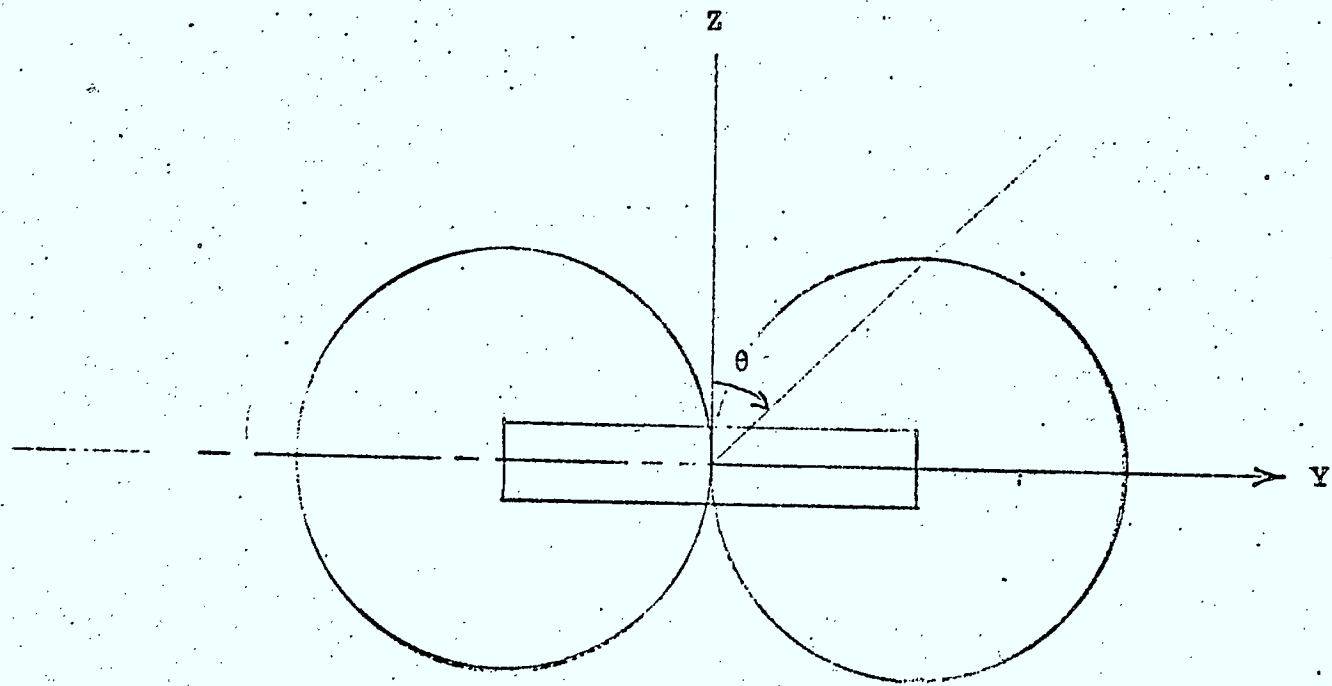


Fig. 4.5 Radiation Pattern of a Small Loop Antenna

The radiation resistance of a small loop of one or more turns is given by

$$R_r = 31,200 N^2 A^2 / \lambda^4 \text{ ohms}$$

where N is the number of turns and A is the area of the loop (i.e. πa^2 for a circular loop and d^2 for a square loop).

Various techniques are known in the literature for increasing the loop diameter, and yet maintaining the uniformity of current distribution [4.3].

4.3. Experimental Investigations:

The experimental program consisted primarily of indoor and outdoor measurements carried out over an experimental line with different leaky coil arrangements and over the 10KHz to 3MHz frequency range. The oscillator used is the IEC F36 AM/FM function generator already mentioned. The receivers used were the HP spectrum analyzer and Singer R.I.F.I., already mentioned, plus HP vector voltmeter, type 8405A, and HP RMS voltmeter type 3400A.

4.3.1. Experimental Line:

The experimental coaxial line consisted of an aluminum pipe forming the outer conductor and a copper pipe forming the inner conductor with the dimensions selected to yield a characteristic impedance of almost 50 ohms as shown in Fig. 4.6. The dimensions were intentionally chosen to be large to allow for flexibility and convenience of locating and aligning the leaky coil.

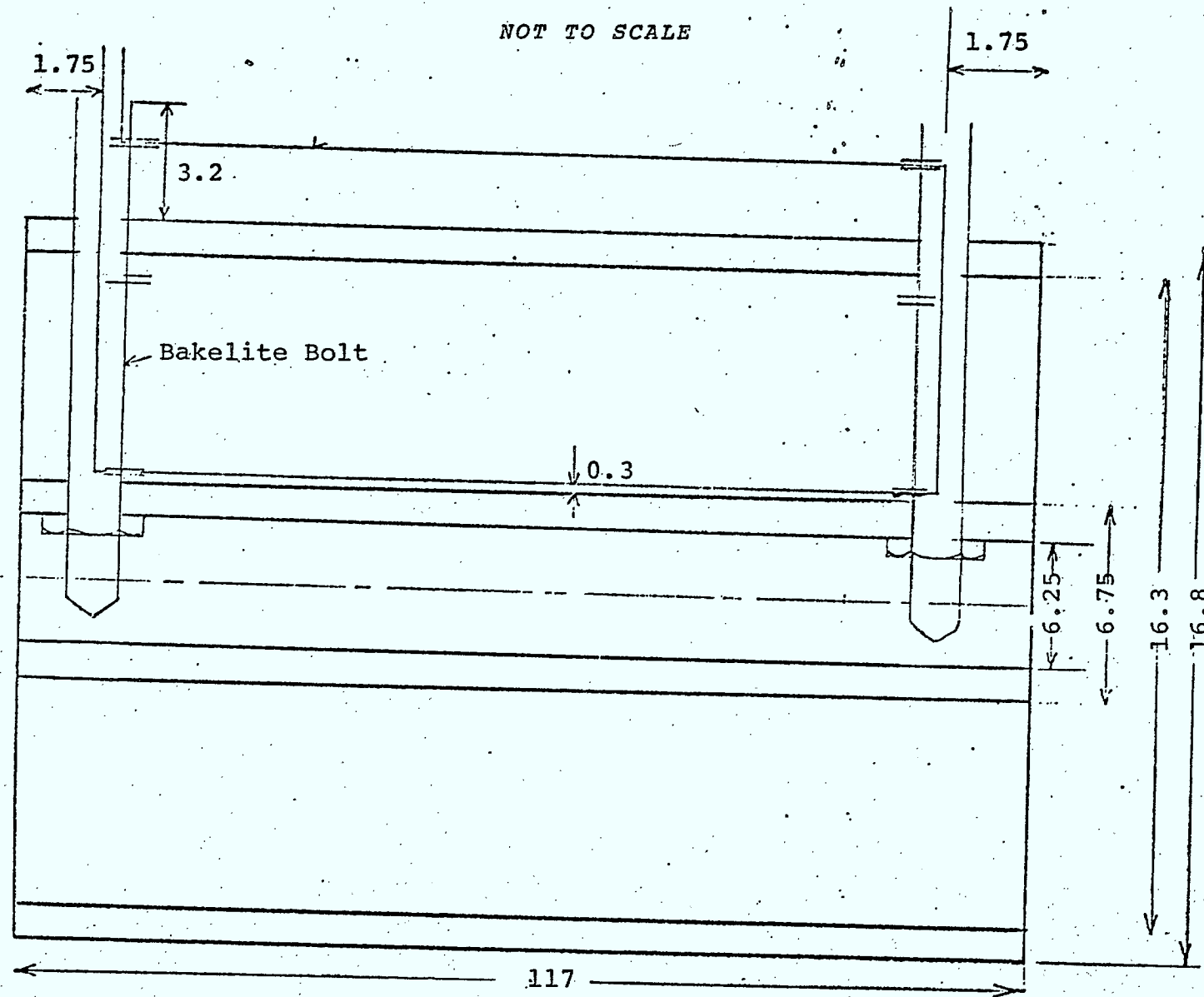
The two ends of the line were connected to N-type connectors to allow for feed from the oscillator and for terminating the line with 50 ohms. The inner conductor was supported in position

and insulated from the grounded outer conductor with the aid of two bakelite discs, one at each end, and such that the entire assembly was rigid.

In order to position and align the coil, two bakelite posts were located, one near each end of the line, and such that they partially protruded through both inner and outer conductors. Each post was threaded on the outside and the lower end was tightened inside the copper pipe with a bakelite nut while the upper end was allowed to extend above the outer conductor surface as shown in Fig. 4:6. Each bolt was bored with an axial hole and three small side holes were also drilled. The enameled wire (Canada wire polythermaleze, size 24) was fed through the axial hole of one bolt and was taken out through the bottom side hole and run through parallel to the inner conductor until the bottom side hole of the second bolt. After stretching, the wire was pulled through the axial hole of the second bolt until either the middle or top side hole (depending on whether arm 4 was to be inside or outside the coaxial line, respectively). The wire was then run through parallel to the outer conductor until the first bolt where it was wrapped and secured leaving the wire terminal for connection together with the starting end. The procedure is repeated to increase the number of turns.

4.3.2. Indoor Experiments:

A number of simple experiments were initially performed to test the basic feasibility of the concept and line construction. The sequence of experiments was as follows:



*all dimensions in centimeters

Fig. 4.6 Geometry of the Experimental Line

Experiment No. 1: The continuity of the coil wire, insulation between the inner and outer conductors, insulation between the coil (single turn) and conductors were tested and confirmed using a VTVM.

Experiment No. 2: With a single turn coil and with arm 4 inside (i.e. coil not leaking) and outside (i.e. coil leaking) the voltage induced was measured as a function of frequency. Table 4.1 presents the results when an RMS voltmeter was employed while Table 4.2 presents the results when the coil terminals were fed directly into the spectrum analyzer. The increase in voltage when arm 4 is outside is obviously due to the larger area of the coil and the larger flux area linked by it.

Experiment No. 3: With arm 4 outside and at a fixed frequency of 3.0 MHz the spectrum analyzer and the loop antenna of the Singer R.I.F.I. meter were used to measure the qualitative effect of moving arm 4 at random and away from being parallel to the outer conductor. The observed variation was below 5 dB for all cases tested. This test confirmed the insensitivity to surroundings and potential of the system.

Experiment No. 4: Since the standard definition of the coupling loss is based on a physical distance of 20 ft away from the line, indoor measurements of the field strength at 20 ft were carried out as a function of frequency using the Singer R.I.F.I. The results are given in Table 4.3.

Experiment No. 5: This experiment is basically a repetition of Experiment No. 2, except for the number of turns which is four(4) in this case. The results are presented in Table 4.4 and show

Table 4.1: Voltage Induced by a Single Turn Loop Using
an RMS Voltmeter (Experiment No. 2)

Noise Level \approx 0.25 millivolts
Generator Voltage: 10 V peak to peak

Frequency	Measured Voltage at Coil Terminals (in Millivolts)	
	Coil Not Leaking*	Coil Leaking**
10 KHZ	0.85	1.20
15 KHZ	1.25	1.50
25 KHZ	2.00	2.30
40 KHZ	3.00	3.50
50 KHZ	3.80	4.30
100 KHZ	7.50	8.40
200 KHZ	15.00	16.00
350 KHZ	26.00	29.00
500 KHZ	37.50	41.00
750 KHZ	57.50	63.00
1 MHZ	75.00	84.00
2 MHZ	160.00	180.00
3 MHZ	270.00	300.00

*Arm 4 in this case is approximately 0.3 cm below
the inner surface of the outer conductor
(i.e. $d_4 = 0.3$ cm)

**Arm 4 in this case is approximately 0.3 cm above
the outer surface of the outer conductor
(i.e. $d'_4 = 0.3$ cm)

Table 4.2: Voltage Induced by a Single Turn Loop Using
HP Spectrum Analyzer (Experiment No. 2)

Generator Maximum Output: 10 V peak to peak

Reference Level: Generator output (0 dB)
when fed directly to Spectrum
Analyzer

Frequency	Measured Voltage at Coil Terminals (in dB)	
	Coil Not Leaking*	Coil Leaking**
10 KHZ	-70	-70
20 KHZ	-64	-65
30 KHZ	-61	-60
50 KHZ	-57	-56
100 KHZ	-51	-50
150 KHZ	-48	-46
200 KHZ	-46	-44
300 KHZ	-41	-40
500 KHZ	-37	-36
750 KHZ	-34	-33
1 MHZ	-31	-30
2 MHZ	-25	-25
3 MHZ	-22	-22

*Arm 4 in this case is approximately 0.3 cm
below the inner surface of the outer
conductor (i.e. $d_4 = 0.3$ cm)

**Arm 4 in this case is approximately 0.3 cm
above the outer surface of the outer
conductor (i.e. $d'_4 = 0.3$ cm)

Table 4.3: Measured Field Strength at 20 ft vs Frequency
(Experiment No. 4)

Frequency (MHZ)	Field Strength (μ V/m)
0.150	1.6
0.200	1.8
0.250	2.1
0.600	3.2
0.750	---
1.000	4.0
2.000	6.2
3.000	22.0

Table 4.4: Measurement of Voltage Induced with a
4-turn Coil inside the Coaxial Line

Frequency (MHZ)	Voltage Induced (Millivolts)
0.010	2.65
0.020	5.20
0.030	8.00
0.050	13.00
0.075	20.00
0.100	26.00
0.200	52.00
0.300	78.00
0.500	140.00
0.750	215.00
1.00	320.00
2.00	1250.00
3.00	7300.00

the expected dependence on the number of turns and frequency within experimental accuracy.

4.3.3 Outdoor Experiments:

In the outdoor experiments, the test LCCX line was employed both as a transmitter and as a receiver with the variables being the frequency, number of turns and coupling distance. Both transmitter and receiver were horizontally polarized.

Tables 4.5 and 4.6 present the results for a single turn coil of the field strength with frequency and coupling distance, respectively.

Tables 4.7 and 4.8 present similar results for a four turn coil as a function of frequency and coupling distance, respectively.

Tables 4.9 and 4.10 are similar to Tables 4.7 and 4.8 except that the test line is used as a receiver.

4.4 Discussion:

Examination of our results for the LCCX line shows that the novel concept of magnetic field coupling in order to feed the radiating element of the leaky line is simple and particularly promising for the lower frequencies, which are of utmost interest.

In order to establish the concept, the dimensions of the experimental line were deliberately chosen large enough for convenience of construction and testing. Even in the few experiments discussed earlier, the behaviour of the line is promising as expected, and deserves more attention in the future. In particular, design charts showing the behaviour with coil size and shape, number of coils per unit length, wire size, number of turns and frequency need to be obtained.

Table 4.5: Variation of Field Intensity ($\mu\text{V}/\text{m}$) with Frequency
(Single Turn)
(Receiving Antenna in Horizontal Position at 20 ft)

Frequency (MHZ)	Field Intensity ($\mu\text{V}/\text{m}$)
0.100	40
0.200	36
0.300	20
0.600	45
0.700	28
1.00	32
2.00	45
3.00	50

Table 4.6: Variation of Field Intensity ($\mu\text{V/m}$) with Distance
(Single Turn), Frequency = 150 KHZ

Distance (Feet)	Field Intensity ($\mu\text{V/m}$)
2	1400
3	420
4	--
5	125
6	--
7	105
8	63
9	40
10	30
11	12.5
12	9.0
19	6.2 - 5.0
20	5.0 - 6.2

Table 4.7: Variation of Field Intensity ($\mu\text{V}/\text{m}$) with Frequency
Receiving Antenna Fixed at 20 ft (4-turn Coil)
Line Terminated in 50 ohms

Frequency (MHZ)	Field Intensity ($\mu\text{V}/\text{m}$)
0.150	3.6
0.200	- -
0.250	2.5
0.300	1.9
0.600	4.8
0.750	3.5
1.0	5.0
2.0	50.0
3.0	90.0

Table 4.8: Variation of Field Intensity ($\mu\text{V/m}$) with Distance
Frequency = 150 KHZ (4-turn Coil)

Distance (Feet)	Field Intensity ($\mu\text{V/m}$)	
2	3600	- 4000
3	1150	- 1600
4	450	- 500
5	160	- 180
6	--	--
7	--	--
8	125	- 145
9	100	
10	64	- 80
11	50	- 55
12	36	- 40
13	20	- 23
14	8.0	- 11.5
15	--	--
16	--	--
17	8.0	- 8.5
18	7.0	- 10
19	--	--
20	3.8	

Table 4.9: Variation of Electric Field Intensity with Frequency
Line Used as a Receiver (4-turn Coil)
Transmitter Fixed at 20 feet

Frequency (MHZ)	Field Intensity ($\mu\text{V}/\text{m}$)
0.150	--
0.200	76
0.300	--
1.500	121
2.000	225
3.000	380

Table 4.10: Variation of Electric Field Intensity with Distance
 Line Used as a Receiver (4-turn Coil)
 Transmitter Frequency = 150 KHZ, Horizontal Polarization

Distance (Feet)	Electric Field Intensity ($\mu\text{V/m}$)
2	1770 - 2850
3	1110 - 1580
4	490 - 792
5	396 - 445
6	197 - 254
7	- -
8	177 - 222
9	- -
10	111 - 127
14	39.6 - 44.5
15	34.8 - 39.6

Also, further work is needed on coil to coil separation along the length of a coaxial line of given dimensions and the resulting transmission loss and radiated field strength. This is in spite of the significant field strengths measured with one coil of one turn.

The simplicity of the proposed LCCX line and the obvious flexibility in its design suggest that it could have a wider scope of applications than conventional LCX lines. In particular, its performance at lower frequencies is most encouraging and worth considering for future rural communication systems.

4.5 References:

- [4.1] Reference Data for Radio Engineers, 4th Edition, International Telephone and Telegraph Corporation, 1956, Ch. 20, p. 249.
- [4.2] Kraus, J. D., Antennas, McGraw Hill, 1950, Chapter 5 and 6.
- [4.3] Jasik, H., Antenna Engineering Handbook, McGraw-Hill, 1961, p.6.3.

GENERAL DISCUSSION

Perhaps the most difficult part of this project was the reproducibility of measurement data at the lower frequencies (below 1 MHz) where available equipment and facilities presented difficulties. Although most of the difficulties were overcome towards the end of the project, using the outdoor lab and reliable equipment borrowed from outside, more effort should, nevertheless, be directed in the future towards alternative measurement methods, particularly at the lower frequencies.

Since a total of five cables were tested in the laboratory, some comments will be offered first concerning observations drawn from specific tables. Three summary tables will then be presented followed by a discussion in the form of a proposal for further contract work on the LCCX cable.

Table 2.8 seems to indicate that the product $E r^2$ is fairly constant, where E denotes the field strength and r the distance between the transmitting and receiving antennas (one of which is the test line). This may be useful for modelling and implies that a 20 ft long LCX cable acts as a short element current radiator, since the $1/r^2$ behaviour is due to the induction term in the radiated field strength corresponding to the 20 ft coupling distance. Thus at the lower frequencies, where applications to rural communications are desirable, the 20 ft coupling distance used to define the coupling loss is a near field distance. This is an argument for changing this distance in the case of rural communications for which present commercial LCX cables are not designed.

With respect to the large coupling loss values in Table 2.9, it should be noted that in conventional environments the corresponding figure is of the order of -134 dB as observed by Martin [1.1, p.5] at a much higher frequency where the transmission losses are obviously larger.

Reference to Table 3.5 indicates that at a distance of 20 ft and frequency of 150 MHz the relative power measured is only 22 dB below the value on the surface, which shows a reasonable external radial power decay characteristic. Obviously the power received by the monopole probe at zero distance is related to the total surface wave power in the line through the internal power profile characteristic extending from the inner conductor surface through the airgap to the outer surface of the dielectric. Based on this behaviour, it is possible to estimate the power profile characteristic, which, along with the 22 dB figure, yields an estimated coupling loss of $42 \text{ dB} \pm 10 \text{ dB}$, as already explained in Chapter 3. On the other hand, commercial LCX and Radiax cables have a published coupling loss ranging from $57 \text{ to } 75 \text{ dB} \pm 10 \text{ dB}$ at the same frequency. Another observation, which shows the advantage of disc loading, can be drawn from Table 3.4 which indicates the feasibility and flexibility (particularly in relation to commercial LCX cables) of controlling the power delivered to the line or minimizing the input VSWR. Hence the idea of disc loading is novel, simple, flexible and quite effective in improving the behaviour of the MGL and therefore deserves further investigation, particularly with regard to optimization of the number of discs and the composition and geometry of each disc for a given MGL. This is particularly

due to the additional effort and cost to construct the line with such discs and the tolerances involved in any potential manufacturing of the cable.

Table 3.7 implies a slower rate of decay of radiated power in the radial direction at 1.5 GHz, which indicates an advantage due to disc loading at the larger distances (beyond approximately 10 cm). Hence significantly higher field strengths can be obtained when the MGL is loaded with a single disc. However, the addition of further discs does not necessarily lead to a higher radiated field strength, but serves the purpose of tuning out line mismatch (caused by bends, connectors, etc.) between successive discs. It should be emphasized that the higher radiated power, due to a disc discontinuity, is associated with higher "insertion loss per disc or subscriber" and consequently less power is available to the next subscriber. This difficulty could be overcome by conventional repeater techniques or higher input power to the line, keeping in mind that the larger insertion loss in this case is largely attributed to disc radiation rather than the remaining small conductor, dielectric and launching losses.

It should be pointed out that the apparent difference of about 10 dB between the data in Tables 4.1 and 4.2 is due to the fact that Table 4.1 is based on RMS voltage measurements, while Table 4.2 is based on a spectrum analyzer measurement. When Table 4.2 is corrected to RMS readings above zero (instead of peak to peak) the resulting data will be reasonably close to that of Table 4.1. In spite of this, Table 4.2 is still considered unreliable because of original lack of calibration accuracy of the spectrum analyzer and difficulty in reading accurately off the screen with a scale of 20 dB/cm.

Tables 4.1 and 4.4 indicate that as N increases from 1 to 4, the induced voltage also increases with frequency by approximately the same ratio (as expected from section 4.2.3) up to around 1 MHz. Also, Tables 4.6 to 4.10 show the expected behaviour with frequency and distance, except for some minor oscillations which are probably due to near field effects and scattering from nearby objects.

Although the LCCX cable proved feasible for both transmission and reception in a preliminary way, it should be pointed out that some circuit difficulties are expected in practice due to the low characteristic impedance (Z_0) of the overall line. The reason for a low Z_0 is the coil wire near the center conductor, which forms a type of parallel wire line with short separation distance. Therefore, as soon as the LCCX line is made long enough to accommodate one or more coils, some method of matching (e.g. using a series transformer or a discrete network) must be devised. Alternatively, the change in Z_0 could probably be made gradual by redesigning the end coils into a trapezoidal (rather than rectangular) shape.

Finally, the salient results for all cables tested are compiled in Summary Tables 1 to 3. The variations of field strength and coupling loss with distance are not shown in these tables. Furthermore, no attenuation loss data are shown for the MGL and LCCX due to lack of definition or lack of a sufficiently long line to make a meaningful measurement at low frequencies. The latter reason is also why no coupling loss data are presented for the LCCX line. However, the tables basically confirm and extend to lower frequencies the available data on the Radiax and Hitachi cables. Also, the tables show that, using the same equipment and measurement techniques, the two

novel cables (MGL and LCCX) appear to be at least competitive if not superior. Such conclusions have to be weighed against the manufacturing requirements and extra cost associated with all novel cables.

Summary Table 1: Electric Field Strength at 20 ft (in $\mu\text{v}/\text{m}$) vs Frequency (in MHz)

Frequency (MHZ)	RADIAX RX4-3A*	HITACHI HW-46**		MGL***		LCCX†	LCCX††
	(V.P.)	(H.P.)	(V.P.)	(H.P.)	(V.P.)	(V.P.)	(V.P.)
0.15	6.2	7.0	3.0	130.0	40.0	1.6	3.6
0.20	8.0					1.8	
0.25	11.4					2.1	2.5
0.30	12.0						1.9
0.60	36.0	12.5	4.5	290.0	90.0	3.2	4.8
0.75							3.5
1.00						4.0	5.0
1.50		70.0	28.0	710.0	115.0		
2.00	45.0					6.2	50.0
3.00	62.0	220.0		1150.0	900.0	22.0	90.
4.00	80.0						
6.00	160.00						
8.00	225.00						
9.00	400.00						
10.00	800.00						

* 20 ft long commercial sample from manufacturer
 **165 ft long commercial sample from manufacturer
 *** 6 ft long experimental line built by contractor

† 3.84 ft long experimental line (with 1 turn coil) built by contractor
 †† 3.84 ft long experimental line (with 4 turn coil) built by contractor

Summary Table 2: Attenuation Loss in dB/20 ft

Frequency (MHZ)	RADIAX CABLE TYPE		HITACHI CABLE TYPE
	RX4-3A	RX5-1	HW-46
0.4	0.01	0	<0.1
0.5	0.01	0	<0.1
0.6	0.02	0.01	<0.1
0.7	0.02	0.01	<0.1
0.8	0.02	0.01	<0.1
0.9	0.04	0.02	<0.1
1.0	0.05	0.02	<0.1
2.0	0.09	0.04	<0.1
3.0	0.11	0.06	<0.1
4.0	0.12	0.06	<0.1
5.0	0.13	0.08	<0.1
6.0	0.17	0.10	0.1
7.0	0.22	0.10	0.2
8.0	0.28	0.20	0.2
9.0	0.28	0.18	0.18
10.0	0.38	0.25	0.2
150.0			1.5
200.0			1.4
250.0			1.8
300.0			1.8
350.0			2.1
400.0			2.4
450.0			2.4
500.0			2.6

Summary Table 3: Coupling Loss in dB (at 20 ft)

Frequency (MHZ)	RADIAX CABLE TYPE RX4-3A		HITACHI CABLE TYPE HW-46 LCX		MGL* (H.P.)
	(H.P.)	(V.P.)	(H.P.)	(V.P.)	
150					42 ± 10**
250	79	78	66	60	
300	68	75	51	57	
350	77	79	63.5	60.5	

*line loaded with a single acrylic disc

**estimated value

PROPOSAL FOR FURTHER INVESTIGATION

With regard to the LCCX cable, it is obvious from previous discussion that the characteristic impedance Z_0 varies in the presence of the short circuited coils. Furthermore, the presence of such coils destroys the field symmetry in the transverse plane unless many identical coils are symmetrically distributed in the transverse plane. As a result, several areas of investigation have been identified and are considered necessary to solve before a final decision on the feasibility and merits of the LCCX cable can be made. These are presently the subject of research theses and include:

- a. variations in Z_0 and transverse field distribution as a result of the presence of the inductive coils and optimal design of the coils and coaxial structure to yield a value of Z_0 equal to 50 ohms and a symmetric field distribution. This study will include the dimensions, number of turns, frequency and actual location of each coil. It is obvious that in the longitudinal plane the coil to coil separation distance needs to be optimized, depending on the application. In addition, the possibility of rotating the angular positions of the coils to control the radiation pattern needs to be investigated. The equivalent circuit of the cable for each of these arrangements and the resulting frequency response and radiation pattern will also be evaluated.

- b. Generation of charts for the transmission loss per km and the coupling loss as a function of radial distance in the transverse plane for a given LCCX cable design.
- c. Investigation of special schemes to reduce the overall cost of a system layout for rural communications. These include the possibility of using LCCX cable only near populated areas and standard coaxial cable elsewhere. Also, the possibility of supplying each subscriber to such a system with a coupling coil for communication purposes will be investigated. Obviously methods to simplify the design of the cable itself and reduce its manufacturing cost are of basic interest.

These areas clearly require elaborate theoretical, numerical and experimental work, particularly in view of the many iterations and modelling attempts that would have to be made to reach a solution for each question.

When comparing the LCCX with other types of leaky coaxial cable, it should be noted that, although the LCCX is in itself novel, it is nevertheless a kind of magnetic analog of the Inieux-Delogne System developed in Belgium and which also consists of discrete radiating elements along the line. The alternative scheme of a continuous longitudinal slot, in the outer conductor, is most likely less costly than the LCCX and has, in fact, been investigated and found suitable for continuous access communications (e.g. in railroads, tunnels, etc. [1.9, 1.10]). However, none of these systems has the capability and adaptability needed to operate a low-loss low frequency rural communication system, as in the case

of the LCCX cable. It is obvious from Tables 4.1 and 4.3 to 4.10 that the LCCX test line radiates significant field strengths at low frequencies using even one coil with one turn. The addition of many more turns and coils at discrete locations, using thin insulated wire, is not expected to present severe testing or manufacturing difficulties or severe limitations on the bending of the cable.

Finally, it should be pointed out that, in addition to the proposed applications already mentioned in the field of communications, there are other applications for the MGL, LCX and LCCX leaky cables in the fields of measurement and instrumentation. Examples of such applications involve the use of a suitably constructed cable as an immersion probe for moisture profile determination of soil and grain (wheat, rice, corn, flour, etc.) as well as on line measurement of snow height and snow parameters in remote areas. It is obvious that the measurement accuracy can be improved by modifying the probing region when two identical probes are immersed in parallel and side by side to make up a single combined probe. In the latter case, the radiating elements (slots, coils, discs, etc.) would naturally be facing each other. It is also obvious that the TDR technique would probably be most suitable for profile measurements, while average type data on snow height, etc. would probably be best done with multifrequency A.C. terminal measurements. In practice, the proposed probes could be constructed with miniature circuitry for manual inspection of moisture content or interrogated by remote sensing techniques if used for snow hydrology or snow avalanche applications.

GENERAL CONCLUSIONS AND RECOMMENDATIONS

Although the contract was limited to a feasibility study with most of the useful experimental work being carried out towards the end, due to the prohibitive winter climatic conditions, it is still possible to offer some meaningful conclusions and recommendations based on what has been done. These are as follows:

1. The performance of commercial LCX Cable samples tested was found to be reasonably close to the data published by the manufacturer in the design frequency band. However, outside this band, and particularly towards the lower frequencies in the Kilohertz range, it was surprising and far better than expected. This performance includes the coupling loss and radiated field strength, while the low transmission loss was expected. Because this happens in the frequency range of most interest for possible application to rural communications, more effort should be directed to fully understand the mechanism of radiation involved.
2. The definition of coupling loss is based on the signal received by a half-wave dipole at a distance of 20 ft in a "clean" environment and was questioned by Martin and others for high frequencies. For our low frequency applications this definition appears even more questionable and less useful, particularly since it is difficult to implement or interpret for rural communications. Perhaps the definition could be retained, provided that field strength compatible with existing receivers is measured. Alternatively, a distance relative to the wavelength rather than a fixed physical distance could be adopted.

3. The time domain reflectometer technique would be used as a complementary method to study the performance of LCX cables over a wide frequency band using a single measurement for each quantity of interest. This method can also be used to separate the 'end effects' and to study such detrimental factors as cable bending, effect of cable burial and as an aid to quick location of cable faults.
4. The modified Goubau Line (MGL) performed reasonably close to theory within the design frequency band. Experimentally the performance outside this band and, particularly, at the same low frequencies, at which the commercial LCX cables were tested, indicated surprising success. Also the leaky MGL, radiating through a single dielectric disc, yielded field strength values much higher than the LCX cable samples. The concept of a sliding dielectric disc also proved useful in matching the leaky MGL to its feed line and hence allowing maximum power into the line. In practical applications it might be preferable to replace the disc by a helical groove or a conducting tape. More work in this area is necessary before the merits of the line could be completely assessed.
5. In spite of the success of the LCX and MGL test lines at low frequencies, it was felt that a better system could still be devised through magnetic field coupling instead of the electric field coupling of the MGL and outer conductor wall current interruption of the LCX. This led to the very simple, novel, and probably patentable line proposed in Chapter 4,

and designated as the leaky coil-coupled coaxial line (LCCX). An experimental line was constructed and tested to establish the basic advantages over all other lines, particularly at low frequencies. Preliminary measurements indicate that the design problems for efficient low frequency transmission and simultaneous radiation can be overcome. It is anticipated that a follow-up investigation would lead to the design procedure and charts for rural communication problems typical of low density populated areas of Canada.

6. It is recommended that all future investigations pertaining to the LCCX line include a parallel study of the feasibility of adopting the concept to existing parallel conductors such as rail tracks, power lines, etc. Also extensive field measurements over buried and overhead LCX and LCCX lines should be carried out. Contracts on such work should include at least one full summer period to facilitate outdoor work and should include burial by the side of a paved highway to assess the additional feasibility of application to vehicular communications.
7. Although this contract did not, and was not intended to advance to the point where concrete cable layout plans for say rural Manitoba could be recommended, there is, nevertheless, some confidence to suggest a preliminary cable communication layout for the sake of discussions only. The factors that must be considered in such a layout for the case of Manitoba are:
 - a. The main highways service areas of highest population densities, whereas the primary 230 KV AC and \pm 450 KV DC Manitoba

Hydro transmission lines do not always pass near the most populated areas.

- b. The railway tracks are similar to the main highways in that they service the most populated areas (mostly cargo rather than passenger service) and reach the Port of Churchill, although the rural rail network may be partially or totally abandoned.
- c. The Manitoba winters are usually quite severe and are usually associated with heavy winds, heavy snowfall, very cold temperatures and significant soil movements.
- d. There is a significant network of 66 KV sub-transmission or distribution lines which service most of the province.

As a result, the preferable and probably most economical layout is to adapt the 66 KV distribution lines for communication purposes, using existing technology. The second choice is to install overhead LCX or LCCX cables wherever necessary along 66 KV lines. The third choice is to bury LCX or LCCX cables along the side of highways or to employ existing rail tracks after solving the associated design problems. For convenience, the Manitoba Hydro power line network is shown on two maps submitted separately.

- 8. Finally, it is recommended that the feasibility of leaky 2-wire transmission lines be assessed and compared with the LCX, MGL and LCCX lines, insofar as the cost and the return and coupling losses are concerned. The proposed line may consist of a conventional 2-wire transmission line feeding a set of dipoles (or folded dipoles) each connected across, and oriented perpendicular to, the

main line. The length of each dipole, and the separation between adjacent dipoles, depends on the frequency and specific application. Basically, the proposed system may be viewed as the electrical analogue of the LCCX system on a 2-wire line. One particular advantage of the proposed line is its flexibility for matching purposes, since the conventional tuning stub method can be employed for impedance matching at the feed points. The possibility of adapting existing power lines to implement the proposed system (e.g. using dipoles or monopoles with power amplifiers fed from contactless pick-up coils) remains to be investigated.

